Epigenetic regulation of muscle stem cell expansion

INAUGURAL-DISSERTATION

zur Erlangung des Doktorgrades der Naturwissenschaften

- Doctor rerum naturalium -

(Dr. rer. nat.)

vorgelegt dem

Fachbereich für Biologie und Chemie (FB 08)

der Justus-Liebig-Universität Gießen

eingereicht von

Ting Zhang

Gießen, 2015

Die vorliegende Arbeit wurde am Max-Planck-Institut für Herz- und Lungenforschung, W.G. Kerckhoff-Institut in Bad Nauheim angefertigt.

Erstgutachter:
Prof. Dr. Dr. Thomas Braun
Abteilung Entwicklung und Umbau des Herzens
Max-Planck-Institut für Herz- und Lungenforschung
Ludwigstraße 43, 61231 Bad Nauheim

Zweitgutachter:
Prof. Dr. Lienhard Schmitz
Biochemisches Institut
Fachbereich Medizin
Justus-Liebig-Universität Gießen
Friedrichstrasse 24, 35392 Giessen

Disputation am 10.Juni 2015

EIDESSTATTLICHE ERKLÄRUNG

„Ich erkläre: Ich habe die vorgelegte Dissertation selbständig und ohne unerlaubte fremde Hilfe und nur mit den Hilfen angefertigt, die ich in der Dissertation angegeben habe. Alle Textstellen, die wörtlich oder sinngemäß aus veröffentlichten Schriften entnommen sind, und alle Angaben, die auf mündlichen Auskünften beruhen, sind als solche kenntlich gemacht. Bei den von mir durchgeführten und in der Dissertation erwähnten Untersuchungen habe ich die Grundsätze guter wissenschaftlicher Praxis, wie sie in der „Satzung der Justus-Liebig-Universität Gießen zur Sicherung guter wissenschaftlicher Praxis“ niedergelegt sind, eingehalten.“

Bad Nauheim, den

ZUSAMMENFASSUNG

Stammzellen der adulten Skelettmuskulatur, auch als Satellitenzellen bekannt, befinden sich normalerweise in einem Ruhezustand und können als Reaktion auf bestimmte Reize aktiviert werden und differenzieren. Durch diese Aktivierung werden Muskelintegrität und –regeneration gesteuert. Störungen der Satellitenzell-Homöostase werden mit Pathologien einiger humaner Muskelerkrankungen in Verbindung gebracht.

Satellitenzellen, die durch die Expression des Transkriptionsfaktors Pax7 identifiziert werden (Pax7+), stammen von stark proliferierenden Pax7+/MyoD+-Vorläuferzellen ab, die während der embryonalen Entwicklung gebildet. Es konnte bereits gezeigt werden, dass Satellitenzellen eine andere chromatinorganisation als Vorläuferzellen beziehungsweise terminal differenzierte Nachkommen Unterschiede besitzen. Dies deutet darauf hin, dass epigenetische Regulatoren in der Zelle an der Schicksalsfindung und Zellidentitätskontrolle ursächlich beteiligt sein könnten, genauere Mechanismen sind bisher nicht bekannt. Durch meine durchgeführten Experimente konnte ich zeigen, dass die Protein-Arginin-Methyltransferase 5 (PRMT5)-ein epigenetischer Modifizierer, der die symmetrische H3R8 Dimethylierung (H3R8me2) in Nukleosomen katalysiert - einen wesentlichen Faktor für Pax7+ Satelliten-Zell-Homöostase bei erwachsenen Skelettmuskel darstellt, Andererseits spielt PRMT5 keine Rolle bei der Pax7+ Muskelvorläuferzellproliferation und Differenzierung während der Entwicklung ist.

Im adulten ruhenden Muskel wird PRMT5 ruhenden Satellitenzellen stark exprimiert. Induzierte Deletion des PRMT5-Gens in Pax7+ Satellitenzellen führt nicht nur zu einem massiven Rückgang der Anzahl der Muskel-Stammzellen während der Alterung, sondern verhindert die Muskelregeneration nach einer akuten Muskelverletzung. Auf zellulärer Ebene ist PRMT5 für Satellitenzellproliferation, während dem frühen Stadium der Zelldifferenzierung und dem Zellüberleben bei Ex-vivo-Differenzierung erforderlich. PRMT5 bindet direkt an die p53-Bindungsstelle am Gen-Locus des Zellzyklusinhibitors p21 und induziert ein epigenetisches Gen-Silencing durch Anreicherung von H3R8me2s, Was zu eine Arretierung der Satellitenzellproliferation führt. Damit übereinstimmend, konnte durch die genetische Deletion von p21 die beobachtete, verminderte Proliferation von PRMT5-negativen Satellitenzellen wiederhergestellt werden. Wird PRMT5 in aus Pax7+ Satellitenzellen abgeleiteten differenzierten Myotuben durch induzierte Ablation entfernt, so können diese Mäuse nach Muskelschädigung die Muskelfasern regenerieren. Diese

Regenerationsfähigkeit ist mit der Wildtyp-Situation vergleichbar und so kann davon ausgegangen werden, dass PRMT5 in differenzierten Myotuben keine signifikante Rolle spielt.

Der genetische Verlust von PRMT5 in Pax7-Vorläuferzellen während der embryonalen Entwicklung führt weder zu Veränderungen der Vermehrung noch der Differenzierung dieser Vorläuferzellen, so dass die These unterstützt wird, dass PRMT5 in der Expansion von Skelettmuskulatur-Vorläuferzellen und der Myotom-Bildung während der Entwicklung keine essentielle Funktion ausübt. Die erzielten Ergebnisse weisen eine einzigartige und essentielle Funktion von PRMT5 in der Satellitenzell-Homöostase nach und zeigen, dass PRMT5 in embryonale Muskel-Vorläuferzellen und differenzierten Muskelzellen keine wichtige Rolle spielt. Hieraus ergibt sich, dass die embryonale Muskelentwicklung und die adulte Myogenese auf unterschiedlichen Regulationsmechanismen basieren.

In weiteren Experimenten konnte ich eine zentrale Rolle von PRMT5 in der Steuerung der regenerativen Myogenese bei Muskel Dystrophien nachweisen. MDX-Mäuse, die ebenso wie humanen Duchenne-Muskledystrophie (DMD) Patienten, nicht das Dystrophin-Protein Expression, wurde mittels induzierter Deletion PRMT5 in Satellitenzellen entfernt. Dies resultierte in einer kompletten Depletion der Muskel-Stammzell-Population, einem dramatischen Verlust von Muskelmasse und einer erhöhten Muskelfibrose, was verschiedene symptome der humanen DMD nur 4 Monaten nach Induktion des PRMT5-Verlustes rekapituliert. Meine Ergebnisse zeigen, dass PRMT5 ein mögliches Target für die Behandlung der humanen DMD hat. Weitere Studien sind nötig, um die Rolle von PRMT5 in der humanen DMD zu verstehen.

SUMMARY

Adult skeletal muscle stem cells known as satellite cells are normally maintained in a quiescent state and could activate, differentiate in responding to environmental cues thereby being responsible for muscle integrity and regeneration in the lifetime. Deregulation satellite cell homeostasis has been implicated in the pathology of several human muscle diseases. Satellite cells that are identified by the expression of transcription factor Pax7 (Pax7+) originate from highly proliferative Pax7+/MyoD+ progenitor cells during development. Interestingly it has been demonstrated that satellite cells show a chromatin organization which is different from the corresponding precursors or terminally differentiated progenies suggesting that epigenetic regulators might be causally involved in cell fate determination and cell identity control. In this study I demonstrated that the protein arginine methyltransferase 5 (PRMT5), an epigenetic modifier catalyzes symmetric H3R8 dimethylation (H3R8me2) in nucleosomes, is an essential factor for Pax7+ satellite cell homeostasis in adult skeletal muscle. In contrast, PRMT5 is not required for Pax7+ muscle progenitor cell proliferation and differentiation during development and the function of differentiated myotubes in adult skeletal muscle.

In adult resting muscle, PRMT5 is highly expressed in quiescent satellite cells. Induced deletion of PRMT5 in Pax7+ satellite cells does not only lead to a massive decline of the number of muscle stem cells during aging, but also completely abolishes muscle regeneration after acute muscle injury. At the cellular level, PRMT5 is required for satellite cell proliferation, early stage of cell differentiation and cell survival upon differentiation *ex vivo*. Mechanistically PRMT5 directly binds to the p53 binding site at the locus of cell cycle inhibitor p21 gene and induces epigenetic gene silencing by depositing H3R8me2s. The up-regulation of p21 in *Prmt5* mutant satellite cells results in an arrest of satellite cell proliferation. Consistently, genetic loss of p21 partially restores the proliferation defects of PRMT5 deficient satellite cells. Importantly, mice with induced ablation of PRMT5 in Pax7+ satellite cell derived differentiated myocytes regenerate skeletal muscle to the same degree wild type mice, suggesting that PRMT5 is dispensable in differentiated myofibers. Furthermore, ablation of PRMT5 in Pax7+ precursors during embryonic development does not alter the precursor cell proliferation and differentiation, indicating that PRMT5 is dispensable for expansion of skeletal muscle progenitor cells and formation of muscle cells during development. Taken together these findings demonstrate a unique and essential role of PRMT5 in satellite cell homeostasis suggesting distinct

genetic and epigenetic requirements for developmental myogenesis and regenerative myogenesis.

In addition, I analyzed the role of PRMT5 in muscle regeneration in a murine model of muscular dystrophy. Induced satellite cell specific deletion of PRMT5 in mdx mice, a model lacking dystrophin expression as that in human Muscular Dystrophy (DMD) patients but showing much less severe and representative muscle phenotypes, results in depletion of the muscle stem cell pool, dramatic loss of muscle mass and increase of muscle fibrosis, recapitulating many pathological features of human DMD patients in only 4 months after PRMT5 ablation. This finding demonstrated that PRMT5 mediated epigenetic regulation of regenerative myogenesis has therapeutic implications for human DMD. Further studies will focus on detailed pathophysiological analyses of PRMT5 and mdx double mutant mice and the role of PRMT5 in human DMD.

TABLE OF CONTENTS

1 INTRODUCTION

Skeletal muscle is the most abundant tissue in the vertebrate body and plays a major role in physiological functions such as locomotion, breathing and energy metabolism. The structural units of skeletal muscle are muscle fibers or myofibers, formation of which is defined as myogenesis. In mammals myogenesis includes developmental and adult regenerative myogenesis. Developmental myogenesis refers to muscle fiber formation during embryonic development, which could be further separated into two stages: embryonic myogenesis and fetal myogenesis (Messina and Cossu, 2009) . Embryonic myogenesis begins with myotome formation at E9.5 followed by fusion of myoblasts and formation of primary (embryonic) fibers at approximately day E11.5. Fetal myogenesis starts with the proliferating myoblasts that do not fuse into primary fibers but continue to proliferate and differentiate only at E14.5–17.5 giving rise to secondary (fetal) fibers (Buckingham and Rigby, 2014; Messina and Cossu, 2009). In the mouse fetal myogenesis is complete three weeks after birth and further muscle mass increase depends on hypertrophic muscle growth without dramatic proliferation of myoblast cells (White et al., 2010). Adult skeletal muscle is a tissue with high potential for regeneration to repair muscle damage after physiological and non-physiological muscle injury. Regenerative myogenesis is defined as the formation of new muscle after muscle injury in adult stage. This largely relies on adult muscle stem cells termed satellite cells, which are derived from the muscle progenitor cells during embryonic muscle development (Yin et al., 2013b).

1.1 Developmental myogenesis

Developmental myogenesis of trunk and limb muscles is initiated in the somites, segmented structures that form from paraxial mesoderm in an anterior-to-posterior manner. The dorsal epithelial region of the maturing somite, the dermomyotome, gives rise to muscle progenitor cells as well as other tissue progenitors developing into endothelial and smooth muscle cells of blood vessels, dermal and brown fat lineages. Muscle progenitor cells within dermomyotome proliferate, differentiate and produce mononucleated myoblasts. At around embryonic day 11 (E11), these postmitotic mononucleated myoblasts start to migrate out from the border regions of the dermomyotome, fusion into multinucleate muscle fibers in the mouse that characterizes “embryonic” or primary myogenesis necessary to establish the basic muscle pattern.

1.1.1 Pax3 is involved in the control of embryonic myogenesis

The formation of muscle during early embryonic development depends on the proliferation, differentiation and migration of muscle progenitor cells, which is tightly regulated by a myogenic transcription factor network including Pax3, Myf5, MyoD and Mrf4. While myogenic transcription factor Myf5 and Mrf4 play a critical role in myogenic progenitors in somites (Braun and Gautel, 2011; Tajbakhsh et al., 1996), Pax3, the paired homeobox containing transcription factor controls cell survival particularly in the hypaxial domain of the somite (Franz et al., 1993; Goulding et al., 1994). Additionally Pax3 marks migrating myogenic progenitor cells that have not yet activated the myogenic determination genes(Bober et al., 1994). Once Pax3-positive myogenic cells have left the dermomyotome and started to form muscle mass, a critical cellular equilibrium has to be maintained between self-renewal of the progenitor pool and embryonic myofiber formation (Buckingham and Rigby, 2014). This could be regulated by FGF signaling pathway. Pax3 directly controls a myogenic enhancer element of Fgfr4 and activates its expression, which promotes progenitors entry into the differentiation program (Lagha et al., 2008). After entering into the myogenic program, Pax3 activates the transcription of myogenic factor Myf5 leading to the activation of other down-stream transcription factors for instance MyoD and Myogenin by regulating its enhancer elements as well (Chang et al., 2004; Francetic and Li, 2011; Tajbakhsh et al., 1997). Therefore Pax3 is critical for controlling embryonic myogenesis by regulating the cellular equilibrium of self-renewal of muscle progenitor cells and myogenic cell differentiation.

1.1.2 Pax7 maintains skeletal muscle stem cells

As muscle development proceeds, the second wave of myogenesis (also called fetal myogenesis) takes place between E14.5 and E17.5 in the mouse and involves the fusion of secondary myoblasts either with each other to form secondary fibers (initially smaller primary fibers) or with primary myofibers. Fetal myogenesis is characterized by growth and maturation of each muscle anlagen and by the onset of innervation (Messina and Cossu, 2009). While Pax3 transcription is down-regulated in fetal muscle with a notable exception being the persistence of Pax3 expression in a subset of satellite cells including those residing in the diaphragm (Relaix et al., 2006), Pax7, a paralog of Pax3, becomes the dominant factor in all myogenic progenitor cells. In the limb, Pax7 is initially co-expressed with Pax3. Genetic tracing experiments showed that all later Pax7-positive cells in the fetal limb are derived from cells that had expressed Pax3 (Hutcheson et al., 2009). Pax7 activates the transcription factor nuclear factor 1/X (Nfix) that in turn, activates fetal specific genes,

including muscle creatine kinase (MCK) and β-enolase, while repressing embryonic genes, such as slow myosin (Messina et al., 2010). The loss of fetal myofibers when the Pax7 lineage is ablated highlights the important role of Pax7+ cells for fetal myogenesis. In late-stage of fetal muscle development, the Pax3 derived Pax7 positive cells begin to adopt a satellite cell position (Kassar-Duchossoy et al., 2005; Relaix et al., 2005), suggesting that this somite-derived population also provides the progenitor cells for postnatal skeletal muscle (Gros et al., 2005). Therefore Pax3+ and Pax7+ cells contribute differentially to embryonic and fetal limb myogenesis respectively.

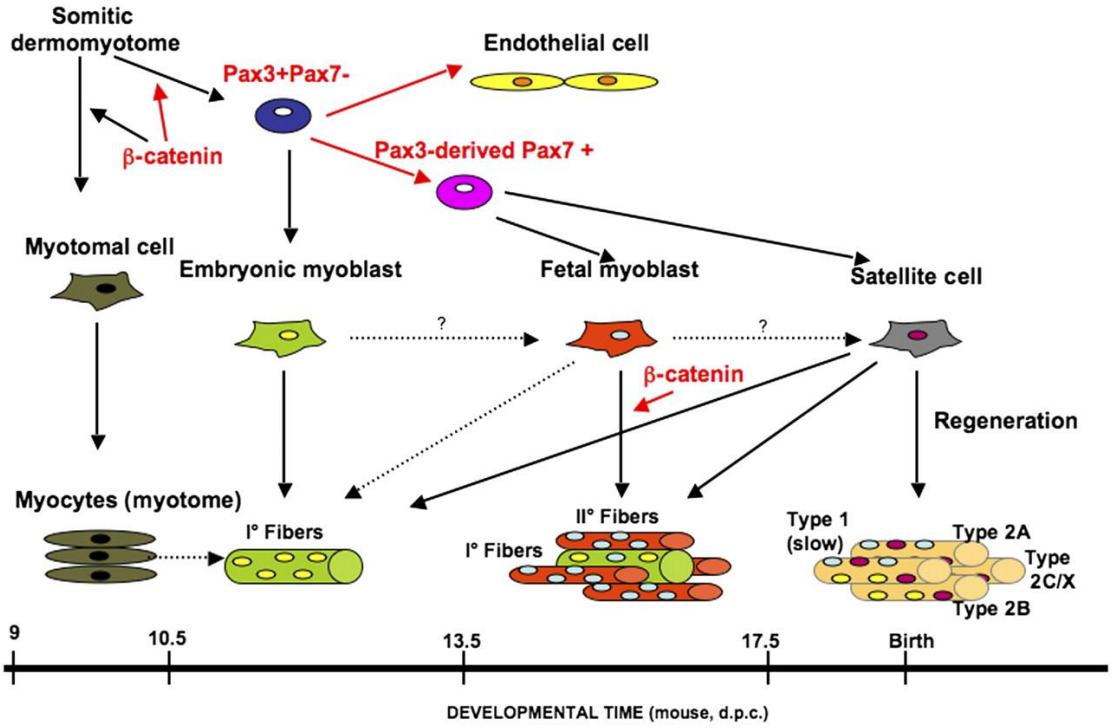

Figure 1.1.1 Model of embryonic and fetal limb myogenesis (Messina and Cossu, 2009)

1.1.3 Developmental myogenesis of head muscle

Emerging evidence demonstrated that head muscle development follows a distinct program compared to limb/trunk muscle development. Initial specification of mouse masseter muscles depends on the bHLH genes MyoR and capsule without the need of Pax3 and Pax7 (Lu et al., 2002). The activation of myogenic program by these two transcription factors leads to formation of head muscle. Additional players are pituitary homeobox 2 (Pitx2) and T-box transcription factor 1 (Tbx1), both of which are expressed widely in the developing mouse embryo. Pitx2 mutants do not properly develop the muscles that are derived from the first branchial arch (Dong et al., 2006) and extraocular muscles due to extensive cell death in the premyogenic mesoderm

(Gage and Camper, 1997). Furthermore induced deletion of Pitx2 using UBC-CreER^{T2} that avoids premyogenic mesoderm apoptosis down-regulates Myf5 and Mrf4 and abolishes the expression of MyoD, indicating that Pitx2 functions upstream of these myogenic factors during head muscle formation (Zacharias et al., 2011). Pitx2 directly activates Myf5 as well as MyoD through binding to the regulatory region at the promoter region. These findings suggest that Pitx2 regulates both progenitor cell survival and myogenic specification at the onset of extraocular muscle formation, mimicking the role of Pax3 at the sites of myogenesis in the body. Tbx1 mutants also suffer from impaired myogenesis in the first branchial arch and lack the muscles that normally originate from other arches due to the severe malformations of these structures (Jerome and Papaioannou, 2001; Kelly et al., 2004). In Tbx1/Myf5 double mutants all muscles derived from the first branchial arch are absent suggesting that Tbx1 functions up-stream of MyoD as well(Sambasivan et al., 2009). Additionally Tbx1 mediated head muscle myogenesis has been linked to Fgf10 and Fgf8 signaling cascade, ablation of which results in inhibition of proliferation of the myogenic progenitor cells (Ng et al., 2002).

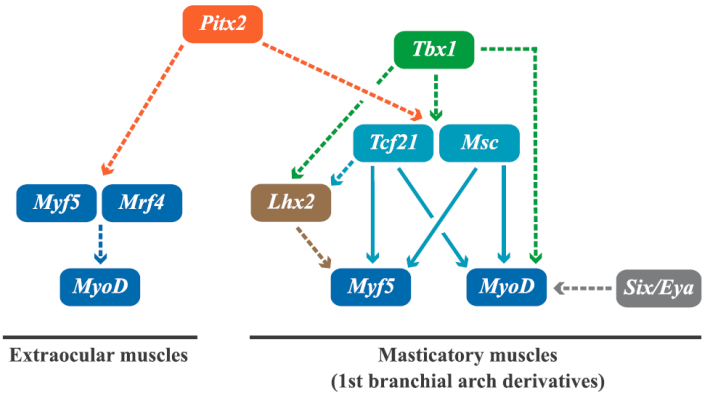

Figure 1.1.3 Gene regulatory network that governs myogenesis in the head and truck/limbs (Buckingham and Rigby, 2014)

1.2 Regenerative myogenesis and muscle stem cells

Unlike *de novo* embryonic muscle formation, regenerative myogenesis in higher vertebrates depends on both the injured tissue retaining an extracellular matrix scaffolding as a template for the formation of muscle fibers and the recruitment of an undifferentiated muscle stem cells also known as satellite cells (Ciciliot and Schiaffino, 2010). These stem cells have been shown to use asymmetric divisions for self-maintenance and, at the same time, giving rise to more committed myogenic progenies (Conboy et al., 2007; Kuang et al., 2007; Shinin et al., 2006).

1.2.1 Characteristics of satellite cells

Skeletal muscle satellite cells are quiescent mononucleated myogenic cells residing between the basal lamina and the plasma membrane of the muscle fibers. Satellite cells could be morphologically distinguished from the fully differentiated myocyte by 1) a relatively high nuclear-to-cytoplasmic ratio with few organelles; 2) a smaller nuclear size compared with the adjacent nucleus of the myotube; and 3) an increase in the amount of nuclear condensed heterochromatin compared with that of the myonucleus (Figure 1.2.1).

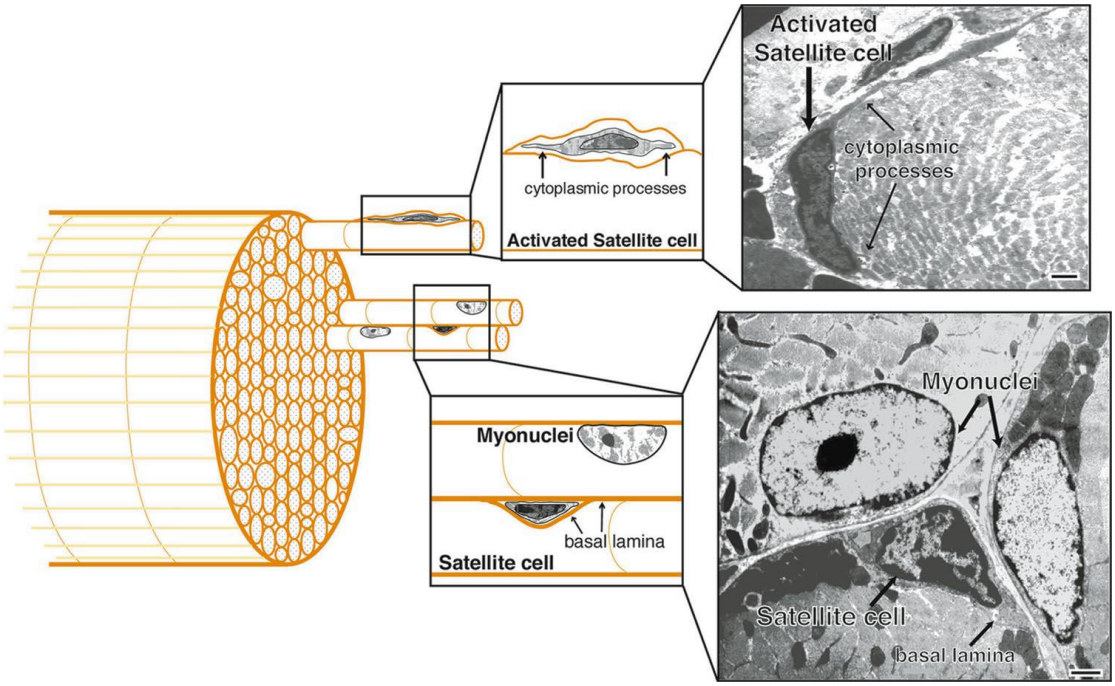

Figure 1.2.1 Characteristics of muscle satellite cells in the myofibers
Satellite cells occupy a sub-laminar position in adult skeletal muscle. The satellite cells can be distinguished from the myonuclei by a surrounding basal lamina and more abundant heterochromatin as shown by electron micrograph picture (Hawke and Garry, 2001). Bar = 1 μm.

Studies from immunohistochemical staining, genetic profiling and mouse transgenic studies have further revealed molecular and cellular markers that can be used to distinguish satellite cells from other cell types. Among them, the most widely accepted markers are CD34, CXCR-4, M-cadherin, Pax7, syndecan-3, syndecan-4, α7-intergin and c-met (Alfaro et al., 2011; Burkin and Kaufman, 1999; Cornelison et al., 2001; Cornelison and Wold, 1997; Ratajczak et al., 2003; Seale et al., 2000). While many of these defined cell markers expressed in satellite cells are not unique to this stem cell population, combination of these markers can be used to isolate pure

satellite cells from skeletal muscle (Fukada et al., 2004; Montarras et al., 2005; Pannerec et al., 2012; Zammit et al., 2006).

1.2.2 Origins of satellite cells

Satellite cells originate from Pax3 and Pax7 expressing cells which initially are derived from the dermomyotome (Relaix et al., 2005; Seale et al., 2000). Along this line inactivation of Pax7 results in severe depletion of muscle stem cells in adult stage and impaired muscle regeneration upon injury (Gunther et al., 2013; Seale et al., 2000). Furthermore by using $MyoD^{iCre/+}$/R26R-EYFP lineage tracing system Kanisicak and colleagues have shown that almost all satellite cells in adult muscle have activated MyoD during satellite cell development even though myoD expression is shut down in most adult satellite cells (Kanisicak et al., 2009). These results strongly support the idea that the majority of adult Pax7+ satellite cells have a somite origin and transit through a Pax7+/MyoD+ state. Inactivation of Pax7 in Myf5 positive lineage using $Myf5^{Cre/+}$/$Pax7^{loxP/loxP}$ mice revealed that the majority of adult satellite cells originates from Myf5-expressing myogenic cells as well (Gunther et al., 2013). Consistently using a Myf5Cre/Rosa26YFP reporter, Kuang et al could show that the majority (90%) of the adult satellite cell pool originates from Myf5+ precursors (Kuang et al., 2007). Notably formation of the satellite cell pool in germline Myf5 or MyoD nulls suggests that Myf5 or MyoD is not required for satellite cell formation most likely due to the compensatory effect of Myf5 and MyoD during skeletal muscle development (Gensch et al., 2008; Haldar et al., 2008).

On the other hand, accumulating evidence also indicates that some adult satellite cells may have alternative origins other than dermomyotome-derived Pax3+/Pax7+ progenitors. For instance studies utilizing TN-APCreERT2 and VE-cadherinCreERT2 alleles have showed that alkaline phosphatase (ALPL) expressing pericytes, but not VE-cadherin-expressing endothelial cells, can develop into postnatal satellite cells and participate in normal development of limb muscles (Dellavalle et al., 2011). Additionally multiple studies have demonstrated that several types of non-satellite cells can reconstitute the satellite cell niche and turn into bona fide satellite cells (Pax7-expressing myogenic cells) after transplantation into regenerating skeletal muscles. These cells include bone marrow-residing hematopoietic stem cell (LaBarge and Blau, 2002), CD45- muscle side population (SP) cells (Asakura et al., 2002), PW1+ interstitial cells (Mitchell et al., 2010), Sca1+/CD34+ fibro-adiogenic progenitors (FAPs) (Joe et al., 2010b) and muscle derived stem cells (MDSCs) (Lee et al., 2000; Qu-Petersen et al., 2002). However, It remains largely unknown to what extent these cells contribute to the adult satellite cell pool and muscle regeneration

under physiological conditions, and the validity of some of these studies have been questioned.

1.2.3 Satellite cells and adult muscle regeneration

The main function of satellite cells is to regenerate muscle upon injury thereby maintaining muscle integrity in adulthood. Muscle regeneration occurs in three sequential but overlapping stages including myofiber necrosis; the inflammatory response; the activation, differentiation, and fusion of satellite cells; and the maturation and remodeling of newly formed myofibers. In intact muscle, satellite cells are sublaminal and mitotically quiescent. Upon exposure to signals from a damaged environment, satellite cells exit their quiescent state and start to proliferate (satellite cell activation) accompanied by the down-regulation of Pax7 and rapid activation of myogenic transcription factors: Myf5 and MyoD. These proliferating satellite cells and their progeny are often referred as adult myoblasts. Subsequent differentiation of myoblasts is marked by the up-regulation of Mrf4, Myogenin and myosin heavy chain (Zammit et al., 2004). Ultimately, these differentiated myoblasts form new multinucleated myofibers or fuse to the damaged myofibers resulting in muscle regeneration (Rudnicki et al., 2008). Some of the activated SCs that do not proliferate or differentiate maintain Pax7 gene expression but down-regulate MyoD expression. These cells eventually withdraw from the cell cycle and regain markers that characterize myogenic quiescence (Nagata et al., 2006). In essence, maintenance of satellite cell homeostasis is critical for the muscle regeneration both in physiological (e.g., extensive exercise) (Parise et al., 2008) and pathological conditions (e.g., myotoxin induced injury and degenerative diseases) (Lepper et al., 2011) by providing sufficient myoblasts for fusion and maintaining the quiescent satellite cell pool (Figure 1.2.3).

The necessary and sufficient role of satellite cells during muscle regeneration is clearly supported by the finding that ablation of the total satellite cell pool (all Pax7 cells) in adulthood completely abolished muscle regeneration (Gunther et al., 2013; Sambasivan et al., 2011). However it has also been reported that several types of non-satellite cells can undergo myogenic differentiation and contribute to muscle regeneration after transplantation into regenerating muscle (Asakura et al., 2002; LaBarge and Blau, 2002; Mitchell et al., 2010; Polesskaya et al., 2003). Nevertheless, the contribution of these cells to adult muscle regeneration seems to be negligible compared with satellite cells, implying that the physiological relevance of non-satellite cell-based myogenesis might depend on Pax7 expression and/or the existence of considerable numbers of satellite cells.

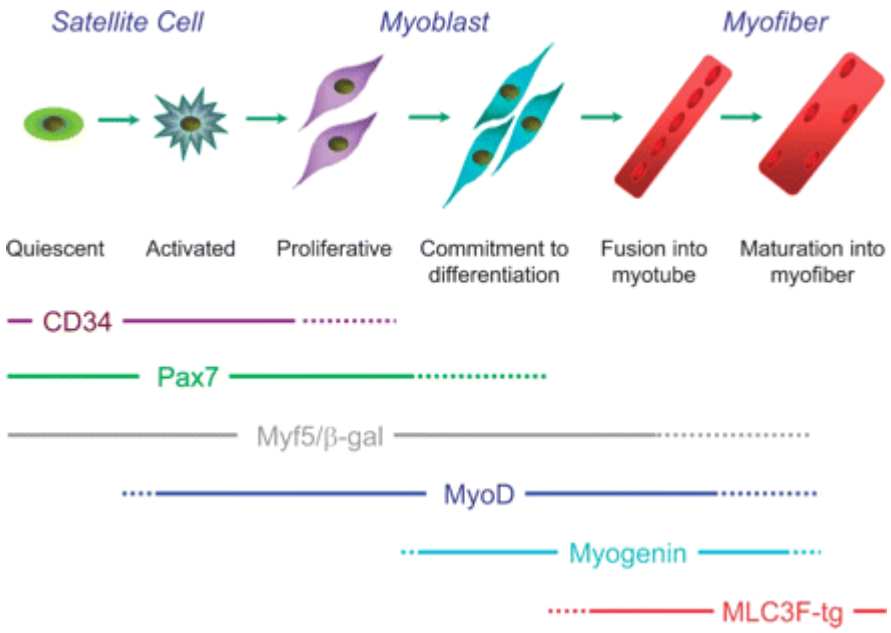

Figure 1.2.3 Schematic stages of satellite cell mediated myogenesis and markers typical for each stage (Zammit et al., 2006).

1.3 Regulation of satellite cell homeostasis

Satellite cells based adult muscle regeneration is highly orchestrated to ensure that specific genes are regulated in a temporally and spatially organized manner according to genetic and environmental factors (Dobreva and Braun, 2010; Yablonka-Reuveni et al., 2008). Regulation of satellite cell quiescence, activation, cell cycle re-entry and differentiation in response to muscle injury involve interplay of multiple muscle-specific transcription factors and epigenetic modifiers together with interaction with the satellite cell niche.

1.3.1 Transcriptional regulation of satellite cell homeostasis

The transcriptional network regulation satellite cell homeostasis has been well established. Pax7-mediated activation of MyoD and Myf5 specify a population of SCs that enters the differentiation program whereas Pax7+/MyoD- cells re-enter the quiescent state and replenish the satellite cell pool (Rudnicki et al., 2008). Furthermore down-regulation of Pax7 in Pax7+/MyoD+ or Pax7+/Myf5+ population coincides with the ability of MyoD and/or Myf5 to induce the transcription of downstream genes and promote terminal differentiation (Olguin and Pisconti, 2012). Consistently MyoD knockout mice show severely deficient skeletal muscle regeneration following injury due to excessive myoblast proliferation and defective differentiation of SCs (Cornelison et al., 2000). One of MyoD targets is the cyclin

dependent kinase (CDK) inhibitor p21(waf1/Cip1), which is induced by MyoD during myoblast differentiation and subsequently permanent cell cycle arrest (Halevy et al., 1995).

While Myf5 and MyoD are expressed in proliferating myoblasts prior to differentiation, Myogenin and MRF4 are only expressed in terminally differentiating cells (Megeney and Rudnicki, 1995). Expression of myogenin is primarily induced by MyoD, which enhances the expression of a subset of genes that are previously initiated by MyoD (Cao et al., 2006). Along this line ChIP-Seq analysis reveals a convoluted hierarchical gene expression circuitry centered on MyoD and its downstream targets: Myogenin and Mef2 transcription factors (Mef2s). Based on the temporal expression pattern of MyoD, Myogenin and Mef2s, a feed-forward regulatory circuit is proposed. In this hypothesis, myogenic differentiation is an irreversible procedure and is driven by the sequential expression of key transcription factors, which are destined to transduce gene expression signals to their target genes (Penn et al., 2004).

1.3.2 Epigenetic regulation of satellite cell homeostasis

Currently emerging evidence demonstrates that the epigenetic mechanisms contribute to the identity and homeostasis of satellite cells as well. Epigenetic circuitry is operated by highly interconnected events including post-translational modifications of histones (e.g. phosphorylation, acetylation, methylation and ubiquitination), chromatin remodeling, nucleosome patterning and DNA modifications. Specific chromatin states and epigenetic events have been shown to maintain the satellite cells homeostasis, and to enable the proper response to external cues (Dilworth and Blais, 2011; Giordani and Puri, 2013).

Histones undergo extensive post-translational modifications thereby influencing the chromatin structure as well as the interaction between DNA and nucleosomes leading to alteration of gene transcription. Histone acetylation has invariably been linked to transcriptional activation and is dynamically regulated by the opposing activities of histone acetyltransferases and histone deacetylases (HDAC) (Haberland et al., 2009). Two nuclear histone acetyltransferases, CREB-binding protein (CBP)/p300 and PCAF have been show to transactivate MyoD promoter by acetylating histone at Myod regulatory regions as well as MyoD itself (Hamed et al., 2013; Polesskaya et al., 2000). Three distinct classes of HDACs are involved in the repression of muscle gene transcription by countering the activities of histone acetyltransferases during myoblast proliferation (Lu et al., 2000; Mal et al., 2001; Puri et al., 2001). While class I HDACs could associate with and inhibit MyoD (Mal et al.,

2001; Puri et al., 2001), class II HDACs (specifically HDAC4 and HDAC5) are dedicated repressors of MEF2 activity (Fulco et al., 2003; Lu et al., 2000; McKinsey et al., 2000a; McKinsey et al., 2000b). Class III HDACs, the NAD(+)-dependent histone deacetylase Sirt1, forms a repressor complex with PCAF and MyoD, silencing muscle gene expression in response to metabolic variations(Fulco et al., 2003).

Histone methylation is another epigenetic means that has been shown to modulate the expression of muscle-specific transcriptional regulators at different stages of SCs. Genome wide epigenetic profiling in satellite cells revealed a fundamental role of H3K27me3 in suppressing factors associated with non-muscle lineages within a proliferative progenitor population (Woodhouse et al., 2013). Along with this, Liu et al demonstrated by ChIP-seq that quiescent SCs possess a permissive chromatin state in which only a few genes are epigenetically silenced by PcG-mediated H3K27me3 whereas a large number of genes encoding regulators that specify non-myogenic lineages are demarcated by bivalent domains at their transcription start sites (TSSs) (Liu et al., 2013). For instance, a transition from a transcriptionally permissive H3K4me3 mark to a repressive H3K27me3 mark was observed on the Pax7 gene locus as proliferating myoblasts turn off this important marker of satellite cell identity and prepare for differentiation (Palacios et al., 2010). Consistently loss of Ezh2, the enzyme responsible for H3K27me3, in Pax7+ satellite cell leads to transcriptional deregulation in non-muscle lineages and impairs muscle stem cell expansion but not terminal differentiation (Juan et al., 2011; Woodhouse et al., 2013). Additionally TrxG/MLL complex that mediates H3K4 methylation in the Myf5 enhancer region has been shown to control satellite cell proliferation by interacting with Pax7 (McKinnell et al., 2008).

Chromatin-remodeling activities have been shown to play an essential role in the activation of muscle differentiation program, especially with the recruitment of the SWI/SNF complex to myogenic loci being of particular relevance (de la Serna et al., 2006; Simone et al., 2004). Differentiation-activated p38α kinase phosphorylates BAF60c on a conserved threonine thereby promoting incorporation of MyoD–BAF60c into a Brg1-based SWI/SNF complex. The ATPase activity of Brg1 and Brm in the complex is essential for chromatin remodeling and active transcription of MyoD-target genes (de la Serna et al., 2006; Forcales et al., 2012; Simone et al., 2004). Furthermore, IGF1 signaling mediated local hyperacetylation at muscle genes by p300/CBP and PCAF HATs is required for the remodeling activity of the SWI/SNF complex (Serra et al., 2007), linking signaling transduction to chromatin remodeling in muscle gene expression.

The condensed heterochromatin formation in satellite cells observed by electron microscope indicates that maintenance of high order chromatin structure is required for satellite cell identity. Differentiation of satellite cells into myocytes is accompanied with loss of condensed heterochromatin and formation of open euchromatin (Hawke and Garry, 2001). This suggests that epigenetic mechanisms regulating high order chromatin structure and/or controlling transition from heterochromatin to euchromatin are causally involved in regulating satellite cell homeostasis. It is tempting to propose that overall genome-wide alteration of DNA or histone modificationsin SCs will permit a full appreciation to what extent these complementary epigenetic marks modulate the myogenic gene expression program and SC homeostasis.

1.3.3 Niche regulating satellite cell homeostasis

Satellite cells are present in a highly specified niche, which consists of the extracellular matrix (ECM), vascular and neural networks, different types of surrounding cells, and various diffusible molecules. It has been shown that the dynamic interactions between satellite cells and their niche regulate satellite cell quiescence, self-renewal, proliferation, and differentiation by means of cell-cell interaction and autocrine or paracrine signals (Yin et al., 2013b).

The myofibers are the primary component of the satellite cell niche due to their direct contact with satellite cells. It has been proposed that the myofibers emanate a “quiescent” signal either by their physical association or by releasing chemical compounds. Along this line, removal of the myofiber plasmalemma drives quiescent satellite cells to activation and proliferation (Bischoff, 1986). Additionally recent studies have revealed that numerous factors that regulating satellite cell homeostasis are presented on myofibers or secreted by myofibers. For example, IL6 and IL4, two cytokines that mediate a paracrine control of SC proliferation and fusion respectively, are expressed in and secreted from the myofibers. Their expression is controlled by transcription factor SRF in the myofibers (Guerci et al., 2012). Transmembrane Notch ligand Delta is reported to be up-regulated in myofibers after muscle injury. Delta binds to the Notch receptor in the satellite cells and activates the Notch signaling cascade thereby inducing cell proliferation in response to injury (Conboy et al., 2003). Therefore the muscle fiber degenerates, which probably leads to niche destruction and a loss of inhibitory signals.

The basal lamina, consisting of a network of the extracellular matrix (ECM), covering the myofibers is another main anatomical hallmark of the satellite cell niche. The molecules within ECM include collagen, laminin, entactin, fibronectin, perlecan, and decorin glycoproteins along with other proteoglycans. Changes in ECM

composition have been indicated to provide instructive cues thereby regulating satellite cell homeostasis and muscle regeneration. Lack of collagen VI in Col6a1$^{-/-}$ mice reduces satellite cell self-renewal capability and impairs muscle regeneration after muscle injury (Urciuolo et al., 2013). Satellite cells express high levels of Laminin receptors α7β1 Integrin (Itg) and dystroglycan (Burkin and Kaufman, 1999; Cohn et al., 2002), lack of both causes blunted muscle regeneration in response to injury (Cohn et al., 2002). Mice deficient for the Laminin-α2 subunit suffer from muscular dystrophy with severely impaired regeneration which can be rescued by transgenic expression of a functional basement membrane-dystroglycan linkage (Bentzinger et al., 2005; Meinen et al., 2007), suggesting that an intact ECM is essential for maintenance of satellite cell properties and for muscle repair.

The satellite cell niche is composed of different cell types such as Ang1-expresssing endothelial cells and fibroblasts as well (Abou-Khalil et al., 2009; Christov et al., 2007). It is becoming clear that other cell types for example fibro-adipogenic progenitors (FAPs) and TCF4+ fibroblasts influence satellite cell behavior in contexts of regeneration and growth (Joe et al., 2010a; Murphy et al., 2011). However it remains to be determined whether such cell types constitute the niche and therefore regulate homeostasis or function as paracrine agents involved in proliferation and differentiation of satellite cell progeny.

Mechanical and structural properties of the niche are also important for satellite cell function. It has been observed that satellite cells cannot be removed from niche and maintained *in vitro* without a loss of stem cell characteristics (Cosgrove et al., 2009; Wilson and Trumpp, 2006). However, recently Gilbert et al demonstrated that isolated satellite cells cultured for short-term on elastic surfaces mimicking the softness of adult skeletal muscle better maintain stem cell properties than cells growing on rigid surfaces (Gilbert et al., 2010).

Taken together these findings suggest that a better understanding of the muscle stem cell niche will eventually help us to develop techniques for the *ex vivo* cultivation of satellite cells, allowing genetic correction and stem cell therapy for satellite cell related muscle diseases.

1.3.4 Different genetic requirement of developmental and regenerative myogenesis

Given that regenerative myogenesis relies on muscle stem cells that are derived from muscle progenitor cells during developmental myogenesis to build up muscle in adult, it has been proposed that the cellular mechanisms controlling adult regenerative myogenesis and developmental myogenesis are similar (Parker et al., 2003). Along

this line, myogenic factors such as MyoD, Myf5 and Myogenin play similar role in developmental and regenerative myogenesis. However recent evidence indicated multiple cellular differences between them. Firstly when cultured *in vitro*, embryonic, fetal and adult myoblasts differ in their appearance, media requirements, responding to extrinsic signaling molecules, drug sensitivity, and morphology of myofibers derived from them. While embryonic myoblasts are elongated cells (Figure 1.3.4.1A) and could differentiate into mononucleated or oligonucleated myotubes, fetal myoblasts show a triangular shape (Figure 1.3.4.1B), proliferate to limited passages in response to growth factors and differentiate into large multinucleated myotubes. Satellite cells on the other hand are the only clonogenic cells with round shape morphology (Figure 1.3.4.1C), undergo senescence after a limited number of passages *in vitro* and differentiate into large multinucleated myotubes.

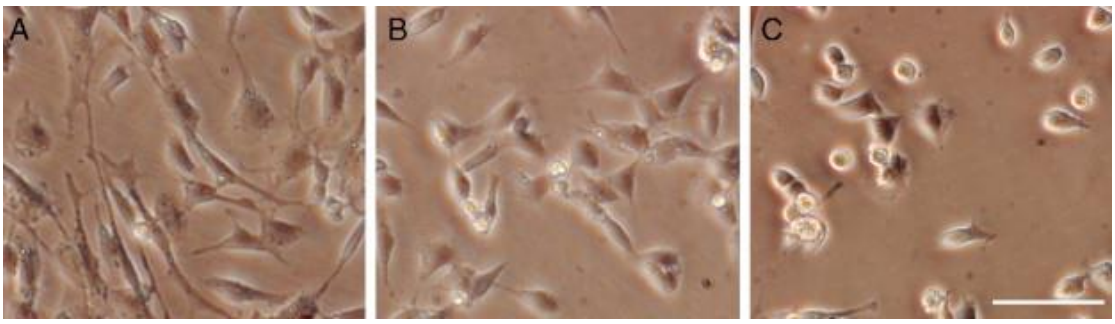

Figure 1.3.4.1 Different morphology of embryonic, fetal and adult myoblasts.
Phase contrast images showing that murine embryonic (A), fetal (B) myoblast and satellite cells (adult myoblasts) (C) were cultured in 20% fetal calf serum containing medium. Scale bar, 50 μm (Biressi et al., 2007).

Furthermore it has been shown that differentiation of embryonic myoblasts is insensitive to signal molecules such as TGFβ and BMP-4 (Biressi et al., 2007), both of which could block differentiation of fetal myoblast and satellite cells. Additionally embryonic myoblasts present a different sensitivity to merocynine 540 and phorbol esters (TPA) as compared to fetal myoblast and satellite cells (Nameroff and Rhodes, 1989) (See also in Table 1).

Secondly while embryonic and fetal muscle development depends on highly proliferative primary and secondary myoblasts without intermittent quiescence, satellite cells under non-regenerative physiological conditions are normally quiescent in vivo. During regeneration, and in contrast to muscle precursors, some activated satellite cells self-renew and return to quiescence to replenish the stem cell pool (Figure 1.3.4.2). This process has been attributed to asymmetric cell divisions of satellite cells (Braun and Martire, 2007; Kuang et al., 2007). Last but not the least, in

	Culture appearance and clonogenicity	Signaling molecule response	Drug sensitivity	Myofiber morphology in culture
Embryonic myoblasts	Elongated, prone to differentiate and form small colonies, do not spontaneously contract in culture	Differentiation insensitive to TGFβ-1 or BMP4	Differentiation insensitive to phorbol esters (TPA), sensitive to merocynine 540	Mononucleated myofibers or myofibers with few nuclei
Fetal myoblasts	Triangular, proliferate (to limited extent) in response to growth factors, spontaneously contract in culture	Differentiation blocked by TGFβ-1 and BMP4	Differentiation sensitive to phorbol esters (TPA)	Large, multinucleated myofibers
Satellite cells/ Adult myoblasts	Round, clonogenic, but undergo senescence after a limited number of passages, spontaneously contract in culture	Differentiation blocked by TGFβ-1 and BMP4	Differentiation sensitive to phorbol esters (TPA)	Large, multinucleated myofibers

Table 1 Summary of characteristics of embryonic, fetal, and adult myoblasts and myofibers (Murphy and Kardon, 2011).

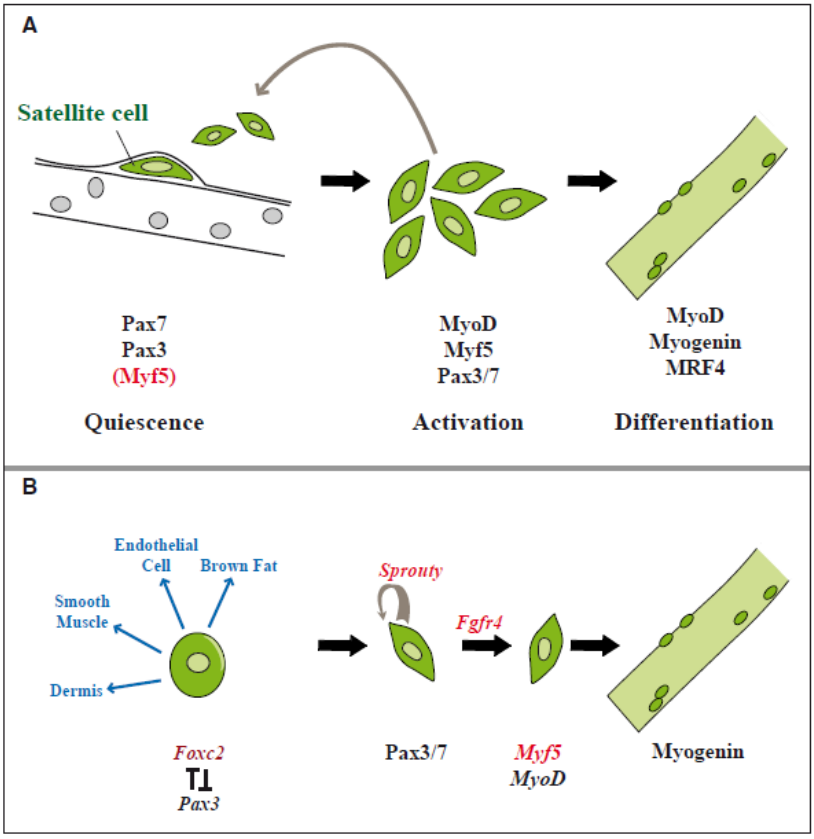

Figure 1.3.4.2 Regenerative myogenesis versus developmental myogenesis
(A) The progression of adult muscle satellite cells toward new muscle fiber formation. (B) The progression of somitic cells toward myogenesis during development (Buckingham and Rigby, 2014).

the developing embryo, rapidly dividing muscle precursors apparently do not receive signals from their microenvironment that would suffice for them to enter quiescence. In contrast, it has been shown that signals emanating from the adult muscle stem cell niche play key roles in regulating stem cell asymmetry, fate and behavior (Chakkalakal et al., 2012). Further studies aiming to identify distinct cellular and molecular characteristics of embryonic myoblasts, fetal myoblasts and satellite cells will help to fully understand the distinct genetic requirements for developmental and regenerative myogenesis.

1.4 Satellite cell proliferation and Duchenne muscular dystrophy

The essential role of satellite cells for muscle regeneration in physiological conditions is further supported by the fact that deregulation of satellite cell homeostasis is causally involved in the pathology of multiply muscle diseases. Among the mostly studied examples is the Duchenne muscular dystrophy (DMD). DMD is a lethal X-linked recessive disease caused by the mutations in the gene encoding the cytoskeletal protein dystrophin, which links the inner cytoskeleton to the extracellular matrix and therefore plays a key role in plasma membrane integrity in both skeletal and cardiac muscles (Petrof et al., 1993). DMD is characterized by severe progressive muscle wasting and chronic cycles of muscle degeneration and regeneration (Bell and Conen, 1968). The disease also affects the cardiac muscle leading to dilative cardiomyopathy (DCM) in 90% of patients. Death usually occurs in the second or third decade of life and is due to respiratory or circulatory failure (de Kermadec et al., 1994; Eagle et al., 2002). Satellite cells and their progeny, myoblasts are thought to gradually lose their proliferative and differentiating capacity, and are eventually exhausted in Duchenne muscular dystrophy, due to repeated activation, proliferation and limited self-renewal capacity (Blau et al., 1983; Blau et al., 1985; Heslop et al., 2000). As a result muscle regeneration is impaired in the advanced state of the disease and muscle tissues are gradually replaced by adipose and fibrotic tissues. Satellite cells isolated from DMD patients exert severe proliferation inhibition and DMD is therefore considered to be stem cell dysfunction disease as well (Blau et al., 1983).

The most widely used animal model for DMD are dystrophin mutant (mdx) mice. The first mice strain (C57BL/10-Dmdmdx), which was described in 1984, arose in an inbred colony of C57BL/10 mice. Despite sharing the same genetic defect as DMD patients (mutations in the dystrophin gene), mdx mice have an almost normal life

span and show slowly progressive muscle pathology, with the exception of the diaphragm muscle. Mdx mice have no widespread formation of fibrous connective tissue and no loss of muscle mass, all of which characterize the human DMD (DiMario et al., 1991; Straub et al., 1997). The similar proliferation rate of satellite cells from wild type and mdx explains the lack of characteristics of DMD within mdx mouse model. Along this line recently Sacco et al. demonstrated that mdx mice lacking telomerase activity show shortened telomeres in muscle cells, impaired proliferation of satellite cells and a severe dystrophic phenotype similar to human DMD (Sacco et al., 2010). Together with a previous report of a 14-fold shortening of telomeres in DMD patients relative to healthy individuals (Decary et al., 2000), these studies suggest that a difference in the length of telomeres between humans (5-15 kbs) and mice (>40 kbs) explains the difference in proliferative potential of muscle satellite cells between DMD patients and mdx mice. This also indicates targeting satellite cell proliferation might provide an alternative therapeutic strategy for human DMDs.

1.5 Protein arginine methyltransferase family (PRMTs)

Histones undergo a variety of post-translational modifications in their globular domains and N-terminal tails, among which lysine acetylation and methylation have been extensively studied (Greer and Shi, 2012; Margueron and Reinberg, 2011). Besides these modifications, arginine residue can also be modified by a distinct group of enzymes termed protein arginine methyltransferases (PRMTs). In eukaryotes, PRMTs catalyze the addition of one or two methyl groups to the guanidino nitrogen atoms of arginine resulting in either ω-NG-monomethylarginine (MMA), ω-NG,NG-asymmetric (aDMA) or ω-NG,N'G-symmetric dimethylarginine (sDMA) (Yang and Bedford, 2013). According to their catalytic activities, PRMTs could be classified as type I, type II or type III enzymes. Type I and type II enzymes catalyze the formation of MMA as an intermediate. Furthermore type I enzymes including PRMT1, 2, 3, 4, 6 and 8 catalyze the formation of aDMA whereas type II PRMTs including PRMT5, 7 and potentially PRMT9 catalyze the formation of sDMA (Figure 1.5.1) (Auclair and Richard, 2013). Certain substrates can only be monomethylated by PRMT7 that is referred as type III PRMTs (Miranda et al., 2004).

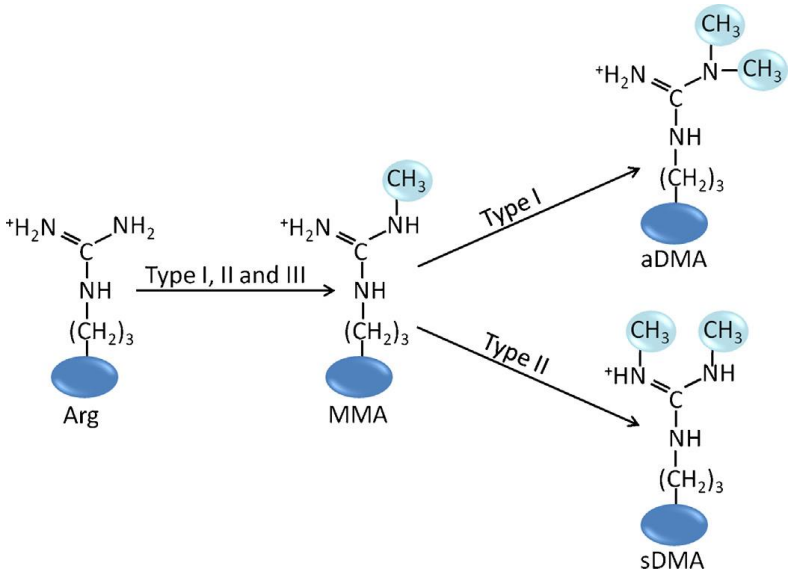

Figure 1.5.1 Protein arginine methylation.
Arginine residues are methylated by members within protein arginine methyltransferase (PRMT) family. PRMTs catalyze either the formation of monomethylarginine (MMA), asymmetric dimethylarginine (aDMA) or symmetric dimethylarginine (sDMA). The type I enzymes form aDMA and the type II enzymes form sDMA and both catalyze the formation of MMA as an intermediate. (Auclair and Richard, 2013)

PRMTs are AdoMet-dependent methyltransferases catalyzing highly specific methyl group transfers from the ubiquitous cofactor S-adenosyl-l-methionine (AdoMet) to a multitude of biological targets in the cell (Wei et al., 2014). PRMTs vary in length, but all contain a conserved core region including a methyltransferase (MTase) domain, a β-barrel, and a dimerization arm. While the MTase binding domain is highly conserved in AdoMet-dependent methyltransferases, the 7 β-barrel domains are quite unique to the PRMT family (Cheng et al., 2005). As shown in Figure 1.5.2, PRMTs have 1–2 highly conserved MTase domains, which include motif I (VLD/EVGXGXG), post I (V/IXG/AXD/E), motif II (F/I/VDI/L/K), motif III (LR/KXXG), and THW loop(Yang and Bedford, 2013).

Similar to other post-translational modifications, methylated arginine motifs serve as binding sites for specialized protein domains. Currently, the tudor domain is one well known domain that binds to methylarginine motifs. the tudor domain can be divided into methylarginine and methyllysine binding classes based on high order structures but not to their primary sequences. Structural studies have revealed that the aromatic cages on methylarginine-binding tudor domains are narrower than the methyllysine-binding cages, which favors the planar methyl-guanidinium group (Liu et al., 2012; Tripsianes et al., 2011). Methylation of arginine leads to an increase of bulk and hydrophobicity of the arginine residue, which facilitates non-electrostatic contacts

with the aromatic cage of the Tudor domain. In the cage, cation-π contacts between aromatic rings and the cationic carbon of the methylarginine residue stabilize the interaction (Liu et al., 2012; Tripsianes et al., 2011). To date there are more than 30 Tudor domain-containing proteins (TDRDs) identified in mammalian genome (Chen et al., 2011).

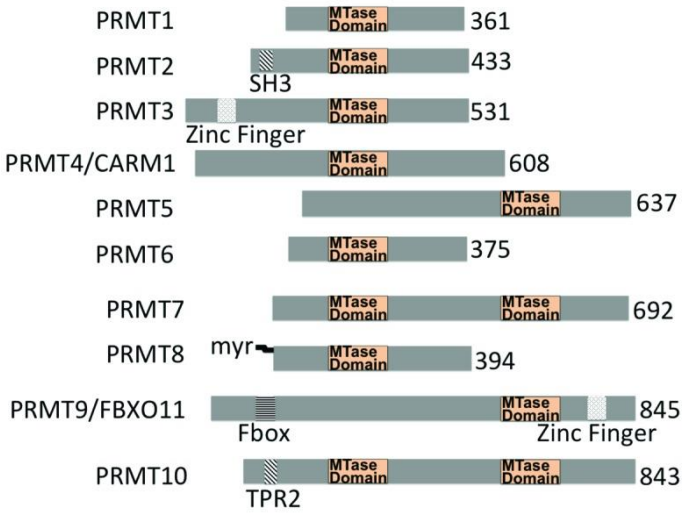

Figure 1.5.2 The schematic domain structure of PRMTs.
All PRMTs universally have 1–2 methyltransferase (MTase) domains (Wei et al., 2014).

Another protein module that has been identified to specifically recognize methylation arginine is the plant homeodomain (PHD) finger. PHD finger within protein RAG2 binds to H3R2me2s/K4me3 doubly modified peptides slightly better than to H3R2me2a/K4me3 and H3K4me3. Further structure analysis revealed that a Tyr residue in this domain that is not conserved in other PHDs, provides a preferred interacting surface for H3R2me2s (Ramon-Maiques et al., 2007). However, the biological significance of the interaction of RGA2 PHD fingers with the doubly modified H3 histone tail (H3R2me2s + H3K4me3) is still not clear. In addition, the PHD finger within the ADD domain of the DNA methyltransferase DNMT3A has been shown to directly bind to H4R3me2s thereby targeting DNA methylation and silencing transcription of the human β-globin locus (Zhao et al., 2009). Given the prevalence of arginine methylation in the cell, it is most likely that only a small proportion of the methylarginine effectors have been identified. New screening approaches aiming to identify additional 'readers' of these methyl modifications will help to understand the signal transduction pathways that emanate from this type of PTM (Yang and Bedford, 2013).

Removal of arginine methylation is biochemically difficult. One possibility is to convert non- or mono- methylated arginine to citrulline (Figure 1.5.3) (Cuthbert et al., 2004; Wang et al., 2004), leading to loss of arginine methylation marks. The key enzymes catalyzing arginine to citrulline belong to a family of proteins called peptidylarginine deiminase (PADIs). PADI4 has been recently shown to convert R2 and R17 at histone H3 tails to citrulline, counteracting arginine methylation catalyzed by PRMT6 and PRMT4, respectively (Cuthbert et al., 2004; Kolodziej et al., 2014).

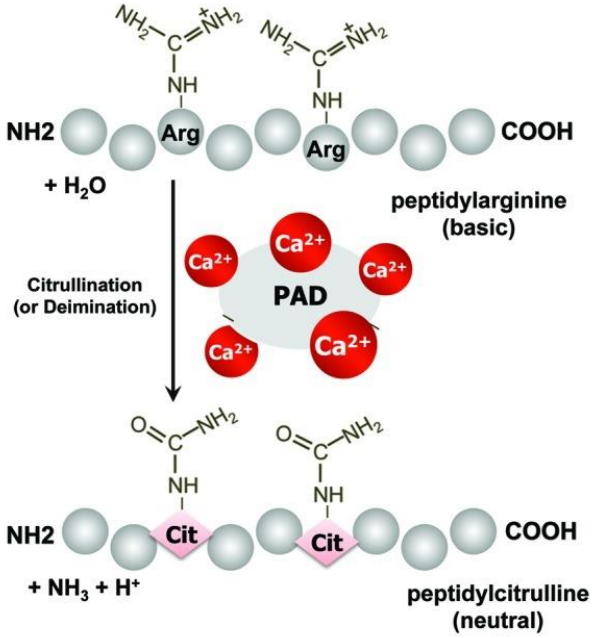

Figure 1.5.3 An outline of the protein citrullination (deimination) process.
Calcium-dependent peptidylarginine deiminases (PADIs) convert peptidylarginine into peptidylcitrulline resulting in altered protein function (Jang et al., 2013).

Additionally it has been shown that Jumonji C domain containing protein JMJD6 is capable of directly erasing mono- and di-methyl arginine marks without altering the protein sequence (Chang et al., 2007) . However, this finding has recently been questioned (Webby et al., 2009). Thus it is still unclear whether there is enzymatic reaction that directly removes methyl groups from arginine in histones or other proteins.

1.6 Protein arginine methyltransferase 5 (PRMT5) and symmetric arginine methylation

PRMT5 is the major symmetric arginine dimethyltransferases and has been shown to play a pivotal role in regulating multiple cellular processes ranging from transcription repression, RNA processing to cell signaling, differentiation, apoptosis and

tumorigenesis (Bedford and Clarke, 2009). Consistently complete loss of this enzyme is not compatible with mouse or cell viability (Tee et al., 2010). PRMT5 exists both in nucleus and in cytoplasm with distinct substrate and functions. In the nucleus, PRMT5 has been shown to symmetrically dimethylate histones H2AR3, H3R8, H4R3 and many transcription factors (Karkhanis et al., 2011). Association of PRMT5 with various binding partners appears to influence its substrate specificity. For instance a nuclear protein called cooperator of PRMT5 (COPR5) was identified as a PRMT5 interacting partner by the yeast two-hybrid assay and might recruit PRMT5 preferentially to methylate histone H4R3 *in vitro* (Lacroix et al., 2008).

1.6.1 Symmetric arginine methylation and transcription repression

Using ChIP and ChIP-seq methods, it has been shown that H4R3me2s is strongly correlated with repression of transcription (Barski et al., 2007; Wang et al., 2008; Xu et al., 2010). Furthermore H4R3me2s has also been shown to be mono-allelic within the H19 imprinting control region (Jelinic et al., 2006), suggesting that symmetric arginine methylation might regulate imprinting gene silencing. Mechanistically H4R3me2s serves as a direct binding target for the DNA methyltransferase DNMT3A, which interacts through the ADD domain with a PHD motif. During the silencing of the human beta-globin gene and C/EBPβ target genes, H4R3me2s is required for DNMT3A binding and DNA methylation in the promoter regions of those genes (Tsutsui et al., 2013). However this finding has not been supported by subsequent structure analysis of the DNMT3A ADD domain (Otani et al., 2009) or by peptide array screening for interaction partners using the same domain (Zhang et al., 2010), suggesting a more complicated situation of H4R3me2s in mediating DNMT3A binding, DNA methylation and gene silencing. In support of this H4R3me2s has also been shown to act independently from repressive epigenetic modifications such as H3K9me3, H4K20me3 and DNA methylation at imprinted gene loci (Girardot et al., 2014). While many findings support an positive correlation of symmetric arginine methylation and gene silencing, a recent ChIP-seq study using another specific antibody show that H4R3me2s is a hallmark of G+C-rich sequence elements, but is generally independent of the transcriptional status or methylated DNA in ES and MEF cells (Girardot et al., 2014), suggesting more complicated transcriptional regulation by symmetric arginine methylation.

1.6.2 Transcription repression by PRMT5

Recent studies indicate that PRMT5 suppresses gene expression by either modifying histones in concert with a variety of other epigenetic modifiers including ATP-

dependent chromatin remodelers and co-repressors or indirectly modulating the activity of specific transcription factors (Dacwag et al., 2007; Hosohata et al., 2003; Pal et al., 2004). Furthermore, PRMT5 has been shown to induce additional repressive epigenetic marks at the fetal globin gene promoter in an erythroid cell line through the assembly of a multi-protein repressor complex containing the histone modifying enzymes Suv4-20h1 and casein kinase 2alpha (CK2alpha), which catalyze tri-methylation of H4K20 and phosphorylation of H4S1, respectively (Rank et al., 2010). Unlike the genome wide studies by ChIP-seq, it has been shown that PRMT5 mediated H4R3me2s recruit Polycomb proteins in a Groucho related protein (Grg) dependent manner leading to tri-methylation of H3K27 and subsequently gene silencing (Tae et al., 2011).

PRMT5 induced transcription repression has also been shown in execution with ATP-dependent chromatin remodelers. Affinity purification and ChIP assay showed that PRMT5 and its binding partner MEP50 form complex within NuRD (Nucleosome Remodeling and Deacetylation complex) (Le Guezennec et al., 2006). PRMT5-NuRD complex co-occupies promoters of target genes including CDKN2A (which encodes p14ARF and p16INK4a). Furthermore, enrichment of PRMT5-NuRD at the promoter of target genes depends on DNA methylation given that treatment with the DNMTs inhibitor 5-aza-2'-deoxycytidine (5-azadC) reduces their association with target promoters (Le Guezennec et al., 2006). Mechanistically PRMT5 reduces the interaction between MBD2 and histone deacetylase within NuRD complex by directly methylating MBD2 thereby lowering the association of NuRD complex with methylated promoter DNA and gene repression (Tan and Nakielny, 2006). PRMT5 forms a complex with other ATP-dependent chromatin remodelers: BRG1- or hBRM-based hSWI/SNF complexes, which is capable of mediating target gene repression by efficiently histone H3 and H4 symmetric arginine methylation (Pal et al., 2004). Notably SWI/SNF-PRMT5 complex induced transcriptional silencing is context dependent as well. For instance at the early stage of skeletal muscle differentiation, PRMT5 is required for myogenin expression by direct binding to the promoter and facilitate SWI/SNF complexes interaction and remodeling at myogenin locus (Dacwag et al., 2009). In multiple cell culture models for adipogenesis, the presence of PRMT5 and H3R8me2s promotes the binding of SWI/SNF complexes, which is required for the binding of PPARγ2 at PPARγ2-regulated promoters and activation of adipogenic genes (LeBlanc et al., 2012). However the transition between activation and repression of PRMT5 function is still unknown.

In addition, PRMT5 has been shown to be involved in RNA mediated gene silencing by methylating the small RNA-binding protein Piwi, which is exclusively

present in germ cells and interacts with a specific class of small non-coding RNAs called piwi-interacting RNAs (piRNAs). In mouse embryonic germ cells, members of the Piwi family repress transcription of transposable elements by inducing *de novo* methylation of their DNA sequences. Biochemical purification of Piwi interacting proteins led to the identification of several Tudor domain-containing proteins including PRMT5. Mutation of specific arginine residues within the N-terminal region of one Piwi protein MILI results in loss of interaction and co-localization with Tudor proteins, suggesting that PRMT5-induced methylation of Piwi proteins is critical for their recognition by the Tudor family of proteins and proper function of the piRNA pathway (Vagin et al., 2009).

1.6.3 PRMT5 methylates transcription factors

Emerging evidence has shown that PRMT5 methylates not only histones but also a host of transcriptional factors including E2F-1, p53, SPT5, p65 and homeobox A9 (HOXA9) in nucleus (Bandyopadhyay et al., 2012; Cho et al., 2012; Jansson et al., 2008; Kwak et al., 2003; Wei et al., 2013). PRMT5 directly methylates E2F-1 in tumor cell lines, through which stabilizes E2F1 protein, increases E2F1 DNA binding activity hence up-regulates E2F1 target gene transcription coordinating with decreased cell growth rate and apoptosis (Cho et al., 2012). PRMT5 has also been shown to interact with and methylate tumor suppressor p53, at R333, R335 and R337 upon DNA damage. Methylation of p53 by PRMT5 leads to inhibition of p53 oligomerization, impairment of recruitment to target genes and suppression of gene expression upon DNA damage (Jansson et al., 2008). Moreover, PRMT5 directly interferes gene expression by methylating the transcription elongation factor SPT5, leading to decreased interaction between SPT5 and elongating RNA polymerase II thereby silencing IκBα and IL-8 gene expression (Kwak et al., 2003). PRMT5 is the only arginine methyltransferase that methylates p65, a subunit of NF-κB, resulting in the enhanced binding of NF-κB to κB elements and gene repression (Wei et al., 2013). The homeobox transcription factor HOXA9 is essential for the induction of proinflammatory proteins in endothelial cells (EC) in response to stimuli and PRMT5 was shown to activate HOXA9 by dimethylating Arg140 within this protein (Bandyopadhyay et al., 2012)

1.6.4 PRMT5 methylates multiple targets in cytoplasm

PRMT5 mediated arginine methylation has been implicated in a variety of cytosolic processes as well, including biogenesis of Sm-class ribonucleoproteins, assembly of the Golgi apparatus and ribosome biogenesis. Sm proteins are components of the

spliceosomal U1, U2, U4 and U5 small nuclear ribonucleoproteins (snRNPs). In the cytoplasm, PRMT5 acts together with pICln and WDR77 as part of the methylosome, which mainly methylates Sm proteins (SmB/B', SmD1, and SmD3), increasing their affinity for the Tudor domain of spinal motor neuron 1 (SMN1) (Friesen et al., 2001; Meister and Fischer, 2002), facilitating their loading onto the Sm site of small nuclear RNA (snRNA) thereby giving rise to U-snRNPs. The absence of PRMT5 results in reduced methylation of Sm proteins and aberrant constitutive splicingThe aberrant splicing of specific mRNAs in neural stem cells of PRMT5 mutant (Bezzi et al., 2013) provides confirmation for the role of PRMT5 in RNA processing.

PRMT5 has been shown to form a complex with GM130, a Golgi matrix protein, and co-localizes with other Golgi markers in Golgi apparatus (Zhou et al., 2010) PRMT5 methylates GM130 at R6, R18 and R23, affecting ribbon formation of Golgi apparatus. Consistently knockdown of PRMT5 reduces GM130 methylation and increases fragmented Golgi apparatus (Zhou et al., 2010). PRMT5 has been shown to interact with and methylate ribosomal protein S10 (RPS10), a member of the ribosome 40S subunit (Gary and Clarke, 1998). Methylation of RPS10 appears to be critical for ribosome assembly, protein synthesis and cell proliferation. Mutations that affect methylated arginine residues result in an unstable protein that is inefficiently incorporated into ribosomes. Moreover, RPS10 knockdown cells grow slower than control cells, and re-expression of wild type, but not mutant RPS10 restores cell proliferation, highlighting the importance of PRMT5-induced methylation in ribosome biogenesis and growth control (Gary and Clarke, 1998).

Interestingly recent studies revealed that cellular localization of PRMT5 appears to be dependent on whether cells are non-transformed or transformed. While in most primary and immortalized cells, PRMT5 is primarily located in the cytosol with a small amount in the nucleus, in transformed cells PRMT5 is mainly enriched in nucleus (Pal et al., 2007). This suggests distinct function of PRMT5 in the control of cell growth and proliferation. For instance, cytoplasmic PRMT5 is capable of directly interacting with and monomethylating R1175 at epidermal growth factor receptor (EGFR), a transmembrane receptor whose activation in turn initiates downstream signaling events associating with cellular proliferation and tumorigenesis, in non-transformed cells (Hsu et al., 2011). Methylation of EGFR suppresses EGFR function by promoting phosphorylation of Tyr1173 and subsequently inhibits ERK signaling, suggesting a crosstalk between arginine methylation and tyrosine phosphorylation in regulating cell proliferation. Relocation of PRMT5 from the cytosol to the nucleus in transformed cells results in reduced EGFR methylation thereby potentiating ERK signaling and enhancing cell proliferation of cancer cells (Hsu et al., 2011). Notably

recent proteomic analysis of symmetric methylated protein revealed that many arginine sites in distinct proteins are modified indicating that PRMT5 is involved in a network regulating distinct cellular processes (Chang et al., 2013). A systematic analysis ofthe role of PRMT5 in the network will further improve our understanding of symmetric arginine methylation and biology of cancer and stem cell.

1.6.5 PRMT5 function in stem cells

The critical role for PRMT5 during embryonic development has been recently demonstrated by a study showing that *Prmt5*-null mice are early embryonic lethal between E3.5 to E6.5 (Tee et al., 2010). In addition, the failure to derive embryonic stem (ES) cells from *Prmt5*-null blastocysts together with down-regulation of pluripotency genes and up-regulation of differentiation genes in PRMT5 knockdown ES cells strongly indicated that PRMT5 is required for stem cell pluripotency. Furthermore PRMT5 promotes somatic cell reprogramming to the induced pluripotent stem (iPS) cells with classical Yamanaka factor protocol (OCT3/4, SOX2, KLF4, MYC) (Nagamatsu et al., 2011; Takahashi and Yamanaka, 2006). Mechanistically cytoplasmic PRMT5 forms a complex with signal transducer and activator of transcription (STAT3) and represses differentiated differentiation gene in ES cells thorugh the leukemia inhibitory factor (LIF) -STAT3 signaling pathway (Tee et al., 2010). PRMT5 not only plays an essential role in embryonic stem cells but also regulate proliferation of adult stem/progenitor cells during development. Recently, it has been demonstrated that PRMT5 controls neural stem/progenitor cells (NPCs) homeostasis (Bezzi et al., 2013). The conditional ablation of PRMT5 in the Nestin+ NPCs leads to the cell cycle block, triggers cell death and finally results in the postnatal death in mice. At the molecular level, the absence of PRMT5 results in reduced methylation of Sm proteins, aberrant constitutive splicing, and the alternative splicing of specific mRNAs with weak 5′ donor sites. Intriguingly, Mdm4 is identified as one of these key mRNAs that senses the defects in the spliceosomal machinery and transduces the signal to activate the p53 response. Consistently, ablation of p53 in NPCs rescues neural stem cell proliferation, providing a mechanistic explanation of the phenotype observed *in vivo* (Bezzi et al., 2013). Given that the proliferation of adult stem cells is following after activation in response to specific signals in their microenvironment, and is always accompanied with self-renewal that governs the stem cells re-entry into quiescence, suggesting that PRMT5 might regulate adult stem cell homeostasis differently.

PRMT5 has also been implicated in epigenetic regulation during mouse germ cell specification by directly interacting with the transcriptional repressor B-lymphocyte-

induced maturation protein (BLIMP1) (Ancelin et al., 2006). Translocation of the BLIMP1–PRMT5 complex from the nucleus to the cytoplasm during embryogenesis results in reduced methylation in H2AR3/H4R3 and de-repression of genes involved in germ cell specification. Moreover, BLIMP1 over-expression in embryonic P19 carcinoma cells results in repression of germ cell specification genes and increased methylation of histones H2AR3 and H4R3 (Ancelin et al., 2006; Eckert et al., 2008). The crucial role of PRMT5 in germ cell formation is further demonstrated by recent genetic studies in Drosophila. Loss of dart5 (also called Capsuleen), the fly ortholog of PRMT5, causes defects in spermatocyte maturation and infertility. While female dart5 mutants are fertile, their embryos fail to form the pole cells that give rise to germ cells in adults (Gonsalvez et al., 2006), supporting the important role of PRMT5 in germ cell formation. At the molecular level, Dart5 is required for the methylation of spliceosomal proteins in oocytes thereby controlling the localization of these proteins in the pole plasma, loss of which leads to impaired germ cell formation (Anne et al., 2007).

1.6.7 PRMT5 acts as an oncogene in cancer

Emerging evidence has shown that PRMT5 plays an important role in tumorigenesis and might be a potential therapeutic target for cancer treatment. Overexpression of PRMT5 has been shown in many patient-derived primary cancers such as liver, pancreas, skin, breast, cervix, prostate, kidney, ovary, bladder and lung, with strikingly elevated expression in colon cancer. Expression of PRMT5 is thus positively correlated with growth rate of cancer cells and inversely correlated with overall patient survival (Wei et al., 2013). Distinct mechanisms by which PRMT5 controls tumorigenesis have been revealed. PRMT5 might function as oncogene-like protein due to its ability to repress the expression of tumor suppressor genes, to control cell cycle progression, to alter epigenetic modifications of cancer cells and to deregulate oncogenic signaling pathways. Pal et al showed that in mouse embryonic fibroblast cell lines, PRMT5 acts as an oncogene by decreasing the expression of tumor suppressor genes like the suppressor of tumorigenicity 7 (ST7) and nonmetastatic 23 (NM23) (Pal et al., 2004). Along this line increased levels of PRMT5 and transcriptional silencing of ST7 are associated with more aggressive disease in patients with glioblastoma (Yan et al., 2014). Chung et al. showed that inhibition of PRMT5 in non-Hodgkin lymphoma cell lines reactivates the Retinoblastoma (Rb) tumor suppressor pathway and Polycomb Repressor Complex 2 (PRC2) silencing thereby inducing lymphoma cell death (Chung et al., 2013). In an orthotopic model of breast cancer, Powers et al showed that PRMT5 methylates

tumor suppressor programmed cell death 4 (PDCD4) at R110 thereby involving in breast cancer control (Powers et al., 2011). In human osteogenic sarcoma SAOS2 cells, PRMT5 ablation induces the expression of p53 resulting in p53-dependent apoptosis and cell cycle arrest in the G1 phase (Jansson et al., 2008). PRMT5 has also been shown to up-regulate cyclin-dependent kinases (CDKs) and the PI3K/AKT signaling cascade, both of which are the key players in cancer (Wei et al., 2012). In human patients with myeloproliferative neoplasms, the strong interaction between PRMT5 and constitutively activated form of JAK2 (JAK2-V617F) inhibits its methyltransferase activity and promotes myeloproliferation (Liu et al., 2011). In multiple endocrine neoplasia type 1 (MEN1) tumor PRMT5 interacts with menin and suppresses the Hedgehog signaling by dimethylating histone H4R3, which also strengthen the role ofPRMT5 as a therapeutic target in treating this tumor (Gurung et al., 2013). Moreover, PRMT5 has also been demonstrated to be an essential component of the hypoxia-inducible factor 1 (HIF-1) signaling pathway involved in attenuating the hypoxic induction of HIF-1α in human lung adenocarcinoma, fibrosarcoma, and mammary carcinoma cell lines (Lim et al., 2012) and of nuclear factor κB (NF-κB) pathway by dimethylating R30 of the p65 subunit in diverse human cancers (Wei et al., 2013).

2. OBJECTIVES

Multiply tissue specific adult stem cells originate from highly proliferative progenitor cells during development. For instance, skeletal muscle contains a rare, specialized subset of myofiber-associated adult stem cells called satellite cells, which are derived from a population of proliferative Pax7+/MyoD+ muscle precursors during early embryonic development. In resting muscle these cells are in quiescent state. Upon muscle injury or excessive exercise, satellite cells exit quiescence, activate, proliferate and differentiate eventually generating new myofibers. Understanding the molecular mechanisms underlying satellite cell homeostasis in adult and muscle progenitor proliferation during development is therefore essential for muscle development and regenerative medicine. Previous studies have shown that quiescent satellite cells maintain high content of compacted heterochromatin structure that distinguishes them from their precursors and progeny (differentiated myocytes). This indicates that distinct epigenetic determinants regulating satellite cell homeostasis during regenerative myogenesis from muscle precursors during developmental myogenesis. To identify and elucidate the epigenetic signatures that could distinguish the molecular requirements between these two biological processes, I have addressed following objectives:

(1) Identifying novel epigenetic modifications and modifiers that are specifically enriched in satellite cells
(2) Investigating if the epigenetic modification and modifiers are required for maintaining satellite cell homeostasis and muscle regeneration in both physiological and pathological conditions.
(3) Identifying molecular targets mediating for the effects of epigenetic modifies in control of satellite cell homeostasis.
(4) Addressing the potential role of novel epigenetic modifiers in myopathies and muscle diseases.

3 MATERIALS

3.1 Chemicals and Enzymes

Table 3.1: Specific reagents

Reagent	Manufacturer
Cardiotoxin (# C-9759)	Sigma-Aldrich Chemie GmbH, Steinheim
Collagen type 1 (# 354236)	BD Biosciences Pharmingen, San Diego, USA
Collagenase type 2 (# 4176)	Worthington Biochemical Corporation, Lakewood, United States
Collagenase P (# 11213857001)	Roche Diagnostics GmbH, Mannheim, Germany
cOmplete Protease Inhibitor Cocktail Tablets	Roche Diagnostics GmbH, Mannheim, Germany
Dispase (# 354235)	BD Biosciences Pharmingen, San Diego, USA
DMSO	Sigma-Aldrich Chemie GmbH, Steinheim
DNase I (# 11284932001)	Roche Diagnostics GmbH, Germany
Dithiothreitol (DTT)	AppliChem GmbH, Darmstadt
Ethidium bromide	Sigma-Aldrich Chemie GmbH, Steinheim
Eosin Y solution, aqueous	Sigma-Aldrich Chemie GmbH, Steinheim
Hematoxylin Gill	Sigma-Aldrich Chemie GmbH, Steinheim
Skimmed milk powder	Roth GmbH, Karlsruhe, Germany
Paraformaldehyde (PFA)	Fluka Chemie GmbH, Buchs
Percoll (# P4937)	Sigma-Aldrich Chemie GmbH, Steinheim
Ponceau S	Fluka Chemie GmbH, Buchs
Protein Standard (Novex ® Sharp Protein Standard)	Invitrogen GmbH, Karlsruhe
Rnase,Dnase-free(#11119915001)	Roche Diagnostics GmbH, Mannheim, Germany
Tissue-Tek ® O.C.T. PolyfreezeTM freezing	Miles Inc., Diagnostic Division, Elkhart, United States
TRIZOL ® reagent	Invitrogen GmbH, Karlsruhe
Matrigel	BD Biosciences, Greiner
Mowiol 4-88	Fluka Chemie GmbH, Buchs
Protein A Agarose	Roche Diagnostics GmbH, Germany
Protein G Agarose	Roche Diagnostics GmbH, Germany
Chelex®100 Resin	BioRad Laboratories GmbH, Munchen

3.2 Ready-reaction systems

Table 3.2: Used Kits

Kit	Manufacture
Click-iT EdU	Invitrogen GmbH, Karlsruhe
In Situ Cell Death Detection Kit, TMR red	Roche Diagnostics GmbH, Germany
DC ™ protein kit	BioRad Laboratories GmbH, Munchen
Masson's trichrome	Sigma-Aldrich Chemie GmbH, Steinheim
Absolute ™ SYBR ® Green Fluorescein Mix	Thermo Fisher Scientific, Rockford, USA
MinElute PCR Purification Kit	QIAGEN GmbH, Germany
Qubit® dsDNA HS Assay Kit	Invitrogen GmbH, Karlsruhe

3.3 Buffers and Solutions

All buffers and solutions were prepared with water that previously available via a Treatment system (MilliQ Plus Water System, Millipore GmbH, Schwalbach/Ts) to the quality grade "double-distilled".

Table 3.3.1: Standard buffers

Standard buffers	Composition
PBS	137 mM NaCl, 2.7 mM KCl, 10 mM Na_2HPO_4, 2 mM KH_2PO_4
PBST	PBS containing 0.1% Tween 20
SDS running buffer (10x)	250 mM Tris base, 1% SDS, 1.9 M Glycine
Semi-dry transfer buffer	25 mM Tris base, 192 mM Glycine, 20% Methanol
Whole cell extraction buffer	100mM Tris-HCl, pH 7.9, 1M $MgCl_2$, 1M KCl, 0.1M EDTA, protease inhibitor cocktail
Red blood cell lysis buffer	1.5M NH_4Cl, 100 mM $KHCO_3$, 10 mM EDTA,add 5 µg/ml Dnase I before use

Table 3.3.2: buffers for ChIP and ChIP-seq

ChIP buffers	Composition
Cell lysis buffer	5mM HEPES pH8, 85mM KCl, 0.5% NP-40, Protease inhibitors
Nuclear lysis buffer	50 mM Tris-HCl, pH 8.0, 10 mM EDTA, 1% SDS, protease inhibitors
ChIP dilution buffer	20 mM Tris-HCl, pH 8.0, 150 mM NaCl, 2 mM EDTA, 1% Triton X-100, complete protease inhibitor cocktail
High salt washing buffer	20 mM Tris-HCl, pH 8.0, 500 mM NaCl, 2 mM EDTA, 1% Triton X-100
LiCl washing buffer	10 mM Tris-HCl, pH 8.0, 250 mM LiCl, 1% Na-deoxycholate, 1% NP40
TE washing buffer	10 mM Tris-HCl pH 8.0, 1 mM EDTA
IP elution buffer	100mM NaHCO3, 1%SDS, freshly prepared

3.4 Culture media

Table 3.4: Culture media

Mediums	Composition
Growth medium for C2C12	DMEM (Dulbecco's Modified Eagle Medium) with 4.5 g / l glucose 10% fetal calf serum, 100 U / ml penicillin / streptomycin, 20 mM glutamine
Growth medium for FACS isolated satellite cells and Freshly isolated myofibers	GlutaMAX ™ DMEM with 4.5 g / l glucose 20% fetal calf serum, 100 U / ml penicillin / streptomycin 15 µg/µl Fibroblast growth supplement (FGS)
Differentiation medium	DMEM with 4.5 g / l glucose, 2% horse serum, 100 U / ml penicillin / streptomycin, 20 mM glutamine

3.5 Oligonucleotides

The oligonucleotides used in this work were from Sigma-Aldrich Chemie GmbH, Steinheim based.

Table 3.5.1: List of primers for genotyping.

Genotyping	Primers	Sequence(5'-->3')
Pax7 ^{CreERT2}	Forward	ACTAGGCTCCACTCTGTCCTTC
	Reverse	GCAGATGTAGGGACATTCCAGTG
ZsGreen	Forward	CTGCATGTACCACGAGTCCA
	Reverse	GTCAGCTGCCACTTCTGGTT
Rosa26-YFP	RosaFA	AAA GTC GCT CTG AGT TGT TAT
	RosaRF	GGA GCG GGA GAA ATG GAT ATG
	Rosa-SpliAC	CAT CAA GGA AAC CCT GGA CTA CTG
mdx	mdx_Forward	GCGCGAAACTCATCAAATATGCGTGTTAGT GT
	mdx WT Reverse	GATACGCTGCTTTAATGCCTTTAGTCACTCA GATAGTTGAAGCCATTTTG
	mdx MT Reverse	CGGCCTGTCACTCAGATAGTTGAAGCCATT TTA
p21	p21 exon 144	GAACTTTGACTTCGTCACGG
	p21 genoU	ACAACACCTCCTGGTCAGAGG
	p21 PGK neo3	GAAGAACGAGATCAGCAG
Pax7 ^{Cre}	ck188	GCTCTGGATACACCTGAGTCT
	ck256	TCGGCCTTCTTCTAGGTTCTGCTC
	ba97	GATCTGGACGAAGAGCATCA
	ck172	GGATAGTGAAACAGGGGCAA
Prmt5	P1	TGTAAATATTAAAGGCGCATAAC
	P2	CTATGGATCTACTTAGGGGCTTC
	P3	CCAGAACTTCCTCTGGTTTCTGG
	P4	GAAAGCTGTGTGTGCTCACAC
HSA ^{CreERT2}	Forward	GAGCCGAGAGTAGCAGTTGT
	Reverse	GGCAAACGGACAGAAGCATT

Table 3.5.2: List of primers for RT-qPCR and ChIP-qPCR.

Name	Primer sequence (5'-->3')	Annealing temperature (°C)	Application
Prmt5 Exon5-7	AGAATGCCCCGACTACACAC	**56**	RT-qPCR
	AGCCTCTGCTGCACCTTAGA		RT-qPCR
p21	CGGTGTCAGAGTCTAGGGGA	**56**	RT-qPCR
	ATTGGAGTCAGGCGCAGATC		RT-qPCR
Pax7	GCTACCAGTACAGCCAGTATG	56	RT-qPCR
	GTCACTAAGCATGGGTAGATG		RT-qPCR
MyoD	GAATGGCTACGACACCGCCTAC	60	RT-qPCR
	TAC		
	CCTACGGTGGTGCGCCCTCTGC		RT-qPCR
	TGGGCTGGGTGTTAGTCTTA		RT-qPCR
Myf5	CCACCTCCAACTGCTCTGAC	56	RT-qPCR
	GCTTCAGGGCTTCTTTTCCT		RT-qPCR
m36B4	AAGCGCGTCCTGGCATTGTCT	56	RT-qPCR
			RT-qPCR
cyclinB1	GGGTGTGCTTTGAATTCTGACA	56	RT-qPCR
	AGGAGTGGCGCCTTGGTAT		RT-qPCR
p53	TGCTGTGCAATTAAAGGCTGT	56	RT-qPCR
	CGTGTTCTCCGAGATACTTGGT		RT-qPCR
p21 Enhancer	CACAGGGAAGAGAGCTCCAG	56	ChIP
	AGCCAGGGCTACACAGAGAA		ChIP
p21 TSS	TCCACAGCGATATCCAGACA	56	ChIP
	GGACACACCTGTGACTCTGG		ChIP
p21 p53 BS	CAAGCCCTTCCCAGACTTCC	60	ChIP
	TCTAGAGATCGCTGCCCAGA		ChIP
p21 +700bp	CCTGTTTCGCGGTAGCCA	60	ChIP
	ACAATGAGTCACCTCCTCGC		ChIP
p53 promoter	TGCTGTGCAATTAAAGGCTGT	60	ChIP
	CGTGTTCTCCGAGATACTTGGT		ChIP

3.7 Plasmids

Table 3.7: Plasmids used

Name	Description	Source
psPAX2	Plasmid for expression of the packaging genes gag, pol, and rev for the production of lentiviruses.	Sigma-Aldrich GmbH, Steinheim
pMD2.G	A plasmid for expression of the viral Hüllpr oteine VSV-G for the preparation of lentiviruses.	Sigma-Aldrich GmbH, Steinheim

3.8 Antibodies

Table 3.8: List of antibodies used in this study, related to the experimental procedures

Antibody	Antigen	Application	Manufacturer
Anti-Pax7 mouse	Pax7	IF	DSHB
Anti-CD34 Rat	CD34	IF	eBioscience
Anti-MyoD rabbit	MyoD	IF	Santa Cruz
Anti-MyoD mouse	MyoD	IF	
Anti-Myogenin rabbit	Myogenin	IF	Santa Cruz
Anti-Myogenin mouse	Myogenin	IF	DSHB
MF20	Myosin heavy chain	IF	DSHB
Anti-Gapdh	Gapdh	WB	Cell signaling
Anti-PRMT5	PRMT5	WB,ChIP	Active Motif
Anti-p53	p53	WB,ChIP	Cell signaling
Anti-H3R8me2s	H3R8me2s	WB,ChIP	Novus
Anti-H4R3me2s	H4R3me2s	WB,ChIP	Abcam
Anti-Histone H3	Histone H3	WB,ChIP	Abcam
Rabbit IgG		ChIP	Diagenode
Mouse IgG		ChIP	Diagenode
Anti-CD11b PE-Cy7	CD11b	FACS	eBioscience
Anti-CD45 PE	CD45	FACS	eBioscience
Anti-CD31 PE	PECAM1	FACS	eBioscience
Anti-CXCR4 APC	CXCR4	FACS	eBioscience
Anti-CD34 A450	CD34	FACS	eBioscience

3.9 Cell lines

C2C12 **ATCC CRL-1772 ™**	A mouse myoblast cell line. These cells are capable of differentiation at a low serum concentration in culture. C2C12 cells were used to study the differentiation of myoblast *in vitro* **(Yaffe and Saxel, 1977)**
HEK293T **ATCC CRL-11268 ™**	A specific cell line originally derived from human embryonic kidney cells. These cells constitutively express the simian virus 40 (SV40) large T antigen. 293T cells are suitable for the production of virus particles **(DuBridge et al., 1987)**.

3.10 Mouse lines

***Pax7*^{Cre}**	A targeting vector was constructed that placed an ires-Cre-FRT-Neo-FRT cassette in the ClaI site within the 3'-untranslated region of the *Pax7* gene following the stop codon in exon 10. This targeting vector was electroporated into R1 ES cells that were then subjected to positive and negative selection. Mice that are heterozygous for the targeted mutation are viable, fertile, normal in size and do not display any gross physical or behavioral **(Keller et al., 2004)**.
***Pax7*$^{Cre/ERT2}$**	A targeting vector was used to insert loxP sites flanking exon 2. Exon 2 was excised via transient Cre mediated recombination to generate the Pax7tm1.1Fan allele. Exon 1 in the *Pax7*^{tm1}.1Fan allele was replaced with a targeting vector containing sequence encoding Cre-ERT2, IRES-DsRed and an FRT flanked PGK-neo cassette. Mice that are heterozygous for the targeted mutation are viable, fertile, normal in size and do not display any gross physical or behavioral abnormalities (Chen-Ming Fan, Carnegie Institution of Washington) (Lepper et al., 2009).
***Prmt5*$^{flox/flox}$**	The *Prmt5*$^{flox/flox}$ mice in the *Prmt5* gene locus encoding the Exon 7 flanked by two loxP sequences. When crossed with the strain expresses Cre recombinase from the targeted locus, Cre-mediated recombination results in tissue-specific deletion of the *Prmt5* sequence. (EUCOMM).
***Pax7*:ZsGreen**	A murine BAC containing the Pax7 locus was modified by replacing the Pax7 coding sequence from exon 1 with a sequence encoding ZsGreen, and transgenic mice were

	generated by pronuclear injection. These mice allow direct access to the satellite cell pool by flow cytometry, enabling the direct isolation of a homogeneous cell population for *in vitro* study (Bosnakovski et al., 2008).
ROSA26-EYFP	A generic ROSA26 targeting vector was constructed. Then the reporter mice generated was by inserting EYFP or ECFP cDNAs into the ROSA26 locus, preceded by a loxP-flanked stop sequence. he resulting EYFP or ECFP expression patterns indicated that the reporter strains function as faithful monitors of Cre activity. (Srinivas et al., 2001)
***p21* null mice**	A targeting vector was constructed containing a 8kb cdkn1a genomic sequence with a PGK-neo cassette, that eliminate a 3kb genomic fragment containing exon 2 of cdkn1a. Its replacement through homologous recombination created a null mutation (Deng et al., 1995).
***mdx* mice**	Duchenne muscular dystrophy (DMD), the Dmd^{mdx} mutants do not express dystrophin and therefore have been routinely used as an animal model of the disease even though the resultant myopathology is much less severe compared to the human disease course.(Jackson's Lab)

4 METHODS

4.1 Isolation of satellite cells and myofibers from adult keletal muscles

4.1.1 Satellite cell isolation and purification by FAC sorting

Satellite cell isolation and purification were performed according to established methods (Gunther et al., 2013). First, limb and trunk muscles were minced, digested with 100 caseinolytic units Dispase (BD) in 20ml DMEM supplemented with penicillin/streptomycin (DMEMps) in a 50ml Falcon tube at 37°C for 30 minutes, and then 20ug type II collagenase (Worthington Biochemicals) was added to the tube to make the final concentration as 0.1%. The tube was vortexed to mix the muscle and incubated in 37°C for additional 30 minutes. Afterward the digested muscle was passed through a 25ml syringe for several times to release the satellite cells from the myotubes, and then was filtered through 100 mm, 70 mm, and 40 mm cell strainers (BD). Cells were collected by centrifugation at 1,200 x g for 10 minutes. The pellets were resuspended in 1.5 ml Red blood cell lysis buffer with 5 µg/mL Dnase I and incubated on ice for 3 minutes. Later on cell suspension was filled up to 5 ml with FAC sorting buffer and then overlaid on the 30%/70% precoll gradient. The tube was centrifuged at 1,200 x g for 20 minutes with the acceleration and break off at 4 °C. After Percoll gradient centrifugation, mononuclear cells were subjected to FACS purification either using immunostaining with fluorescence coupled primary antibodies (CD11b-, CD45-, CD31-, CXCR4+ and CD34+) or GFP fluorescence of satellite cells from Pax7:ZsGreen mice and Pax7^{CE}/ROSA-YFP mice.

4.1.2 Isolation single myofibers from the Flexor Digitorum Brevis (FDB) muscles

The FDB muscles from the rear foot of adult mouse were isolated and digested with 0.2% collagenase II (Roche) in 2ml DMEM medium without serum at 37°C for 60 minutes. The digestion was stopped by transferring the muscles to 1 ml of the serum-containing medium (DMEM with 10% FCS and penicillin/streptomycin) in 15ml Falcon tube. Then the single myofbers were released by pipetting with a 1 ml Eppendorf pipette (tips were cut to a large diameter with blade). The isolated myofibers was washed with warm PBS twice and fixed with 4% PFA for further immunofluorescence staining. For culture, single fibers were washed 3 time with warm serum-containing medium and cultured in GlutaMAX ™ DMEM medium with

20% FCS and FGF (15 µg/µl) in suspension. Half of the medium was replaced with fresh culture medium every day. Fixed fibers were stained and the number of satellite cells was quantified per fiber.

4.2 Cell culture

4.2.1 C2C12 culture

Mouse C2C12 myoblasts (American Type Culture Collection, **(Yaffe and Saxel, 1977)** were maintained in DMEM supplemented with 10% FCS and 1% penicillin/streptomycin at 37°C and 5% CO_2 at a cell concentration between 1.5 X 10^5 and 1.0 X 10^6 viable cells/75 cm^2. The differentiation medium contained 2% horse serum instead of 10% FCS. The cells were passaged by trypsinization (0.5% trypsin in 0.5mM EDTA, Gibco BRL) from the culture plate at 70% confluence. For storage, cells were frozen in DMEM supplemented with 20% FCS and 5% (v/v) DMSO and kept in liquid nitrogen.

4.1.2 Culture of satellite cell

The plates and dishes were coated with matrigel before using. matrigel was gradually dissolved on ice and diluted 1:20 in ice cold culture media to coat 3.5-cm dishes. Covered the surface of dishes with 1ml matrigel solution, then immediately removed the matrigel. Each microliter matrigel solution was used to coat maximum 3 dishes. The dishes were placed in 37°C incubator for 1 hour and then in the hood with the lid open to air-dry for 1 hour. To coat 384-well mClear plates (BD Biosciences, Greiner) plates, the matrigel was diluted 1:50 in culture media. The surface of each 384 well-micro plate was covered with 40 µl of matrigel solution. Plates were placed at room temperature for 1 hour and then in 37°C incubator for at least 1 hour before the cells were seeded.

FACS-isolated satellite cells suspension was diluted with warm growth medium. 500 cells were seeded in each well of 384-well plate and 1.0 X 10^4 cells were seeded in one 3.5-cm dish. The medium was changed every day with fresh warm growth medium. For Cre recombinase mediated *in vitro* ablation of *Prmt5*, the cells were culture with 0.4 uM 4-OH-tamoxifen in the growth medium for at least 4 days.

4.3 *in vitro* EdU labeling assay

To determine the proliferating rate of satellite cells, a thymidine analogue, 5-ethynyl-2'-deoxyuridine (EdU) was used to label active DNA synthesis. Wild type and *PRMT5* knockout satellite cells were cultured on Matrigel-coated 384-well mClear plates (BD

Biosciences, Greiner). EdU (Invitrogen) was added to the culture 3 hours before fixation in a final concentration of 40 mM. Incorporated EdU is detected with a Click-iT® EdU Kit. Detection of EdU was done with Alexa Fluor 594 (Invitrogen) following standard protocols. Image acquisition and analysis were performed on Keyence BIOREVO BZ-9000 microscope.

4.4 TUNEL assay

In Situ Cell Death Detection Kit TMR red (Roche) is used to detect apoptotic cells based on the principle of TUNEL method. The hallmark of apoptosis is DNA cleavage, which may yield double-stranded and single-stranded DNA breaks (nicks). Both types of breaks were detected by labeling the free 3'-OH termini with TMR-dUTP, which was catalyzed by the enzyme terminal deoxynucleotidyl transferase (TdT). Briefly, the cells or the cryosetions were fixed by 4% PFA and permeabilized on ice with freshly prepared solution (0.1% triton x-100 in 0.1% sodium citrate) for 2 min. After washing with PBS, the samples were incubated with the TUNEL reaction solution which contains the Label solution and the Enzyme solution (9:1) at 37°C for 1 hour. DNase treated sample was used as a positive control. Image acquisition and analysis were performed on Keyence BIOREVO BZ-9000 microscope using the excitation wavelength in the range of 520-560nm and detection in the range of 570-620nm.

4.5 Senescence cell staining

The senescent cells were detected by the senescence cells histochemical staining kit(Sigma). The assay is based on a histochemical staining for β-galactosidase activity at pH 6. Under these conditions, β-galactosidase activity is easily detectable in senescent cells, but undetectable in quiescent, immortal, or tumor cells. The staining is following the standard protocol. The cells were fixed for 7 min at room temperature with fixing buffer which contains 2% formaldehyde, 0.2% glutaraldehyde, 7.04 mM Na_2HPO_4, 1.47 mM KH_2PO_4, 0.137 M NaCl, and 2.68 mM KCl. After washing with PBS for three times cells were incubated with stain mixture at 37°C without CO2 until the cells are stained blue (2 hours to overnight). The cells were observed under Keyence BIOREVO BZ-9000 microscope. Blue-stained cells and the total number of cells were counted. The percentage of cells expressing β-galactosidase (senescent cells) was calculated.

4.6 Freezing and sectioning of muscles and embryos

Tibialis anterior and soleus muscles were dissected and placed with one end in 10% gum tragacanth on a flat piece of cork. The muscle should extend above the level of the gum. The specimen are then inverted and submerged for 10 - 12 seconds in isopentane cooled by liquid nitrogen. Very quickly, working on dry ice, wrap the frozen muscle in aluminum foil, place the wrapped specimen in a biohazard bag, and place it immediately onto dry ice or in a -80°C freezer. Do not allow any opportunity for partial thawing. The dated embyos were embedded in OCT compound and frozen isopentane cooled by liquid nitrogen. Frozen sections (5-10 µm thick) were prepared. Tissues and embryos were sectioned at -20^{o}C using a cryostat (Leica, Germany). The cryosections were collected on Vectabond-coated glass slides, dried at room temperature and stored at -20^{o}C.

4.7 Immunofluorescence

4.7.1 Cells and myofibers staining

Satellite cells and myofibers were washed with PBS and fixed with 4% paraformaldehyde (PFA) in PBS for 10 minutes at room temperature. After washing twice with PBS, the cells and myofibers were permeabilized with PBS containing 0.3% Triton X-100 for 5 minutes at room temperature and followed with the other three-time washing with PBS. Then the cells and fibers were blocked with 5% horse serum (Invitrogen^{TM}) for 1 hour at room temperature and incubated with the primary antibodies overnight at 4^{o}C. The cells and fibers were washed three times with PBS with 0.01% Triton X-100 and incubated with the secondary antibody for 1 hour at room temperature in dark. After three times of washing with PBS with 0.01% Triton X-100, the cells were counterstained with 1 µg/ml DAPI for 2 minutes. The fibers were transferred to a glass slide suitable for microscopy. Remove any excess of PBS. Apply mounting medium and then add coverslip. Proceed to visualize myofibers under a Carl Zeis, Axiophot microscope. The stained cells were kept in PBS and analyzed by Keyence BIOREVO BZ-9000 microscope.

4.7.2 Cryosection staining

The sections were fixed with cold acetone for 15 minutes at 4 ^{o}C and then air dried at room temperature for 30 min. After fixation, sections were pretreated with blocking solution (5% bovine serum albumin, or mouse IgG blocking solution(M.O.M kit) for mouse IgG1 antibody) for 1 hour. The incubation of primary antibody and secondary antibody is following the protocol of cell staining. After counterstained with DAPI, the

sections were mounted with Mowiol medium and analyzed by fluorescence microscopy on a Carl Zeis, Axiophot microscope.

4.8 Haematoxylin-eosin staining (H&E)

H&E staining was performed followed the standard protocol (Fischer et al., 2008). Briefly frozen sections were fixed in cold acetone for 5 minutes in Coplin jar and completely dried at room temperature for 30 minutes. Afterward the sections were rinsed in distilled water and stained in haematoxylin solution (Merck, Germany) for 10 minutes. After 10 minutes under running tap water the access color was removed. Stained sections were additionally stained with Eosin 0.5% (diluted in distilled water) for 6 minutes. Sections were dehydrated through 96%, 100%,100% ethanol dilution steps. Afterward sections were cleared in xylol 2 times for 10 minutes. At the end sections were mounted with Entellan and coverslips.

4.9 Masson's trichrome staining

Trichrome stains are used primarily for distinguishing collagen from muscle tissue. The staining was performed using ACCUSTAIN® trichrome staining (Masson) kit. Briefly, the sections were mordant in preheated Bouin's Solution, at 56°C for 15 minutes and washed in running tap water for 25min to remove yellow color. Afterwards, the samples were stained in Working Weigert's Iron Hematoxylin Solution for 5 minutes and washed in running tap water for 5 minutes. Then the sections were placed successively in Biebrich Scarlet-Acid Fucshin for 5 minutes, in Working Phosphotungstic/Phosphomolybdic Acid Solution for 5 minutes, in Aniline Blue Solution for 5 minutes, and in 1% Acetic Acid for 2 minutes. Finally the slides were dehydrated through alcohol, cleared in xylene and mounted.

4.10 RNA extraction

Total RNA from satellite cells and muscles was isolated using the Trizol reagent (Invitrogen). All plastic- and glassware used was rinsed with water containing 0.05% DEPC and autoclaved before use to inactivate RNAses. The cell pellet was dissolved in 1ml Trizol and incubated at RT for 5 min. 200ul chloroform were added and the solution was mixed vigorously for 15 sec, incubated at RT for 2-3 min followed by a centrifugation step at 4°C and 12000 g for 20 min. The supernatant was transferred to a new tube and well mixed with 500 μl isopropanol. After incubation at RT for 5 - 10 min the solution was centrifuged at 4°C and 12000g for 10 min. The supernatant was discarded and the pellet was washed with 70% EtOH (prepared with RNAse-free water) followed by a centrifugation at 4°C at 10000 g for 5 min. The resulting pellet

was dried and dissolved in 20 µl RNAse free water. RNA concentration was measured using Nanodrop (Thermo).

4.11 RT-qPCR

1µg RNA was subjected to a reverse transcriptase reaction in the presence of 25 ng/ml random primers and 2.5 mM dA/C/G/TTP with 10 U/ml SSII reverse transcriptase and without enzyme in negative control reactions. The RNA in 10 µl RNAse-free water was mixed with the random primers to a final volume of 11 µl and incubated at 65°C for 5 min followed by 5 min on ice. After addition of 4 µl 5 x firststrand Buffer, 1 µl 0.1 M DDT, 0.5 µl RNAsin, 1ul dNTPs and 1 µl SSII reverse transcriptase (200 U/µl), the mixture was incubated for 55 min at 42°C and for 10 min at 70°C. 1 µl of the mixture were used in gene-specific PCR reactions. Quantitative PCR was performed using the iCycler^{TM} (Bio-Rad) and ABsolute^{Tm} QPCR SYBR® Green Fluorescein Mix (ABgene®, U.K.). For the reaction mix 7 µl of cDNA, 7.5 µl of SYBR green and 0.5uM of each primer per reaction were used. A list of the primers is supplied in Table 7. For each experiment the amounts of targets and endogenous constitutively expressed housekeeping gene (GAPDH or m36B4) was determined from the standard curve. The target values (starting quantities) were normalized to the endogenous reference: SQtarget/SQGAPDH or SQtarget/SQm36B4.

4.12 Westerns blotting

The cultured cells were harvested, washed with ice cold PBS and lysed in cell lysis buffer (20 mM Tris (pH 7.5), 400 mM NaCl, 1 mM EDTA, 1 mM EGTA, 1% Triton X-100, 2.5 mM Sodium pyrophosphate, 1 mM β-glycerophosphate, 1 mM Na3VO4, 1 µg/ml Leupeptin) for 10 min on ice, followed with the sonication. The concentration of the isolated proteins was determined using BCA Protein Assay Reagent (Pierce, Rockford, IL). Samples were mixed with 4 x SDS sample buffer and incubated at 95°C of 10 min. 10 µg whole cell lysate of each sample was loaded on a 10-15 % SDS gel, depending on the size of the interested protein. The gel was blotted onto nitrocellulose membrane (Millipore, Billerica, MA) and blocked with 5% milk/TBS-T 1hour at room temperature. The primary antibody was applied over night at 4°C. Blots were washed twice for 10 min with TBS-T and blots were incubated with the secondary antibody for 1 hr at room temperature. Blots were washed three times for 10 min with TBS-T. Protein expression was visualized using an enhanced chemiluminescence detection system (GE Healthcare, Little Chalfont, United Kingdom) and quantified using a ChemiDoc gel documentation system (Bio-Rad).

4.13 Chromatin immunoprecipitation (ChIP)

100,000 satellite cells were cross-linked with 1% formaldehyde for 10 min, and then were quenched by 0.125 M glycine. The cross-linked cells were washed with ice-cold PBS for three times and spun down at 1200 g. The cell pellets xwere snap-frozen in liquid nitrogen, and stored at -80°C before use.

The pellets were re-suspended in 150ul Nuclear Lysis Buffer with protease inhibitors and incubate for 10 min on ice. Sonication was carried out with Bioruptor(Diagenode), which was used at energy level high and pulses of 30 sec. The number of pulses depended on the cell type and the amount of chromatin in the sample. After sonication, 5 µl of the sheared chromatin was reverse cross-linked in 50ul 10% Chelex/H2O, then loaded on a 2% agarose gel to check the fragment sizes, which should be around 300bp.

DNA concentration in the sheared chromatin was determined with Nanodrop (Thermo) and samples were diluted to 50 µg/ml DNA and split into portions of 1 ml in 1.5 ml eppendorf tubes. The tubes were either subjected to immunoprecipitation or stored at -80°C until further use. Fragmented, precleared chromatin lysate was incubated overnight with indicated antibodies: Histone H3 (Abcam), H3R8me2s (Novus) and PRMT5 (Active Motif), Rabbit IgG(Diagenode). And then was mixed with pre-blocked protein A agarose beads for 2 hours. The beads were spin down and washed with Low Salt buffer, High Salt buffer, LiCl2 buffer and TE buffer. Finally, the reverse cross-linking was performed in 10% Chelex. The supernatant was used for real-time PCR. Primers used for ChIP-qPCR are listed in Table 7.

4.14 ChIP sequencing

The proliferating and 2-day differentiated C2C12 cells were cross-linked with 1% formaldehyde/PBS for 10 min, and then were quenched by 0.125 M glycine. The cross-linked cells were washed with ice-cold PBS for three times. Spin down and resuspend the cells in ice-cold Cell Lysis Buffer with protease inhibitor, and stay on ice for 10min. The cells were pelleted and snap-freezed in liquid nitrogen, and stored at -80°C before use.

The pellets were re-suspended in 150ul Nuclear Lysis Buffer with protease inhibitors and incubate for 10 min on ice. Sonication was carried out with Bioruptor (Diagenode), which was used at energy level high and pulses of 30 sec. The number of pulses depended on the cell type and the amount of chromatin in the sample. After sonication, 5 µl of the sheared chromatin was reverse cross-linked in 50ul 10%

Chelex/H2O, then loaded on a 2% agarose gel to check the fragment sizes, which should be around 300bp.

DNA concentration in the sheared chromatin was determined with Nanodrop (Thermo) and samples were diluted to 100 µg/ml DNA and split into portions of 1 ml in 1.5 ml Eppendorf tubes. The tubes were either subjected to immunoprecipitation or stored at -80°C until further use. Fragmented, precleared chromatin lysate was incubated overnight with indicated antibodies: Histone H3 (Abcam), H4K20me1 (Abcam), H4K20me2 (Abcam) and H4K20me3 (Abcam), then was mixed with pre-blocked protein A agarose beads for 2 hours. The beads were spun down and washed with Low Salt buffer, High Salt buffer, LiCl2 buffer and TE buffer. After last wash, remove the last traces of buffer. Elution was carried out in 500ul freshly prepared IP Elution Buffer (100mM NaHCO3, 1%SDS) for 30min in room temperature on a rotating wheel. Transfer the supernatant to a clean tube. Reverse the crosslinking by adding NaCl to final concentration of 0.3M and shaking at 65° for 6h, then with 20ug/ml RNase (DNase free) at 37° for 1h, followed with 0.01M EDTA, 0.04M Tris pH6.8 and Proteinase K, at 45° for 1h. Finally the ChIPed DNA was purified by the mini-elute PCR kits (Qiagen). Measure the DNA concentration using Qubit® Fluorometric Quantitation (Life Science). Sequencing was performed on an Illumina HiSeq 2000 following a standard protocol.

ChIP-seq reads were converted to fastq format and aligned to a precompiled mm9 reference index with BOWTIE (Langmead, 2010). Peaks calling was performed using MACS (Zhang et al., 2008) . All downstream analyses were done in R/BioConductor (http://www.bioconductor.org) which includes the multiple packages: GenomicRanges, GenomicFeatures and chipseq.

4.15 Transgenic mice

Pax7^{CreERT2}/*Prmt5*$^{fl/fl}$ mice (*Prmt5*^{sKO}) were obtained by breeding knock in *Pax7*^{CreERT2} mice with animals bearing floxed *Prmt5* alleles (EUCOMM). Genomic DNA was prepared from tail or muscle tissue and genotyping was performed by polymerase chain reaction (PCR), as previously described. Specific oligonucleotide sequences used as primers for PCR are listed in Table 6.

4.16 Tamoxifen injections

A single pulse of 2 mg Tamoxifen (Sigma, T5648) in Miglyol® 812 (Caesar & Loretz GmbH) was given to adult mice (7-9 weeks old). Inducible mice were preceded for muscle regeneration assay after one week of the Tamoxifen administration.

4.17 Muscle regeneration assay

Before the treatment of muscle injury mice were anaesthetized intraperitoneally with 2,2,2-tribromoethanol. The stock solution of 1 g/ml was made in isobutane. The working solution for injections contained 120 µl of the stock solution in 10 ml of sterile PBS buffer (12 mg/ml). To anaesthetize mice 25 µl of the working solution per 1 g of body weight was injected intraperitoneally using a 27-gauge needle. To introduce a muscle injury, 50 µl of 0.06 mg/ml cardiotoxin from Naja mossambica mossambica (Sigma, Germany) in 0.9% NaCl was injected into the tibialis anterior of adult mice using a 27-gauge needle and a 1 ml syringe. The needle was inserted deep into the muscle longitudinally towards the knee from the ankle. The anterior tibial muscles were analyzed 7 and 14 days after the injectio. Cardiotoxin (Sigma) was injected into tibialis anterior muscles in a volume of 50 µl.

4.18 Magnetic resonance imaging

All MRI experiments were performed on a 7.0T superconducting magnet (Bruker Biospin, Pharmascan, 70/16, 16 cm; Ettlingen, Germany) equipped with an actively shielded imaging gradient field of 300 mT/m. The frequency for the 1H isotope is 300.33MHz. A 60 mm inner diameter linear polarized 1H volume resonator was used for RF pulse transmission and signal reception (Bruker Biospin). Localizer images were acquired using a spin-echo sequence and corrections of slice angulation were performed, if necessary. RARE-(Rapid Acquisition with Relaxation Enhancement) sequences (TR=2500 ms, TE=36.7 ms slice thickness=1 mm) in axial and coronal orientation were used to determine exact positioning of the lower part of the mouse body. Afterwards a coronal MSME-(Multi-Slice-Multi-Echo) spin-echo-sequence with an echo time TE=8,6 ms, repetition time TR=453 ms, a field of view FOV=7x7 cm^2, matrix size MTX=512x256 and a slice thickness of 1 mm was recorded. For volumetric quantification of fat and muscle tissue we used a plugin developed at our institute for the image processing software ImageJ. A list of anatomically defined landmarks are set by the operator and used to derive tissue specific signal intensity thresholds and to define the region of interest for intensity sensitive region growing segmentation. The resulting tissue voxel volumes inside the region of interest is counted and returned as cubic millimeters for each tissue class. Mice were measured under volatile isoflurane (1.5 – 2.0 % in oxygen and air with a flow rate of 1.0 L/min) anesthesia; the body temperature was maintained 37°C by a thermostatically regulated water flow system during the entire imaging protocol.

4.19 Calcium phosphate transfection

The production of the self-inactivating lentiviral particles was performed in HEK293T cells with standard protocol (The RNAi Consortium (TRC) Broad InstituteThe RNAi Consortium). shRNA-encoding vector (Table 7.) with psPAX2 the plasmid for the packaging genes (gag, pol, and rev), encoding and pMD2.G were co-transfected in HEK293T cells. A day before transfection, 7×10^5 of HEK293T cells were plated per well of a 6-well plate plated. For transfection, 1 µg of shRNA lentiviral control vector (pLKO.1) and 0.9 µg and 0.1 µg of the packaging virus pPAX2 or pMD2.G with MilliQ H_2O were mixed in a total volume of 450 µl. After addition of 50 µl of 2M $CaCl_2$ and 500 HBS buffer, the mixture was added dropwise to the medium where the cells are. The transfection culture plates were gently agitated and incubated at 37 ^oC. Transfected cells were incubated for 18 hours. Media was changed to remove the transfection reagent and replaced by high serum growth media. Afterward cells were sequentially incubated for 24 hours before harvesting the viral-containing media at 24-48 hours post infection. All subsequent steps were according to the Gene Technology Act Made (GenTG) under the security measures of the security level S2

4.20 Lentivirus infection of C2C12 cells

Lentivirus infection was performed with minor modification from standard protocol (The RNAi Consortium (TRC) Broad Institute, The RNAi Consortium). FACS sorted SCs were cultured individually in 30% FCS GlutaMAX™ media supplemented with PenStrep on matrigel-coated 96 well µClear plates (BD Biosciences, Greiner) as described previously (Ustanina et al., 2007). After one day of culturing, cells were infected with the lentivirus-containing media with 2µg/µl polybrene. Medium was removed and replaced by 30% FCS GlutaMAX™. 75-85% infection efficiency was observed by YFP expression at 3 days after infection.

4.21 Immunprecipitaion

C2C12 cells were washed with ice-cold PBS, resuspended in hypotonic buffer containing 0.1% Triton X-100. After incubation on ice for 7 minutes, nuclei were centrifuged at 1,500 x g for 5 minutes, 4 ^oC. Nuclei were lysed in IP buffer (20 mM Tris-HCl, pH 8.0, 400 mM NaCl, 1 mM EDTA, 1 mM EGTA, 1% Triton X-100, complete protease inhibitor cocktail) at 4 ^oC for 10 minutes. The lysate was sonicated with bioruptor for 15 min and cleared by centrifugation at 16,000 x g for 10 min, 4 ^oC. Nuclear extracts were pre-cleared by incubation with protein A/G Sepharose (Amersham) at 4 ^oC for 1 hour. After pre clearing, the lysates were incubated with HA beads for 4 hour at 4 ^oC. After successive washing with wash buffer (20 mM Tris-HCl,

pH 8.0, 200 mM NaCl, 1 mM EDTA, 1 mM EGTA, 1% Triton X-100), bound proteins were eluted from beads in 1 x SDS loading buffer and analyzed on western blots.

4.22 Stable isotope labeling by amino acids in cell culture

C2C12 cells that are ectopically expressing PR-Set7-HA were grown in heavy medium (Arg8, Lys10), while C2C12 cells with empty vector were labeled with nature arginine and lysine (light, Arg0, Lys0). The cells were cultured for at least six passages in heavy and light media to metabolically incorporate heavy amino acids into synthesised proteins. Growth media were replaced with fresh media every three days over a period of a week. Affinity purification of the HA-tagged PR-Set7 was then performed separately following the protocol described above and immunoprecipitates were mixed from both cell lysates within proliferating and differentiating conditions and resolved on a 4–20% SDS–PAGE (NuPAGE, Life Technologies). The gel was stained with Coomassie blue, cut into 15 slices and processed for mass spectrometric analysis using standard in gel procedure. Briefly, In-gel digests (components from Sigma) were performed with the protease LysC (Wako Chemicals GmbH, Neuss, Germany), and peptides were loaded onto STAGE-tips for subsequent MS analysis after extraction. The mass spectrometry and data analysis were performed as described before (Looso et al., 2010).

5 RESULTS

5.1 PRMT5 expression in adult muscle stem cells and during embryonic development

PRMT5, histone symmetric arginine dimethytransferase catalyzing histone H3R8 and H4R3 methylation, has previously been shown to be required for maintaining pluripotency of embryonic stem cells and controlling proliferation of neuronal progenitor cells (Bezzi et al., 2013; Eckert et al., 2008; Tee et al., 2010). To investigate the role of PRMT5 in developmental myogenesis and/or regenerative myogenesis, I firstly monitored PRMT5 expression in quiescent muscle stem cells and differentiated myocytes by performing immunofluorescence assay using freshly isolated myofibers. PRMT5 is highly enriched in Pax7 expressing quiescent satellite cells but not in differentiated myonuclei, suggesting that PRMT5 may be required for satellite cell function (Figure 5.1A). Furthermore activation and differentiation of quiescent satellite cells purified by FACS sorting from Pax7-ZsGreen reporter mice (refxx) correlates with reduction of PRMT5 expression together with down-regulation of Pax7 expression and up-regulation of Myogenin expression, a molecular marker for early myogenic differentiation (Figure 5.1B).

Given that adult satellite cells originate from a population of highly proliferative Pax7+/MyoD+ muscle progenitors during embryonic and fetal muscle development, I then analyzed the expression profile of PRMT5 during embryonic development. A transgenic mouse line carrying one allele of *Prmt5*$^{tm2a(EUCOMM)Wtsi}$ (*Prmt5*$^{tm2a/+}$), which contains an IRES:LacZ tracing cassette and a FRT promoter-driven neo cassette inserted into the sixth intron of *Prmt5*, allowed me to detect expression of PRMT5 during embryonic development *in vivo*. The *Prmt5*$^{tm2a/+}$ mice were crossed with C57Bl/6j wild type mouse and staged embryos were dissected for whole mount lacZ staining. While wild type littermates did not show LacZ staining, mice with transgenic allele of LacZ within *Prmt5* loci showed strong expression of E9.5 embryos with decreased staining in the E11.5 especially in the somites, suggesting that down-regulation of PRMT5 in late stages of developmental myogenesis. I concluded that PRMT5 is highly enriched in quiescent satellite cells in adult skeletal muscle and the expression is reduced during embryonic myogenesis and upon differentiation *in vitro*.

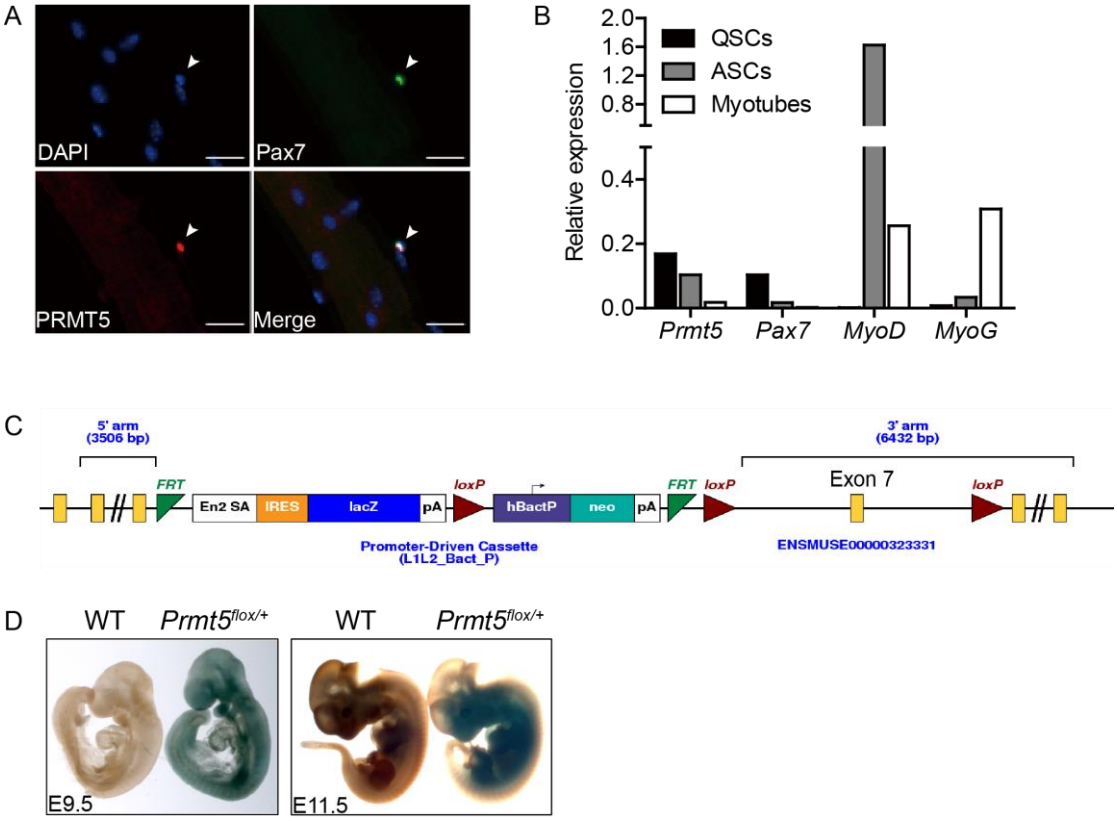

Figure 5.1 PRMT5 is highly enriched in satellite cells

(A) Immunofluorescence assay showing PRMT5 (red) is highly expressed in Pax7+ satellite cells (green) from freshly isolated FDB myofibers. Scale bar indicates 20 μm.

(B) RT-qPCR analysis of Prmt5, Pax7, MyoD and MyoG expression in quiescent satellite cells (QSCs), activating satellite cells (ASCs) and differentiated myotubes. Expression levels of distinct mRNAs are normalized to mRNA of GAPDH.

(C) Schematic of Prmt5 knockout first allele (*Prmt5*^{tm}) from EUCOMM. The 'knockout-first' allele (tm2a) contains an IRES:*lacZ* trapping cassette and a human beta-actin promoter--driven *neo* cassette between two FRT sites, inserted into the sixth intron of Prmt5 . The exon seven is flanked by loxP site.

(D) Whole mount LacZ staining showing *Prmt5* expression at embryonic day 9.5 (E9.5) and day 11.5 (E11.5) in wild type and *Prmt5*$^{fl/+}$ embryos.

5.2 PRMT5 controls satellite cell homeostasis and muscle regeneration

To address the physiological function of PRMT5 in adult satellite cells, I adopted an inducible knockout system due to the early embryonic lethality upon PRMT5 ablation (Tee et al., 2010). The *Prmt5*$^{tm2a/+}$ mouse was firstly crossed with a FLP recombinase mouse line leading to deletion of FRT cassette. The resulting *Prmt5*$^{fl/+}$ mice were interbred to generate homozygous *Prmt5*$^{fl/fl}$ mice, which were further crossed with tamoxifen (TAM) inducible *Pax7*^{CreERT2}(*Pax7*^{CE}) mice (Lepper et al., 2009). The resulting *Pax7*^{CE}/*Prmt5*$^{fl/fl}$ mouse strain (hereafter referred to as PRMT5 satellite cell

specific knockout mouse, *Prmt5*^{sKO}) allows inducible inactivation of PRMT5 by intraperitoneal administration of TAM and enabled us to specifically probe the role of PRMT5 in satellite cells in adult mice (Figure 5.2.1A).

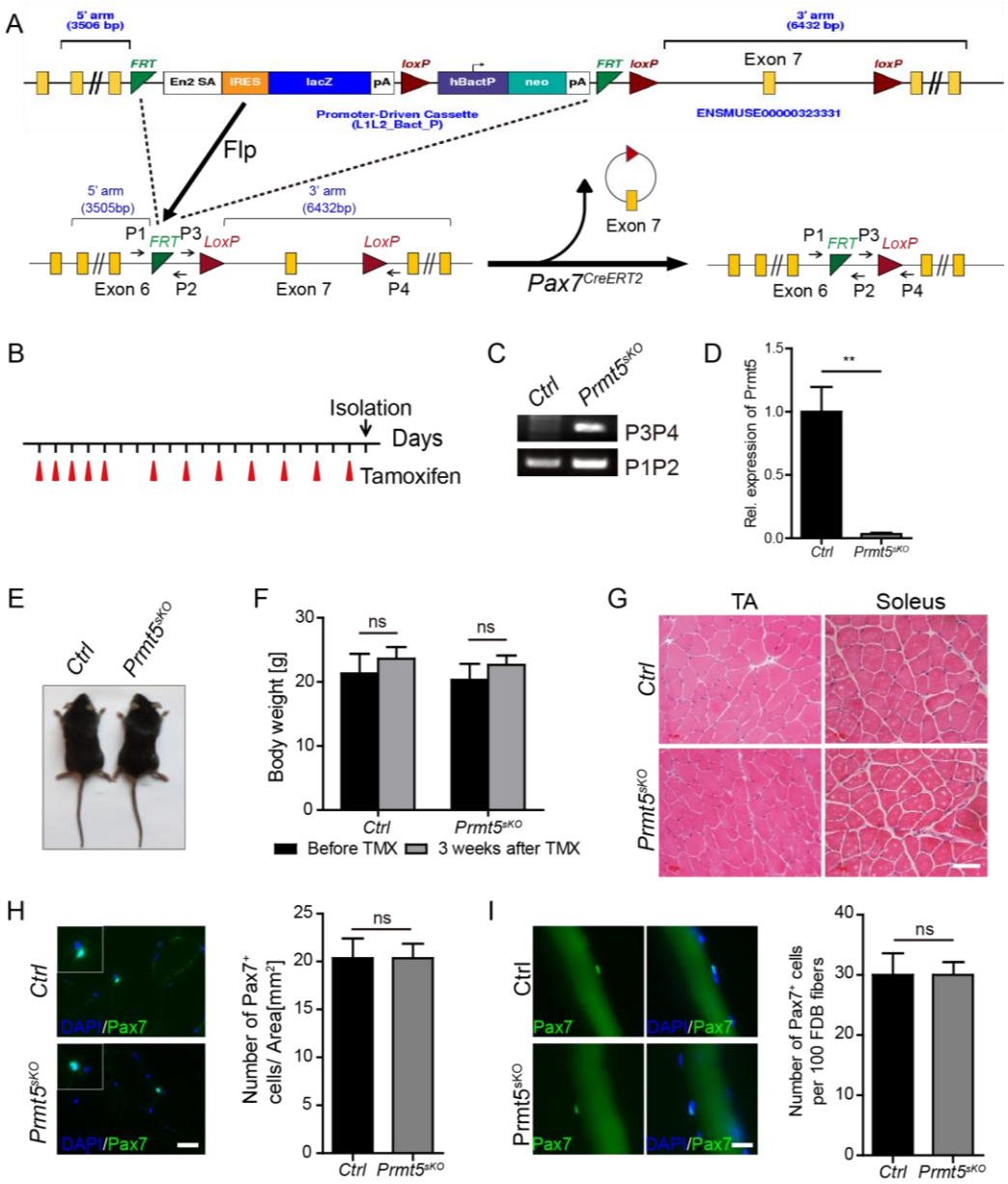

Figure 5.2.1 PRMT5 is dispensable for short-term satellite cell maintenance and muscle integrity

(A) Schematic outline of generation of *Prmt5* flox line. The 'knockout-first' allele are converted by FLP-mediated recombination *in vivo* to a conditional allele, which is referred to as *Prmt5*^{fl}. *Pac7*^{CreERT2} deletes the floxed exon 7 of the *Prmt5*^{fl} allele to generate a frameshift mutation upon tamoxifen induction. Red arrow head indicates loxP site. P1/P2 primer pair covers upstream and downstream of FRT site, whereas P3/P4 primer pair locates outside of two loxP sites and could be used to monitor Cre mediated recombination.

5.2.1 PRMT5 is dispensable for short-term maintenance of muscle homeostasis.

2-month old *Prmt5*^{sKO}/Pax7-ZsGreen (n=3) and *Pax7*^{CE}/*Prmt5*$^{fl/+}$/Pax7-ZsGreen (referred to as Control or Ctrl later) littermates (n=3) were treated with 3mg Tamoxifen per 40g body weight for 5 consecutive days followed by 10 additional injections every other day (Gunther et al., 2013) (Figure 5.2.1B). Recombination of the *Prmt5* locus was efficient as assessed by PCR genotyping (Figure 5.2.1C) and RT-PCR (Figure 5.2.1D) using the FACS purified satellite cells from each group of mice. Interestingly, TAM treated *Prmt5*^{sKO} mice remained viable and displayed no obvious short-term phenotypes under physiological conditions 21 days after treatment (Figure 5.2.1D). No significant change of bodyweight and no morphological alterations of skeletal muscle tissue were observed (Figure 5.2.1F&G). Cryosectioned tibialis anterior (TA) muscle and freshly isolated flexor digitorum brevis (FDB) myofibers of control and *Prmt5*^{sKO} littermates showed no difference in satellite cell numbers, suggesting that PRMT5 is not required for short-term maintenance of muscle homeostasis under normal physiological conditions (Figure 5.2.1H&I).

5.2.2 PRMT5 is required for muscle regeneration and long-term maintenance of satellite cells pool.

Satellite cells are responsible for muscle integrity and repair after chronic and acute

---

(B) Schematic of experimental procedure through which *Prmt5* exon 7 could be deleted upon tamoxifen administration for 3 weeks.

(C) Representative genomic PCR analysis using primer pair P3/P4 from FACS sorted satellite cells showing *Pax7*^{CE} mediated deletion of exon 7 in *Prmt5*^{sKO} mice (n=3) after tamoxifen administration. P1/P2 PCR is used as an internal control.

(D) Semi-quantitative RT-PCR analysis showing a dramatic reduction of *Prmt5* mRNA in FACS-sorted satellite cells from *Prmt5*^{sKO} mice (n=3) as compared with control littermates (n=3). m36B4 mRNA is used as an internal control.

(E) Representative image of control and *Prmt5*^{sKO} mouse 3 weeks after tamoxifen administration.

(F) Bodyweight of control and *Prmt5*^{sKO} mice (n=3) upon tamoxifen administration. The error bars represent standard deviations of the mean (t-test: p >0.1).

(G) Hematoxylin&Eosin (H&E) staining of TA and Soleus muscle after tamoxifen treatment in control and Prmt5^{sKO} mice (n=3). Scale bar indicates 50 µm.

(H) &(I) Immunofluorescence assay of Pax7^{+} cells in TA cryo-sections (H) or in freshly isolated FDB myofibers (I) showing no difference of satellite cell numbers between control and Prmt5^{sKO} mice *in vivo* 3 weeks after tamoxifen treatment. The number of Pax7^{+} per 10mm^{2} section area (H) or 100 myofibers (I) is counted. Error bars represent standard deviations of the mean (t-test: p>0.5, n=3).

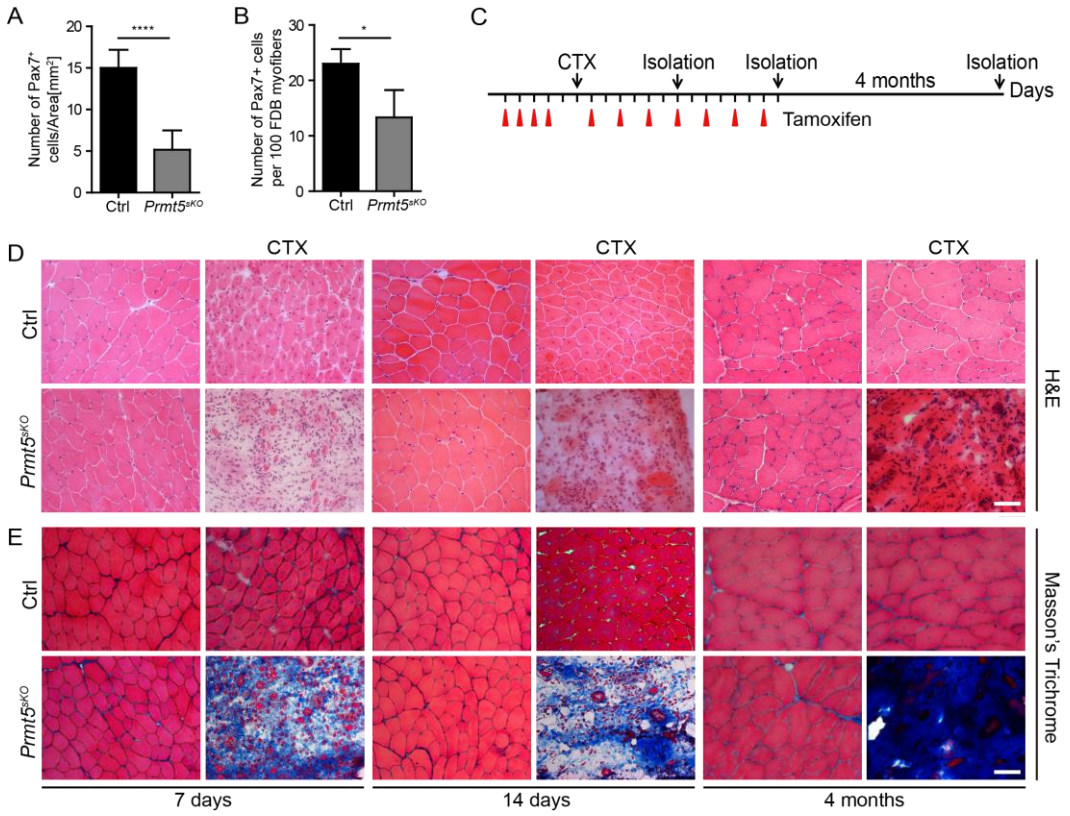

Figure 5.2.2 PRMT5 is required for long-term maintenance of satellite cell pool and muscle regeneration upon acute muscle injury in vivo

(A) &(B) Immunofluorescence assay of Pax7+ cells in cryo-sections from TA muscle (A) or in freshly isolated FDB myofibers (B) revealing a reduced number of satellite cells from *Prmt5*^{sKO} mice compared with control littermates 4 months after tamoxifen administration. The number of Pax7^{+} per 10mm^{2} section area (A) or per 100 fibers (B) is counted. Error bars represent standard deviations of the mean (t-test: ****$p < 0.0001$; *$p < 0.05$; n=4).

(C) Schematic of short and long term muscle regeneration assay upon acute muscle injury in control and *Prmt5*^{sKO} littermates (n=3) upon tamoxifen administration for 3 weeks. TA muscle injury was induced by cardiotoxin (CTX) injection 5 days after initial tamoxifen injection and muscle regeneration was analyzed at different time points as indicated.

(D) &(E) H&E staining (D) and Trichrome staining (E) of TA muscle showing impaired muscle regeneration and fibrosis of injured muscle in *Prmt5*^{sKO} mice as compared to control littermates (n=3) after CTX injection at 7 days, 14 days and 4 months. Scale bar indicates 50 µm.

muscle injury (Gunther et al., 2013; Sacco et al., 2010). Therefore I first investigated whether PRMT5 deficient satellite cells still contribute to muscle regeneration upon acute muscle injury *in vivo*. To this end, TAM treated *Prmt5*^{sKO} and control littermates were subjected to muscle injury via CTX injection into the TA muscle (Figure 5.2.2A). In control animals I noted a robust regenerative response resulting in the formation of regenerated muscle fibers with centrally located nuclei 7 days, 14 days and 4 months after injury (Figure 5.2.2B). Strikingly, muscle regeneration was completely abolished at all of the indicated time-points in conditionally ablated *Prmt5*^{sKO} mice. Hardly any

intact muscle fibers could be detected via H&E staining (Figure 5.2.2B), which went along with a massive increase of fibrotic tissue as visualized via Masson's Trichrome staining (Figure 5.2.2C). To address the role of PRMT5 in long-term maintenance of satellite cell pool, I performed immunofluorescence assay to monitor Pax7 positive satellite cells on the cryosections of TA muscles 4 months after tamoxifen administration. Significant reduction of satellite cell numbers from *Prmt5*^{sKO} mice was revealed as compared to control mice (Figure 5.2.2D). Moreover, the numbers of satellite cells on the freshly isolated FDB myofibers were also reduced upon PRMT5 knockout (Figure 5.2.2E). Taken together, these findings demonstrated that PRMT5 is not required for short-term maintenance of the satellite cell pool but is essential for long-term satellite cell maintenance and muscle regeneration upon acute muscle injury *in vivo*.

5.3 Loss of PRMT5 in a muscle regenerative environment results in decreased muscle mass and depletion of muscle stem cell pool

The failure of maintaining SC pool after long-term treatment together with the loss of muscle regenerative potential upon acute muscle injury in PRMT5 mutant mice *in vivo* support the idea that PRMT5 is required for satellite cell expansion and/or replenishment of the muscle stem cell niche in adult mice. To further prove this, I generated satellite cell specific PRMT5 knockout mice in a constant regenerative or activated environment by crossing *Prmt5*^{sKO} with *Dmd*^{mdx} mice and analyzed muscle integrity and satellite cells within double knockout mice after long-term treatment with tamoxifen. Mdx mice are commonly used animal model for Duchenne muscular dystrophy characterized by a constant muscle degeneration/regeneration cycles, and constitutive activation and turnover of satellite cells. Importantly, despite constant muscle degeneration this histological phenotype is macroscopically characterized by a pronounced muscle hypertrophy in adult mdx mice (Pastoret and Sebille, 1993). The *Prmt5*^{sKO}/mdx and control mice were treated with TAM for 3 weeks starting at the age of 8 weeks and monitored for bodyweight every week until they were sacrificed (Figure 5.3A). While PRMT5 deficient mice and mdx mice progressively gained weight, *Prmt5*^{sKO}/mdx mice failed to increase the bodyweight any more after TAM treatment (Figure 5.3B) and were smaller in size (Figure 5.3C). Consistently, MRI measurements revealed a massive decrease in muscle volume of *Prmt5*^{sKO}/mdx

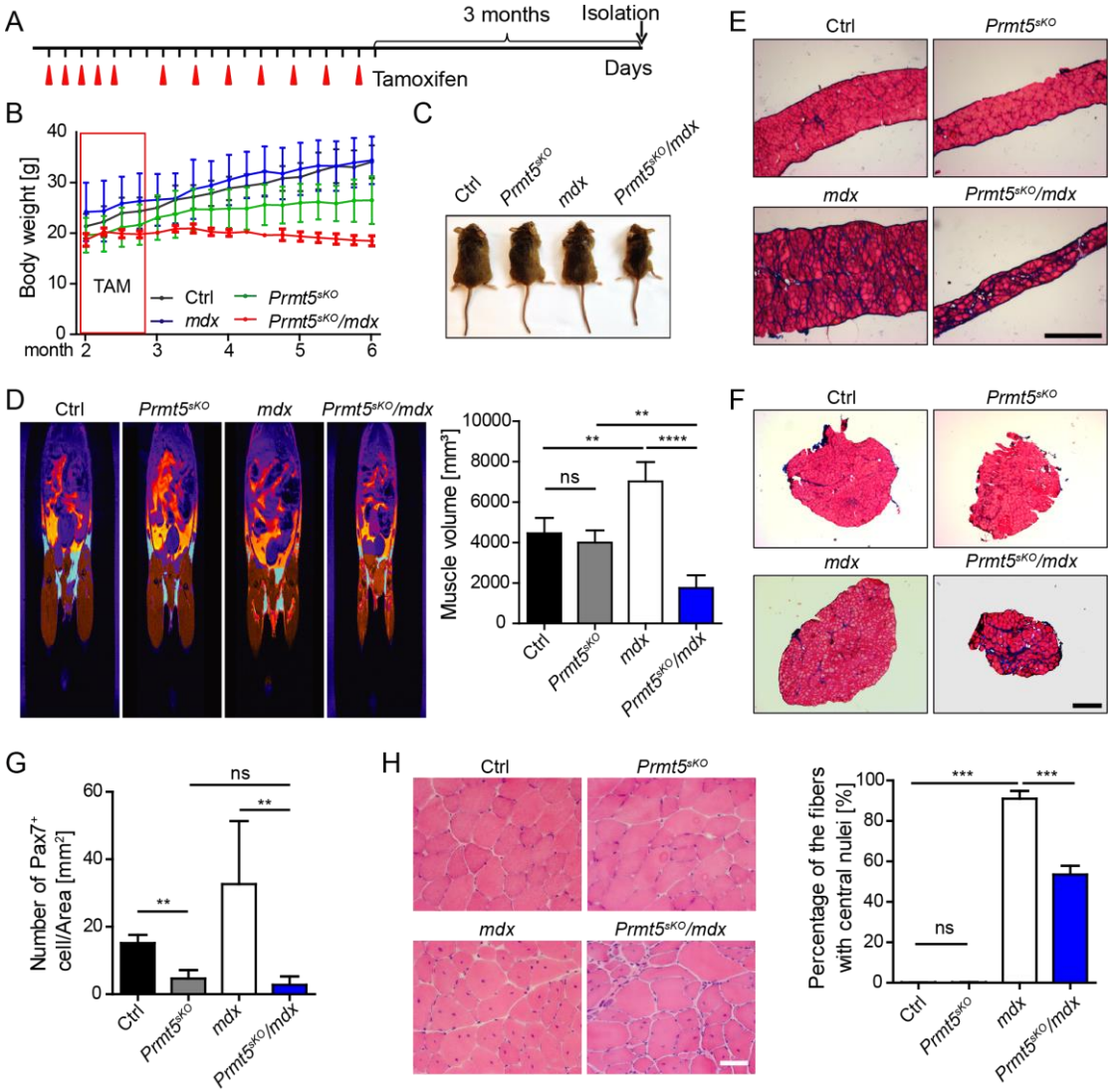

Figure 5.3 Loss of PRMT5 during chronic muscle injury results in decreased muscle mass and depletion of muscle stem cell pool

(A) Schematic of the experimental procedure showing control, *Prmt5*^{sKO}, mdx and *Prmt5*^{sKO}/mdx littermates for 3 weeks tamoxifen administration followed by additional 4 months maintenance.

(B) Bodyweight measurement of the indicated mice for 4 months showing Prmt5^{sKO}/mdx mice stop gaining body weigh after tamoxifen administration.

(C) *Prmt5*^{sKO}/mdx mice showing smaller body size as compared with control, mdx and *Prmt5*^{sKO} mice 4 months after tamoxifen administration.

(D) MRI measurements of muscle mass of control, *Prmt5*^{sKO}, mdx and *Prmt5*^{sKO}/mdx littermates 4 months after tamoxifen administration. Quantification of muscle volume is shown on the right. Error bars represent standard deviations of the mean (t-test: ****p<0.0001, **p < 0.01, ns P>0.05).

(E) &(F) Masson's trichrome staining showing *Prmt5*^{sKO}/mdx mice have thinner diaphragm muscle (E) and more fibrosis in the soleus muscle (F) as compared with control, mdx and Prmt5^{sKO} mice 4 months after tamoxifen administration. Scale bar indicates 400 µm.

(G) Immunofluorescence assay of Pax7+ cells in TA cryo-sections of indicated mice revealing a reduction of satellite cells in the muscle from *Prmt5*^{sKO}/mdx mice as compared with both control and mdx littermates. The number of Pax7^{+} cells per 10mm^{2} section area is counted. Error bars represent standard deviations of the mean (t-test: **p < 0.01, ns P>0.05, n=3).

(H) H&E staining of TA muscle showing more hypertrophic myofibers without central nuclei in the *Prmt5*^{sKO}/mdx mice as compared to mdx mice. Quantification is shown on the right. Error bars represent standard deviations of the mean (t-test: ***p<0.001, ns P>0.05, n=3)

(Figure 5.3D) but not in PRMT5 single knockout mice and mdx mice, demonstrating that PRMT5 is required for long-term maintenance of muscle mass during the chronic muscle injury. These mice were sacrificed at the age of 6 months shortly before the *Prmt5*^{sKO}/mdx mice died. Masson's trichrome staining revealed a strong increase of fibrosis in the soleus muscle compared to *Prmt5*^{sKO} and mdx mice (Figure 5.3F). Notably diaphragm muscles from double mutant mice 3 months after TAM administration underwent dramatic pathological changes, suggesting that respiratory failure might be the main cause of premature death of double mutant mice (Figure 5.3E). Accordingly, both *Prmt5*^{sKO} and *Prmt5*^{sKO}/mdx displayed a decreased number of Pax7 positive satellite cells (Figure 5.3G) compared to controls clearly supporting the idea that satellite cells require PRMT5 to replenish the muscle stem cell pool and to maintain muscle mass during regeneration.

5.4 PRMT5 controls satellite cell proliferation, differentiation and survival

Regeneration of skeletal muscle depends mainly on adult satellite cells. Upon muscle injure, quiescent SCs are activated, enter the cell cycle, and give rise to a population of muscle precursors that proliferate (Pax7+MyoD+), differentiate (Pax7-MyoG+) and then fuse to form new fibers allowing muscle architecture restoration. In parallel, a subset of SC is able to return to its quiescent state, thereby replenishing the initial pool and allowing repeated repair of the tissue (Figure 5.4.1A) (Buckingham and Rigby, 2014; Rudnicki et al., 2008; Zammit et al., 2006). To address PRMT5 mediated cellular mechanisms responsible for satellite cell reduction and impaired muscle regeneration in *Prmt5*^{sKO} mice, I dissected the function of PRMT5 in satellite cell activation, proliferation and differentiation.

5.4.1 PRMT5 is required for the proliferation of satellite cells

To examine whether PRMT5 is required for satellite cell proliferation, satellite cells were sorted from TAM treated control and *Prmt5*^{sKO} mice, cultured *in vitro* for three days and pulse-chased with EdU for three hours before analysis. PRMT5 deficient SCs showed a dramatic reduction of the number of EdU-incorporating proliferating cells, indicating abrogation of satellite cell self-renewal (Figure 5.4.1B). Furthermore *ex vivo* myofiber culture of TAM treated *Prmt5*^{sKO} and control littermates showed myogenic colonies of self-renewing Pax7 positive satellite cells in control SCs (28±3) while Pax7 expression was still apparent but almost no colonies were formed in myofibers from *Prmt5*^{sKO} mice (1= ±1) (Figure 5.4.1D) demonstrating that PRMT5

deficient SCs failed to proliferate and re-enter the cell cycle. In addition, gain of function assays demonstrated that overexpression of PRMT5 in wild type satellite cells *in vitro* increased EdU-incorporated satellite cells compared to control cells (Figure 5.4.1C). In aggregate these data indicated that PRMT5 is indispensable for satellite cell proliferation.

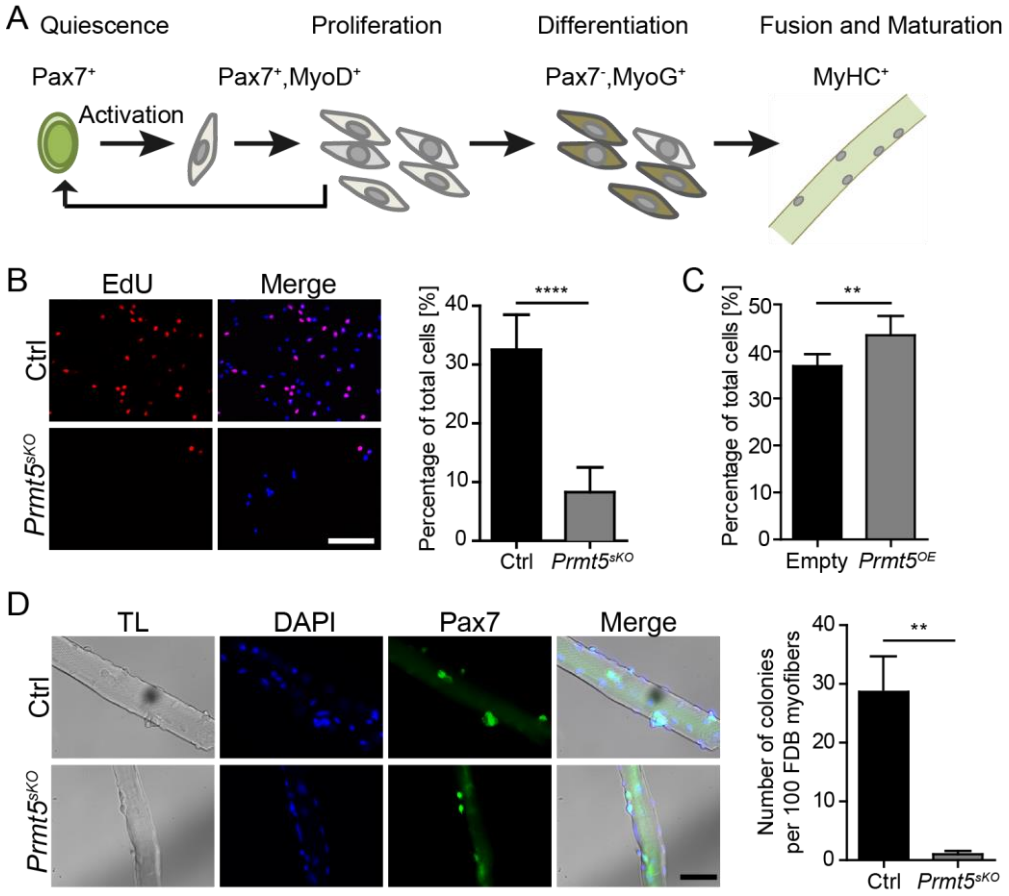

Figure 5.4.1 PRMT5 is required for SC proliferation

(A) Model depicting satellite cell homeostasis control and muscle regeneration.

(B) EdU incorporation assay showing an impaired satellite cell proliferation upon PRMT5 deletion. Quantitation of the percentage of EdU+ cells within Pax7+ cells isolated from *Prmt5*^{sKO} mice as compared to control mice. (unpaired t-test: **P<0.01,n=5) Scale bars indicate 50 µm.

(C) EdU incorporation assay showing an increased satellite cell proliferation upon overexpressing Prmt5. Quantitation of the percentage of EdU+ cells from Pax7+ cells infected with lentivirus overexpressing PRMT5 as compared to control lentivirus. Error bars represent standard deviations of the mean. (unpaired t-test: **P<0.01,n=5)

(D) Immunofluorescence assay of Pax7 positive colony in 3-day cultured FDB myofibers from control and *Prmt5*^{sKO} mice. Totally Pax7 positive colonies from 100 myofibers are counted. Quantification of Pax7 positive colonies in total YFP^{+} cells is shown on the right. Error bars represent standard deviations of the mean (t-test: **p < 0.01; ***p < 0.001,n=3). Scale bars indicate 50 µm.

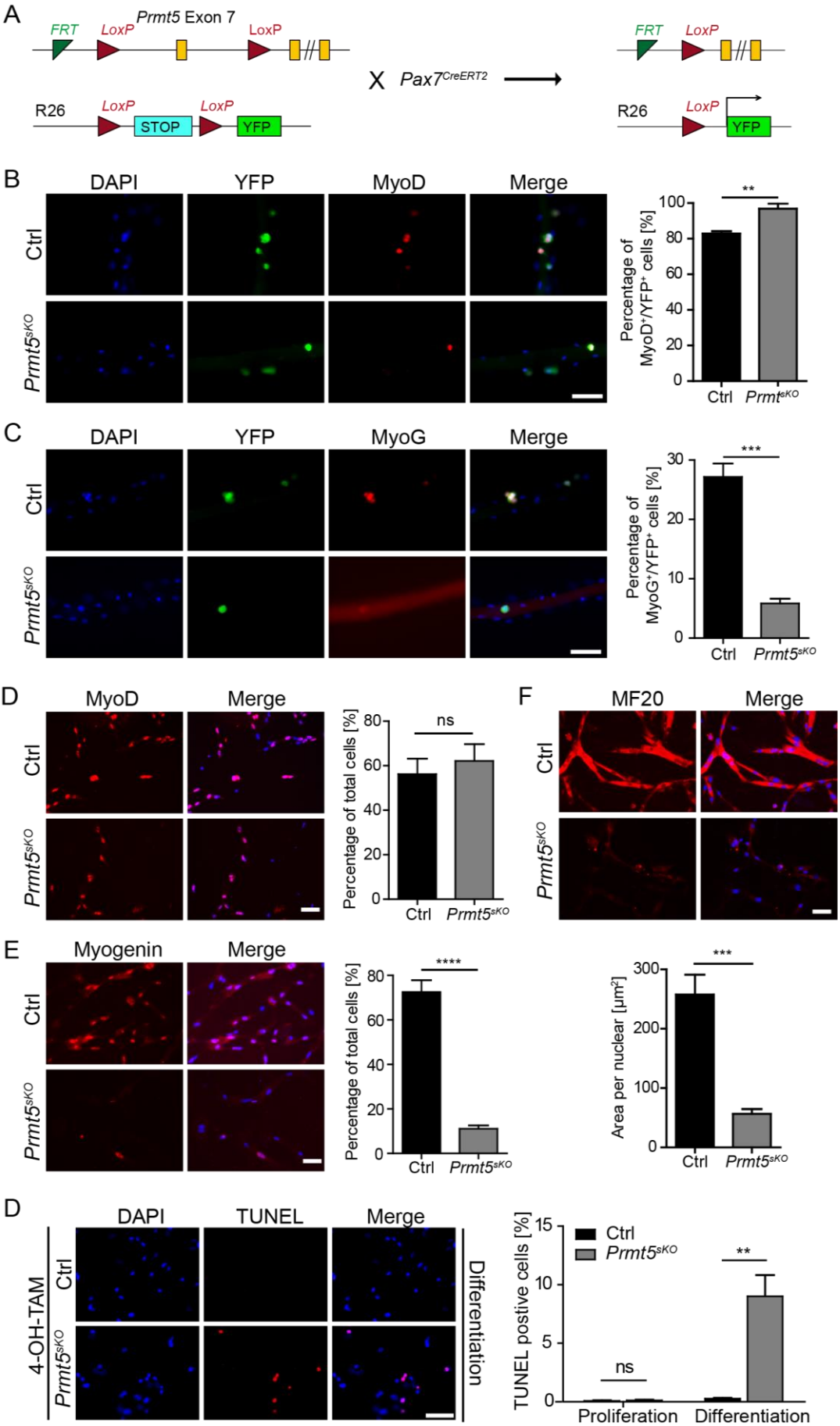
A
Prmt5 Exon 7
FRT
LoxP
LoxP
X
Pax7CreERT2
R26
LoxP
STOP
LoxP
YFP
B
DAPI
YFP
MyoD
Merge
Ctrl
Prmt5sKO
Percentage of MyoD+/YFP+ cells [%]
Ctrl
Prmt5sKO
C
DAPI
YFP
MyoG
Merge
Percentage of MyoG+/YFP+ cells [%]
D
MyoD
Merge
Percentage of total cells [%]
ns
F
MF20
Merge
E
Myogenin
Merge
****
Area per nuclear [µm²]
***
D
DAPI
TUNEL
Merge
4-OH-TAM
Differentiation
TUNEL postive cells [%]
Proliferation
Differentiation

5.4.2 PRMT5 is required for satellite cell differentiation

The impairment of satellite cell proliferation upon PRMT5 ablation prompted me to investigate the fate of PRMT5 deficient SC in adult muscle by lineage tracing approach in control and *Prmt5*^{sKO} mice in which the YFP-reporter transgene is integrated into the Rosa26 locus. Cre recominase expression in Pax7+ satellite cells leads to remove of the floxed-STOP sequence in the ROSA26 locus leading to expression of YFP fluorescent protein upon TAM induction. Satellite cells and their derived progeny then will be permanently labeled by YFP based on the constitutive expression from the Rosa26 locus (Figure 5.4.2A). After 3-week TAM administration, FDB myofibers were isolated from the control and *Prmt5*^{sKO} mice and cultured *in vitro* for 3 days. Notably, PRMT5 deficient progeny identified by an anti-YFP antibody were still capable of expressing MyoD indicating that SC activation is normal (Figure 5.4.2B). Along this line *in vitro* assay of YFP+ cells sorted from *Prmt5*^{sKO} and control littermates did not show any difference of MyoD expression after three-day culture as well (Figure 5.4.2C).

Figure 5.4.2 PRMT5 is required for satellite cell differentiation

(A) Breeding scheme of *Pax7*^{CreERT2}*:Prmt5*$^{fl/fl}$ mouse with Rosa26-YFP reporter mouse.

(B) &(C) Immunofluorescence assay of double YFP/MyoD (B) and YFP/MyoG (C) positive cells in 3-day cultured FDB myofibers from control and Prmt5^{sKO} mice. Quantification of the ratio of MyoD^{+}/YFP^{+} (B) and MyoG^{+}/YFP^{+} (C) in total YFP^{+} cells is shown on the right. Error bars represent standard deviations of the mean (t-test: **p < 0.0, ***p < 0.001). Scale bars indicate 50 μm.

(D) Immunofluorescence assay of MyoD positive cell in 3-day cultured YFP postive cells from TAM treated control and *Prmt5*^{sKO} mice. Quantification of percentage of MyoD+ cells in total cells is shown on the right. Error bars represent standard deviations of the mean (t-test: ns p > 0.5). Scale bar indicates 50 μm.

(E) Immunofluorescence assay of MyoG positive cells in 2-day differentiating YFP positive cells from control and *Prmt5*^{sKO} mice. Quantification of percentage of MyoG^{+} in total cells is shown on the right. Error bars represent standard deviations of the mean (t-test: ****p < 0.0001). Scale bar indicates 50 μm.

(F) Immunofluorescence assay of MF20 positive cells in 2-day differentiating YFP positive cells from control and *Prmt5*^{sKO} mice. Quantification of red area per nuclear is shown on the right. Error bars represent standard deviations of the mean (t-test: ***p < 0.001). Scale bar indicates 50 μm.

(G) Representative images from TUNEL assay showing increased apoptotic cells in PRMT5 deficient cells as compared to control cells after 2-day differentiation. Quantification of percentage of TUNEL positive cells in proliferating and differentiating cells is shown on the right. Error bars represent standard deviations of the mean (t test: **p < 0.01, ns p>0.05, n=3). Scale bar indicates 50 μm.

However when myofibers were stained with an antibody against MyoG, which is an early marker of muscle stem cell differentiation, I observed reduction of the ratio of MyoG+/YFP+ cells in PRMT5 deficient progeny indicating that lack of PRMT5 inhibited differentiation of SCs (Figure 5.4.2D). Consistently *in vitro* assay of YFP+ cells sorted from *Prmt5*^{sKO} and control littermates indicated an impaired muscle cell differentiation in mutant mice monitored by MyoG and myosin heavy chain expression (Figure 5.4.2E&F).

Importantly cell apoptosis analysis showed that while there were no detectable apoptotic cells in proliferative medium in both wild type and mutant mice, upon differentiation significantly more apoptotic cells were detected in mutants (Figure 5.4.2G), indicating that PRMT5 is required for SC survival during differentiation. In aggregate, these data demonstrated that PRMT5 is necessary for muscle stem cell proliferation, and required for cell differentiation and survival, cellular mechanisms responsible for long-term muscle stem cell maintenance and muscle regeneration upon acute or chronic muscle injury.

5.5 PRMT5 is dispensable for myofiber maturation

To investigate whether PRMT5 plays a role in the late stage of differentiation and myofiber maturation during skeletal muscle regeneration, *Prmt5*$^{fl/fl}$ mice were crossed with HSA^{CreERT2} mice, where Cre mediated recombination occurs only in postmitotic myofibers but not in satellite cells (Lai et al., 2004). The resulting *HSA*^{CreERT2}*/Prmt5*$^{fl/fl}$ mouse strain allows specific inactivation of PRMT5 in differentiated myotubes upon tamoxifen administration during muscle regeneration. TAM treated TA muscles from wild type, *HSA*^{CreERT2}*/Prmt5*$^{fl/+}$ and *HSA*^{CreERT2}*/Prmt5*$^{fl/fl}$ littermates were subjected to CTX injection (Figure 5.5A). 14 days after injury, the size of TA muscle were normal between injured and uninjured muscles from wild type, *HSA*^{CreERT2}*/Prmt5*$^{fl/+}$ and *HSA*^{CreERT2}*/Prmt5*$^{fl/fl}$ mice indicating full regeneration of skeletal muscle (Figure 5.5B). Furthermore, myofibers with central nuclei in all mice were detected in cross-sections by hematoxylin and eosin (H&E) staining (Figure 5.5C, 1X injury). Thus, the findings demonstrated that PRMT5 is dispensable for the late stage of muscle differentiation and myofiber maturation during muscle regeneration. Taken together by using different Cre lines, I could show that inactivation of PRMT5 in satellite cells but not in differentiated myocytes impairs muscle regeneration.

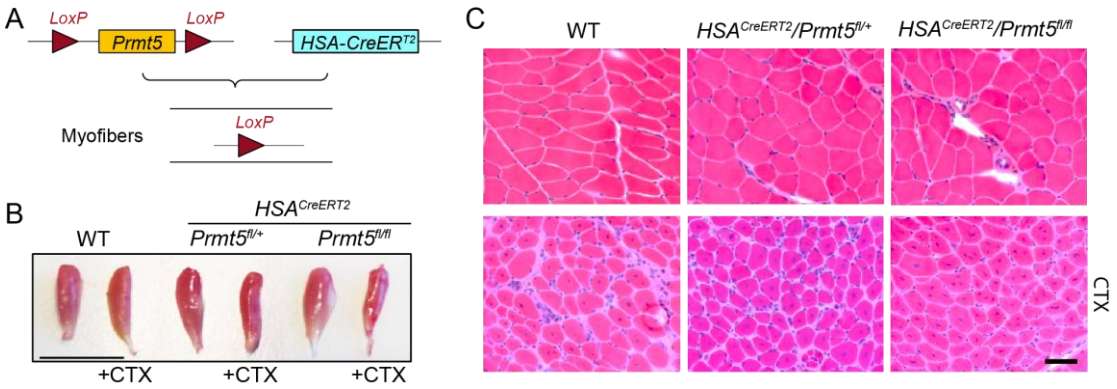

Figure 5.5 Genetic ablation of PRMT5 in differentiated myonuclei results in normal muscle regeneration upon acute muscle injury

(A) Breeding scheme of Prmt5$^{fl/fl}$ mice with *HSA*^{CreERT2} mice.

(B) Representative images of TA muscles of wild type, *HSA*^{CreERT2} */Prmt5*$^{fl/+}$ and *HSA*^{CreERT2} */Prmt5*$^{fl/fl}$ littermates (n=3) 14 days after CTX injection.

(C) H&E staining of TA muscles from wild type, *HSA*^{CreERT2} */Prmt5*$^{fl/+}$ and *HSA*^{CreERT2} */Prmt5*$^{fl/fl}$ littermates (n=3) 14 days after CTX injection. Scale bar indicates 50 µm.

5.6 Molecular mechanism underlying PRMT5 function in satellite cell proliferation

5.6.1 Transcription up-regulation of cell cycle inhibitor *p21* gene upon PRMT5 deletion in satellite cells

Satellite cell homeostasis is controlled by transitions of cells between quiescence and proliferation, and the hallmark of the proliferating population is progression through the cell cycle (Cheung and Rando, 2013). The strong inhibition of satellite cell proliferation upon PRMT5 ablation prompted us to investigate cell cycle regulation by PRMT5, which led to the identification of the cell cycle inhibitor p21 as a potential PRMT5 target gene. p21 belongs to the Cip/Kip family of G1-specific cell cycle dependent kinase inhibitors and has well established roles in inhibiting cyclin-CDK complexes (Choudhury et al., 2007; Parker et al., 1995; Spencer et al., 2013) and satellite cell homeostasis (Carlson et al., 2008; George et al., 2013). qPCR analyses of freshly FACS sorted satellite cells revealed a dramatic up-regulation of *p21* gene expression in PRMT5 deficient SCs indicating a transcriptional inhibition of *p21* by PRMT5 *in vivo* (Figure 5.6.1A). Consistently, transcriptional profiling of satellite cells from *Prmt5*^{sKO} mice, culture-amplified and subsequently treated with 4-hydroxy-tamoxifen (4-OH) (Figure 5.6.1B), revealed a dramatic depletion of PRMT5 and up-regulation of *p21* (Figure 5.6.1C&D). In addtition, I observed a dramatic down-regulation of the cell cycle regulator *CyclinB1*, a p21 target gene(Figure 5.6.1D).

Interestingly, transcription of myogenic factors including Pax7, MyoD and Myf5 was not affected in PRMT5 deficient SCs suggesting that PRMT5 does not directly influence transcription of these genes (Figure 5.6.1D).

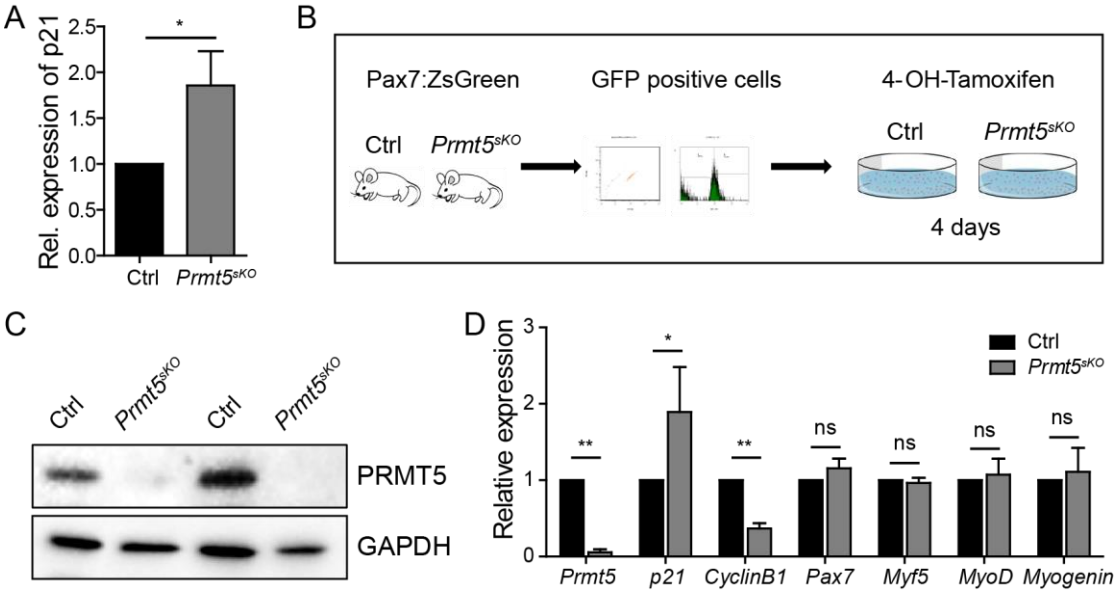

Figure 5.6.1 cell cycle inhibitor *p21* gene is identified as a downstream target of PRMT5 by RNA-seq assay

(A) RT-qPCR analysis showing an up-regulation of p21 expression in satellite cells isolated from Prmt5sKO mice. The expression level of mRNAs is normalized to mRNA of GAPDH. Error bars indicate the standard deviation (Paired t test: *P<0.05, n=3).

(B) Experimental strategy showing ablation of PRMT5 upon 4-OH-tamoxifen administration *in vitro*.

(C) Western blots showing depletion of PRMT5 protein in isolated satellite cells from Prmt5^{sKO} as compared to control littermates after 4-OH tamoxifen administration *in vitro*. GAPDH is used as protein loading control.

(D) RT-qPCR analysis of *Prmt5*, *p21*, *CyclinB1* and myogenic factor expression in cultured satellite cells where PRMT5 ablation is induced upon 4-OH-tamoxifen administration. The expression level of different mRNAs is normalized to mRNA of *Gapdh*. Error bars indicate the standard deviation (Paired t test: *P<0.05, **P<0.01, n=3).

5.6.2 Identification of *cis*-regulatory elements in *p21* gene locus

To determine whether PRMT5 directly binds the *p21* locus thereby suppressing its expression, I carried out chromatin immunoprecipitation (ChIP) experiments in isolated control and PRMT5 deficient satellite cells. First, I did a comprehensively survey of cis-regulatory elements across the entire mouse *p21* gene by analyzing published ChIP-seq results in various cell lines using GEO browser in order to

identify potential transcription factor binding sites (TFBS) and chromatin modification profiles, which is not known in mouse *p21* locus so far.

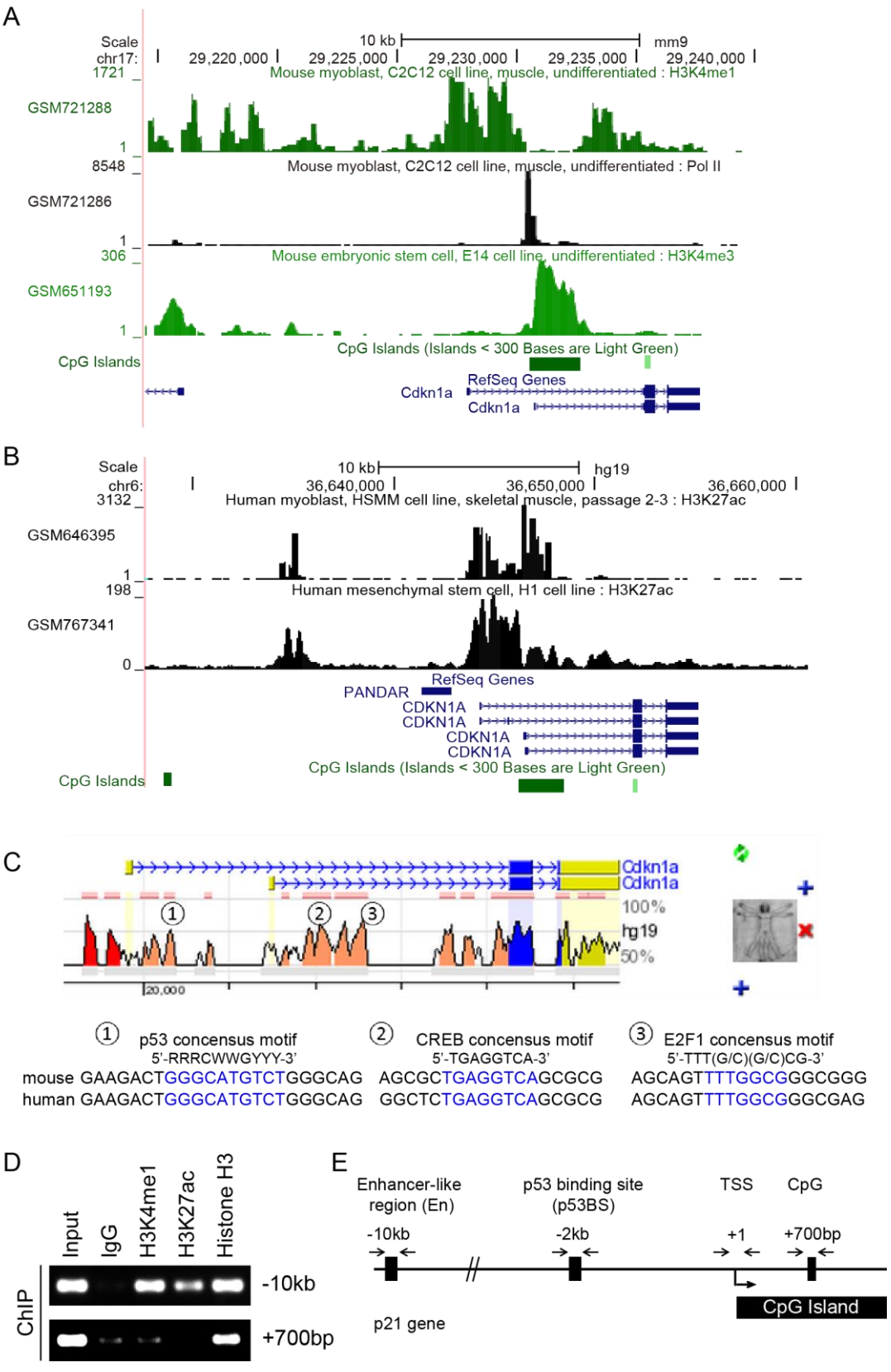

I examined RNA polymerase II (Pol II), H3K4me3 and H3K4me1 in mouse cell lines and H3K27ac in human cell lines. While Pol II signals mark the transcription start site (TSS) of the active *p21* transcription, H3K4me3 modification is enriched between TSS and 1.5kb downstream of TSS within the first intron. This region is also a GC-rich region and is targeted by transcription factor Sp1/KLF family member promoting p21 expression in human cells (Siatecka et al., 2010) (Figure 5.6.2A). Phylogenetic alignment of evolutionarily conserved transcription factor binding sites within *p21* loci from mouse and human revealed a consensus E2F1 and CREB binding sites embeded in this region (Figure 5.6.2C). Furthermore, both H3K4me1 (mouse cell lines) and H3K27ac (human cell lines) are peaked at around 10kb upstream of TSS indicating a potential enhancer region (Figure 5.6.2A&B), which was confirmed by ChIP using antibodies against H3K4me1 and H3K27ac in mouse ES cells (Figure 5.6.2D). In addition, I found a conserved p53 consensus motif at the proximal promoter that is enriched with both H3K4me1 and H3K27me3 (Figure 5.6.2C). In aggregate, four *cis*-regulatory regions in murine *p21* locus: up-stream enhancer region (-10kb,En), p53 binding site (-2kb, p53BS), transcription start site (+10bp,TSS) and down-stream intronic CpG island (+700bp, CpG) were identified by bioinformatics and experimental analyses (Figure 5.6.2E).

5.6.3 PRMT5 mediated H3R8me2s at the p53BS of *p21* gene

Next I examined the association of PRMT5 and distinct histone modifications with these four regulatory regions in the murine *p21* gene locus in control and PRMT5 deficient satellite cells by ChIP analysis. PRMT5 was highly enriched at the En and p53BS loci but not at the TSS and CpG loci in control SCs. Tamoxifen administration led to loss of PRMT5 association to the En and p53BS loci (Figure 5.6.3A).

Figure 5.6.2 Important regulatory regions within murine p21 locus

(A) NCBI genome browser indicating the potential enhancer, promoter and transcription start site of murine p21 locus by analyzing published ChIP-seq results of H3K4me1, H3K4me3 and Pol II in different murine cell lines.

(B) NCBI genome browser indicating the enhancer region of p21 by analyzing published ChIP-seq results of enhancer marker H3K27ac in different human cell lines.

(C) Evolutionary conserved region analysis by ECR browser identified p53, CREB and E2F1 binding sites.

(D) ChIP-PCR of H3K4me1 and H3K27ac at p21 locus in murine ES cells showing a 10kb region upstream of p21 transcription start site as an enhancer like region.

(E) Schematic of four regulatory regions: enhancer like (En), p53 binding site (p53BS), transcription start site (TSS), and intronic CpG island (CpG) within murine p21 locus identified by bioinformatics analyzing the published ChIP-seq data.

Consequently, significant reduction of histone H3 arginine 8 symmetric dimethylation (H3R8me2s), an enzymatic product of PRMT5 (Bedford and Richard, 2005), was found at the p53BS locus (Figure 5.6.2B). Consistent with transcriptional activation of *p21* upon PRMT5 ablation, a significant loss of nucleosome occupancy was detected at the TSS locus as monitored by histone H3 ChIP (Figure 5.6.2C). In addition, an increase of the euchromatic histone mark H3K4me3 was detected in PRMT5 deficient satellite cells at the CpG locus, indicating that PRMT5 mediated H3R8 symmetric dimethylation induced heterochromatin formation at the p53BS resulting in *p21* gene suppression (Figure 5.6.2D).

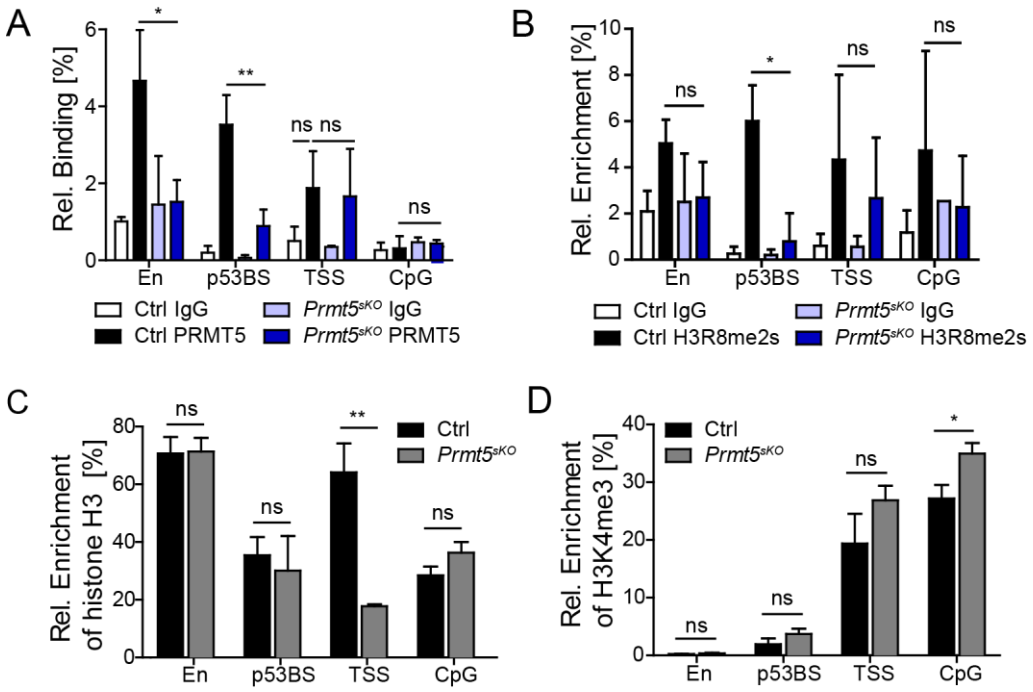

Figure 5.6.3 Ablation of PRMT5 in satellite cells results in loss of H3R8me2s at p53 binding site and formation of euchromatic structure at TSS and CpG island within murine p21 locus

(A), (B), (C)&(D) ChIP-qPCR analysis of Prmt5 (A), H3R8me2s (B), histone H3 (C) and H3K4me3 (D) at four regulatory regions (enhancer-like, p53 binding site, TSS and intronic CpG island) within p21 gene locus in satellite cells isolated from Prmt5^{sKO} mice and control littermates. The relative enrichment of Prmt5 and H3 is normalized against the input DNA and the enrichment of H3R8me2 and H3K4me3 is normalized to histone H3. Error bars represent standard deviations of the mean (t test: **p < 0.01, *p < 0.05, ns p>0.05).

5.6.4 Up-regulation of *p21* upon PRMT5 deletion is p53-independent

p53-dependent and independent activation of *p21* gene expression has been described during cell growth and differentiation and upon DNA damage (Macleod et al., 1995; Parker et al., 1995). My transcription analysis of *p21* gene expression in p53 and PRMT5 double knockout (*p53*$^{-/-}$*/Prmt5*^{sKO}) satellite cells revealed an up-

regulation of *p21* compared to control cells indicating that *p21* up-regulation in satellite cells upon PRMT5 ablation occurs independently of p53 (Figure 5.6.4E).

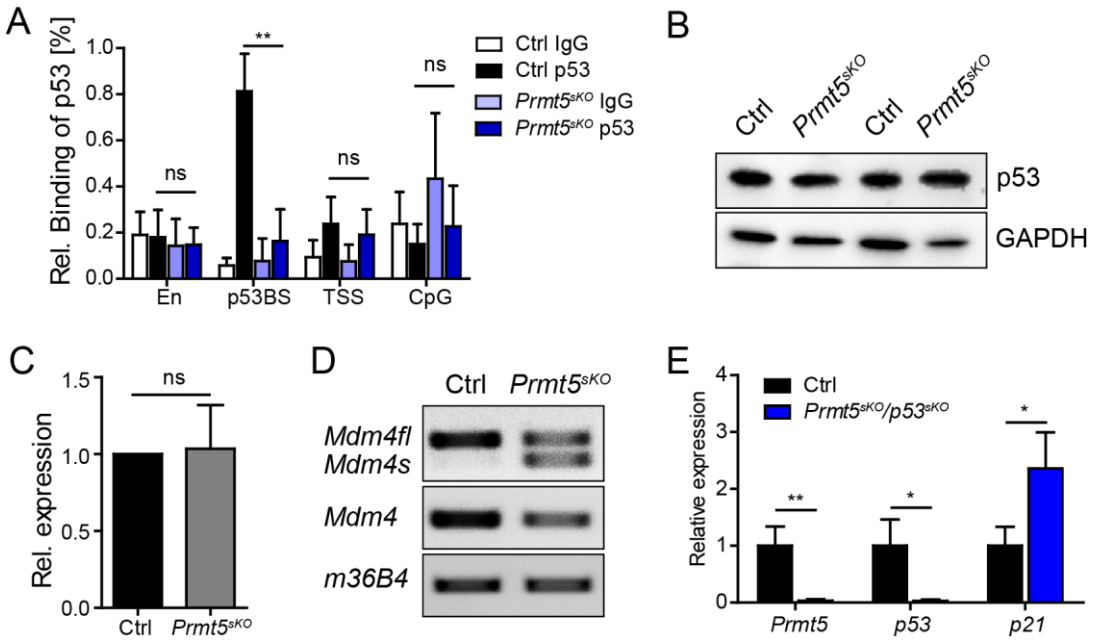

Figure 5.6.4 Ablation of PRMT5 activates p21 gene expression in a p53 independent manner

(A) ChIP-qPCR assay showing a reduction of p53 binding to p21 locus in PRMT5 deficient satellite cells. The relative enrichment of p53 is normalized against the input DNA. Error bars represent standard deviations of the mean (t test: **p < 0.01, n=3).

(B) Western blot showing the protein level of p53 in satellite cells from *Prmt5*^{sKO} mice and control littermates (n=2) after 4-OH tamoxifen administration *in vitro*.

(C) RT-qPCR showing the relative transcription of p53 gene in satellite cells from *Prmt5*^{sKO} mice as compared to control littermates. Error bars represent standard deviations of the mean (t test: ns p>0.05, n=3).

(D) Semi-quantitative RT-PCR showing the Mdm4 full-length transcripts (Mdm4fl) and splicing variant (Mdm4s) in satellite cells from *Prmt5*^{sKO} mice and control littermates. The transcripts of Mdm4 using primers in 3'UTR detecting both Mdm4f and Mdm4s and transcripts of m36B4 are shown below as RNA loading control.

(E) RT-qPCR showing the relative transcription of *Prmt5*, *p53* and *p21* gene in satellite cells from *Prmt5*^{sKO} mice as compared to control littermates. Error bars represent standard deviations of the mean (t test: *p<0.5; **p<0.01, n=3).

5.6.5 *p21* deletion partially restores the proliferative capacity of *Prmt5*^{sKO} SCs

To further address whether p21 is the main downstream factor that mediates impaired cellular functions of SCs upon PRMT5 ablation, I generated double mutant mice by crossing *Prmt5*^{sKO} mice to *p21* null mice (Deng et al., 1995). The resulting *Prmt5*^{sKO}/*p21*$^{-/-}$ mice allowed me to analyze whether the inhibition of proliferation of PRMT5 deficient SCs is rescued in a *p21* null background. A pure population of

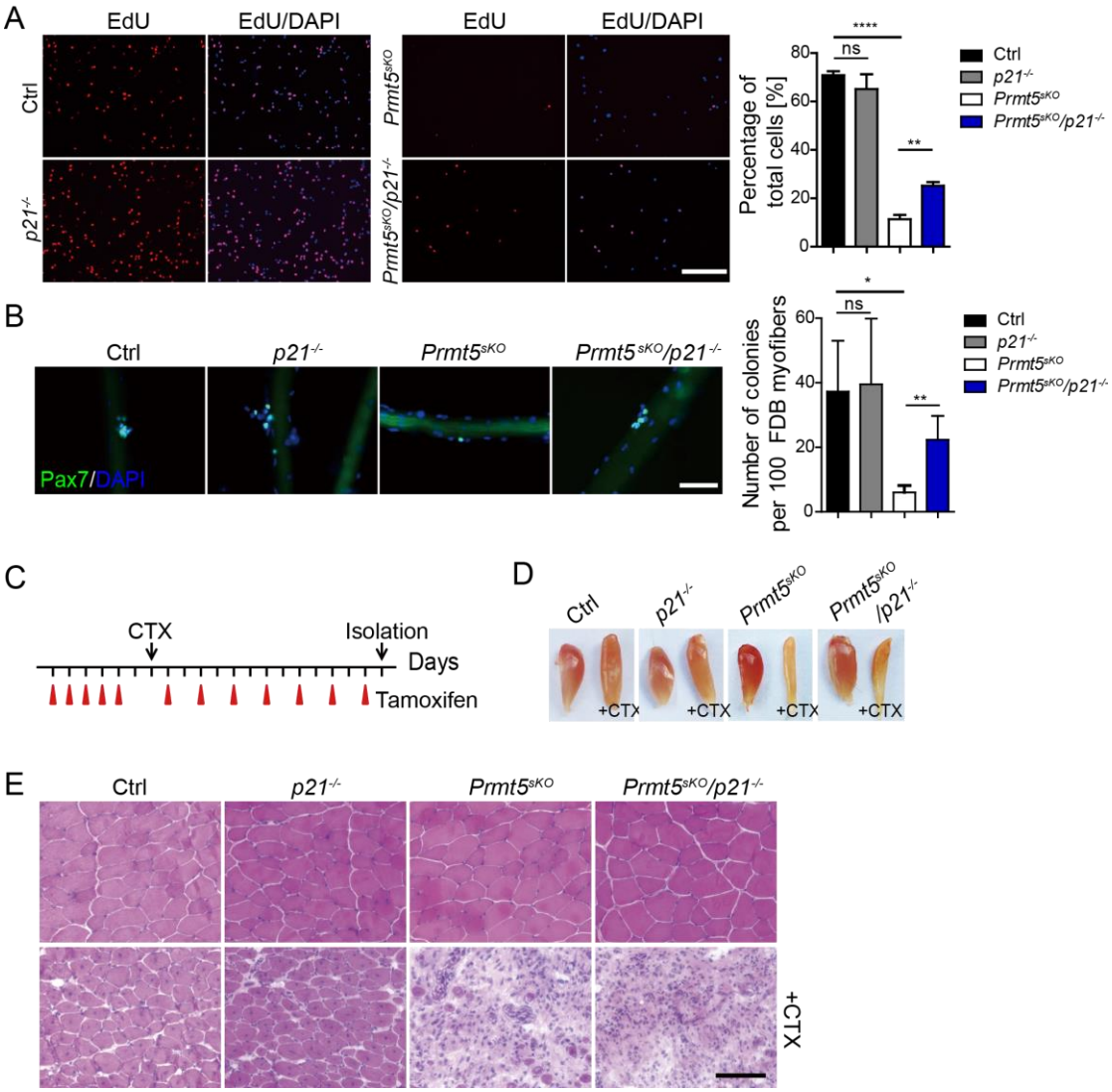

Figure 5.6.5 Genetic ablation of p21 gene partially restores the proliferation capability of PRMT5 deficient satellite cells

(A) EdU incorporation assay in isolated SCs from single and double knockout mice revealing a partial but significant recovery of SC proliferation from *Prmt5*^{sKO}/*p21*$^{-/-}$ mice (n=3) as compared to *Prmt5*^{sKO} mice (n=3). Quantification of EdU positive cells is shown. Error bars represent standard deviations of the mean (t-test: **p < 0.01). Scale bar indicates 200 µm.

(B) Immunofluorescence assay of Pax7 positive colonies in isolated myofibers cultured for 3 days showing an increased number of proliferating Pax7+ colonies in *Prmt5*^{sKO}/*p21*$^{-/-}$ mice (n=4) as compared with *Prmt5*^{sKO} mice (n=4). Pax7 positive colonies from 100 myofibers are counted. Quantification of Pax7 positive colony is shown. Error bars represent standard deviations of the mean (t-test: **p < 0.01). Scale bar indicates 100 µm.

(C) Schematic of muscle regeneration assay upon acute muscle injury in control and *Prmt5*^{sKO} littermates (n=3) upon tamoxifen administration for 3 weeks. TA muscle injury was induced by cardiotoxin (CTX) injection 5 days after initial tamoxifen injection and muscle regeneration was analyzed 2 weeks later.

(D) Representative images of TA muscles of from single and double knockout littermates (n=3) 14 days after CTX injection.

(E) H&E staining of TA muscles from single and double knockout littermates (n=3) 14 days after CTX injection. Scale bar indicates 50 µm.

satellite cells was isolated by FACS sorting using negative cell surface markers CD11b, CD45 and CD31 that exclude leucocytes and endothelial cells, and positive

markers alpha integrin and CD34 that label the satellite cells. *In vitro* EdU incorporation assay in SCs isolated from single and double knockout mice revealed a partial but significant restoration of SC proliferation in *Prmt5*^{sKO}/*p21*$^{-/-}$ mice compared to *Prmt5*^{sKO} mice (Figure 5.6.5 A). Consistently, *ex vivo* clone numbers on isolated myotubes cultured for 3 days increased significantly in double knockout mice as compared with *Prmt5*^{sKO} mice as well (Figure 5.6.5 B). However, satellite cell mediated muscle regeneration upon CTX injection was still impaired in *Prmt5*^{sKO}/*p21*$^{-/-}$ similar to *Prmt5*^{sKO} mice (Figure 5.6.5 C,D&E). These data indicate that epigenetic regulation of the *p21* gene locus by PRMT5 directly controls satellite cell proliferation during satellite cell expansion, and additional PRMT5 targets in SCs might be required for mediating PRMT5 function during later phases of muscle regeneration.

5.7 PRMT5 is dispensable for embryonic and fetal muscle development and Pax7 expressing muscle progenitor expansion

Muscle progenitors and satellite cells use similar regulatory molecules during developmental myogenesis and regenerative myogenesis respectively (Kang and Krauss, 2010). Hence, I reasoned that PRMT5 might not only control satellite cell proliferation and muscle regeneration but might also play a role in expanding muscle precursors and formation of skeletal muscle tissue during development. To test this I used a Pax7^{Cre} knock-in mouse strain (Pax7^{Cre}) that enables deletion of PRMT5 in Pax7 expressing cells during development (Keller et al., 2004) (Figure 5.7A). I isolated wild type and Pax7^{Cre}/*Prmt5*$^{loxP/loxP}$ (hereafter referred to as conditional muscle specific PRMT5 knockout, *Prmt5*^{mKO}; Pax7^{Cre}/*Prmt5*$^{loxP/+}$ as control (Ctrl)) mutant embryos at distinct embryonic days E9.5, E12.5 and E16.5. Surprisingly, embryos lacking PRMT5 in the Pax7 lineage were indistinguishable from wild type embryos isolated from the same pregnant mother mice at all indicated time points (Figure 5.7B). Detailed analyses on cross-sections of embryonic muscle from fore limbs of E12.5 and E14.5 embryos revealed indistinguishable immunofluorescent detection of Pax7+, MyoG+ and MF20+ cells in control and *Prmt5*^{mKO} embryos (Figure 5.7C&D), demonstrating that PRMT5 is dispensable for Pax7+ myogenic precursor cell expansion and muscle differentiation during early embryonic muscle development similarly. At E16.5, a later time-point when Pax7+ muscle progenitor cells already play an important role in fetal muscle growth (Hutcheson et al., 2009), inactivation of PRMT5 in muscle progenitors had no obvious effect on Pax7+, MyoD+

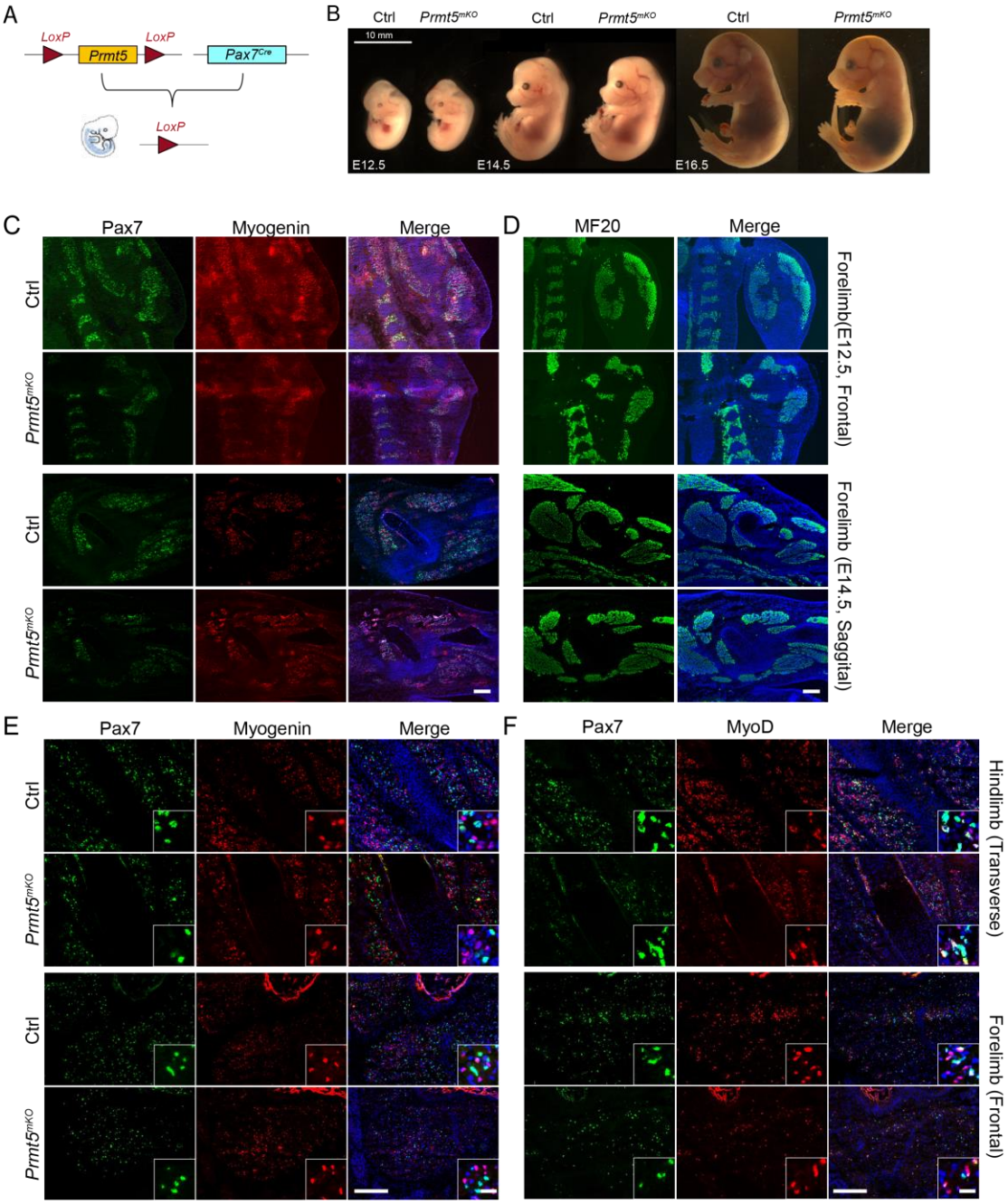

Figure 5.7 PRMT5 is dispensable for embryonic Pax7+ muscle progenitor cell proliferation and differentiation

(A) Breeding scheme of Prmt5$^{loxp/loxp}$ mice with *Pax7*^{ICN} mice.

(B) Representative images of control and *Prmt5*^{mKO} embryos at embryonic day E12.5, E14.5 and E16.5. Scale bar indicates 10 mm.

(C) Representative immunofluorescence images of cryo-sections of forelimb (E12.5 Frontal, upper panel; E14.5 Saggital low panel) showing expression of Pax7 (green) and Myogenin (red). DNA is stained with DAPI (blue). Scale bar indicates 200 µm.

(D) Representative immunofluorescence images of cryo-sections of forelimb (E12.5 Frontal, upper panel; E14.5 Saggital low panel) showing expression of MF20 (green). DNA is stained with DAPI (blue). Scale bar indicates 200 µm.

(E) &(F) Representative immunofluorescence images of cryo-sections of hindlimb (E16.5 Transverse, upper panel) and forelimb (E16.5 Frontal, low panel) showing expression of Pax7 (green) and Myogenin (red) in (E), and Pax7 (green) and MyoD (red) in (F). DNA is stained with DAPI (blue). Scale bar indicates 200 µm. For the inserts scale bar indicates 20 µm.

and MyoG+ expression in both fore and hind limbs as well indicating that myogenic cell proliferation and differentiation was not affected and muscle development was normal (Figure 5.7E&F). These results demonstrated that PRMT5 is dispensable for Pax7+ myogenic precursor cell expansion during embryonic and fetal muscle development, highlighting a distinct genetic requirement for PRMT5 in regulating muscle progenitor cell expansion and satellite cell proliferation.

5.8 The role of PRMT5 in high order chromatin organization of satellite cells

Quiescent satellite cells differ from fully differentiated myocytes is repect to the organization of heterochromatin indicating that control of high order heterochromatin organization is causally involved in the regulation of muscle stem cell homeostasis (Shi and Garry, 2006). Consistently, loss of Pax7 leads to loss of heterochromatic structure within nucleus of satellite cells and impairment of muscle regeneration (Gunther et al., 2013). The high enrichment of PRMT5 in nucleus of satellite cells prompted me to investigate whether PRMT5 controls high order chromatin structure.

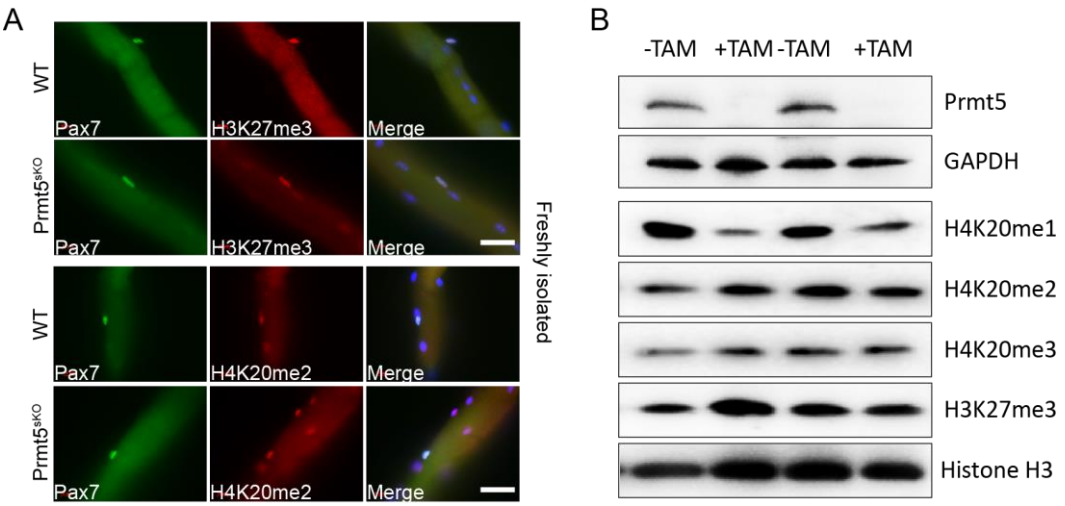

Figure 5.8 Global alterations of histone modifications in satellite cells lacking PRMT5

(A) Immunofluorescence analyses showing no alteration of H4K20me2 and H3K27me3 in satellite cells on freshly isolated myofibers from control and *Prmt5*^{sKO} mice.

(B) Western blot showing the changes of histone modifications in satellite cells from *Prmt5*^{sKO} mice and control littermates (n=2) after 4-OH tamoxifen administration *in vitro*. Histone H3 is used as a histone loading control.

The high order heterochromatin structure was monitored by immunofluorescence assay using antibodies against heterochromatic histone modification marks such as H3K27me3 and H4K20me2 in freshly isolated myofibers. The enrichment of H3K27me3 and H4K20me2 within nuclei of satellite cells did not change in *Prmt5*^{sKO}

mutant compared to control mice, suggesting an intact chromatin structure in PRMT5 deficient satellite cells (Figure 5.9A).

Furthermore, western blot assay of histone modifications using *in vitro* 4-OH-tamoxifen treated *Prmt5*^{sKO} satellite cells and control cells revealed no alteration of H3K27me3 and H4K20me2 in both control and PRMT5 deficient satellite cells (Figure 5.9B). Surprisingly, I detected a dramatic reduction of H4K20me1 in PRMT5 deficient cells (Figure 5.9B). This might be due to a strong cell cycle block given that H4K20me1 has been linked to cell cycle regulation(Beck et al., 2012b). Further detailed analyses of chromatin structure of satellite cells from wild type and PRMT5 deficient mice using MNase digestion and electron microscopy will help to understand the role of PRMT5 in chromatin structure control.

5.9 Genome wide epigenetic profiling of H4K20me1 and its correlation with active transcription.

The enrichment of H4K20me2 within SCs prompted me to identify genes that are labeled by H4K20me2 together with H4K20me1 and H4K20me3 using chromatin immunoprecipitation coupled to high-throughput sequencing (ChIP-seq). I used proliferating as well as differentiating C2C12 cell, a myogenic cell line derived from satellite cells. For each sequencing sample, 10ng ChIPed DNA was collected and subjected to Illumina HiSeq. Around 20 million reads were obtained for each sample.

5.9.1 H4K20me1 is enriched within gene body.

After read mapping to the genome and peak calling, high enrichment of H4K20me1 on gene bodies especially in differentiated C2C12 cells was observed whereas no significant the peaks for H4K20me2 and H4K20me3 were identified in both proliferating and differentiating C2C12 cells. Therefore I focused my further experiments and the analyses on H4K20me1. The ChIP-seq data were confirmed by ChIP-qPCR on randomly picked single gene Med2d (5.10.1A&B). Bioinformatics analysis of the H4K20me1 peak distribution revealed that H4K20me1 are more enriched in the intronic and exonic regions and are strongly depleted in intergenic regions in differentiated C2C12 cells in comparison with the distribution in proliferating cells as well as genomic control annotations (“all”), (5.10.1C). This indicates that H4K20me1 is more enriched within gene bodies especially in differentiated cells. Next, the gene-body regions were binned into 50 bins of variable size (corresponding to gene size) and clustered using hierarchical k-means. Heat map showed that Cluster I that is highly enriched of H4K20me1 contains around 420 genes and shows a strong binding within the gene body (5.10.1D). Gene ontology

analysis of cluster I genes revealed a population of highly expressed housekeeping genes indicating that H4K20me1 correlates with transcription activation.

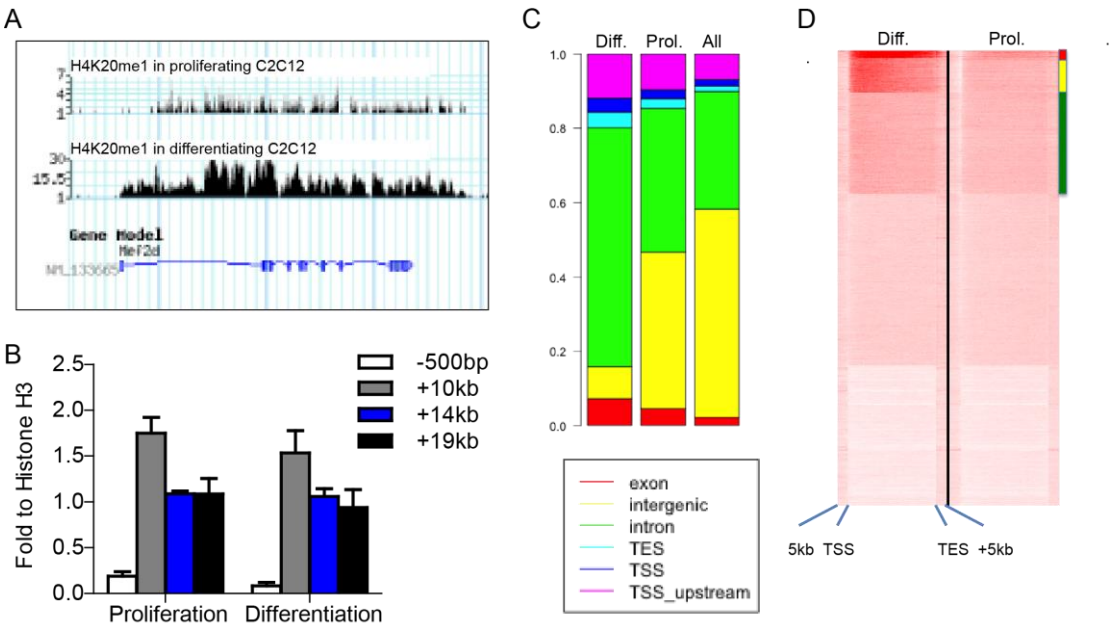

Figure 5.9.1 Genomic distribution of H4K20me1 in proliferating and differentiating C2C12 cells

(A) Representative example of ChIP-Seq enrichment peaks for H4K20me1 at Mef2d gene.

(B) Confirmation of H4K20me1 association at Med2d gene by ChIP-qPCR.

(C) Basic distribution analysis of H4K20me1 ChIP-seq results showing an increased association of H4K20me1 within exons and introns.

(D) Heat map profile showing high enrichment of H4K20me1 within the gene body in differentiating C2C12 cells. Each row of the heatmap represents the binding pattern of H4K20me1 across the −5 kb to +5 kb region flanking the TSS and TES. Gene body region was binned into 50 bins of variable size (corresponding to gene size) and clustered using hierarchical k-means.

5.9.2 H4K20me1 correlates with RNA polymerase II and gene transcription level

To further validate my results, I carried out bioinformatics analysis on the correlation of H4K20me1 with published ChIP-seq data of several known molecular markers that indicate active transcription in C2C12 cells (Asp et al., 2011). Consistently I detected a strong correlation between H4K20me1 and Pol II in differentiating C2C12 cells while the correlation in proliferating cells was weaker (Figure 5.10.2A). Moreover, average binding (number of reads per body/gene length) was calculated and used as a measurement to bin the set of mouse genes into 10 equal-size bins sorted for binding. Average binding was increased from bin 1 to 10. When plotting bins against gene expression values determined from GEO entry GSE11415, I observed an increased level of average gene expression which followed the increased H4K20me1

enrichment, indicating gene expression is positively associated with the H4K20me1 bound nucleosomes (Figure 5.10.2B).

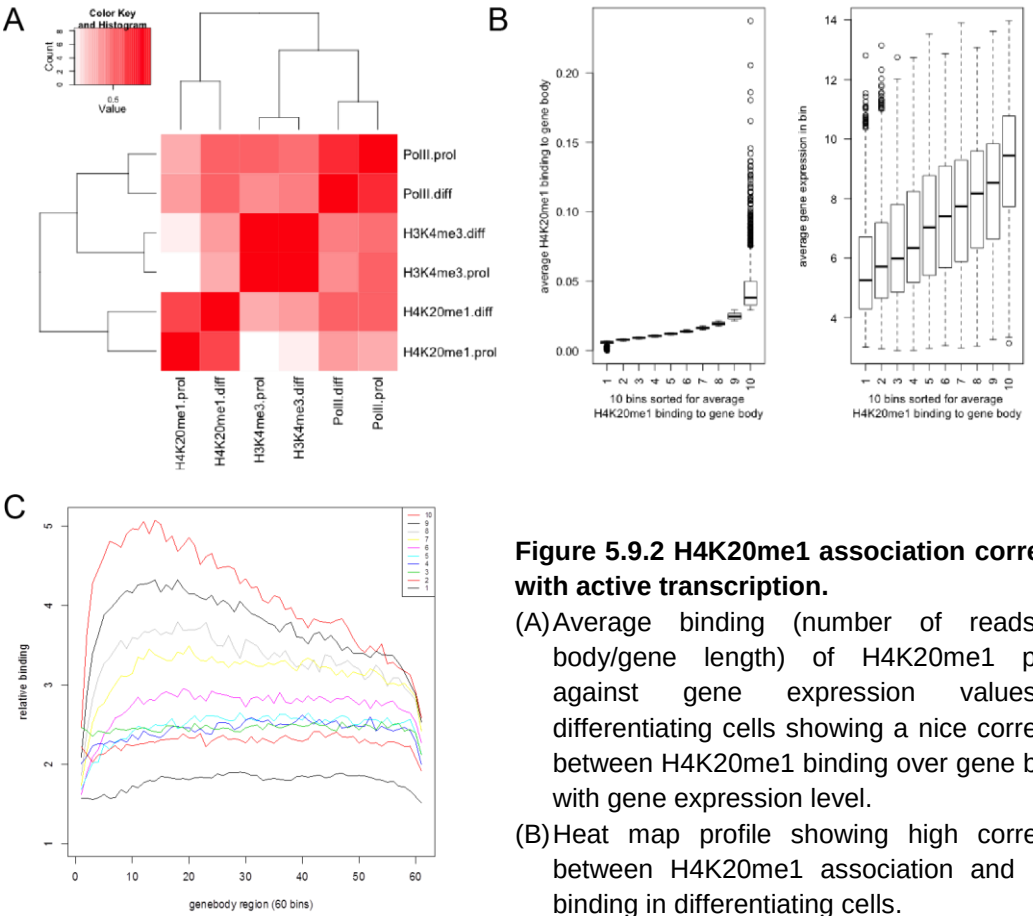

Figure 5.9.2 H4K20me1 association correlates with active transcription.

(A) Average binding (number of reads per body/gene length) of H4K20me1 plotted against gene expression values in differentiating cells showing a nice correlation between H4K20me1 binding over gene bodies with gene expression level.

(B) Heat map profile showing high correlation between H4K20me1 association and Pol II binding in differentiating cells.

(C) H4K20me1 is associated with high CpG promoter in differentiating cells. Average binding (number of reads per body/gene length) of H4K20me1 in differentiating cells was plotted against the CpG density rank of each promoter. Gene body data is plotted as 60 bins spanning the whole gene body of 27000 mouse ref-seq genes. For each promoter the CpG density was calculated and 10 promoter classes were assigned based on the CpG density rank (from 10 = highest density to 1=lowest density).

Then I analyzed promoter characteristics of H4K20me1 bound genes. It has been shown that high CpG density correlates with active gene transcription (Deaton and Bird, 2011). To address whether H4K20me1 associated with genes that show a high CpG density, I separated the gene promoters into 10 classes according to the CpG density (from 10 =highest density to 1=lowest density) and plotted the average H4K20me1 binding to different promoter classes. Notably, the nucleosomes in promoter with higher CpG density were always decorated with more H4K20me1 (Figure 5.10.2C), indicating H4K20me1 is involved in transcriptional regulation of CpG-rich promoters.

5.9.3 H4K20me1 and H3K36me3 show different distribution within the gene body.

To further understand how H4K20me1 is involved in active gene transcription, I examined the average normalized tag densities across all genes or subsets of genes according to their respective expression levels. H4K20me1 distribution within the gene body showed a peak close to the promoter at the transcription start site with a decreased association at the end of the genes. This pattern is different from the distribution of another histone modification H3K36me3, which has been shown to positively correlate with gene activation and is enriched in gene bodiesl. H3K36me3 peaked later at the transcription end site (TES) (5.10.3 A&B). Consistently Set2 in yeast (homolog HYPB in human), the epigenetic modifier catalyzing H3K36me3, is capable of binding directly to RNA polymerase II with COOH-terminal domain (CTD) phosphorylated on Ser2 (Ser2P) that is highly enriched in TES (Hossain et al., 2013). These findings indicated that H4K20me1 might be involved in the early stage of transcription elongation.

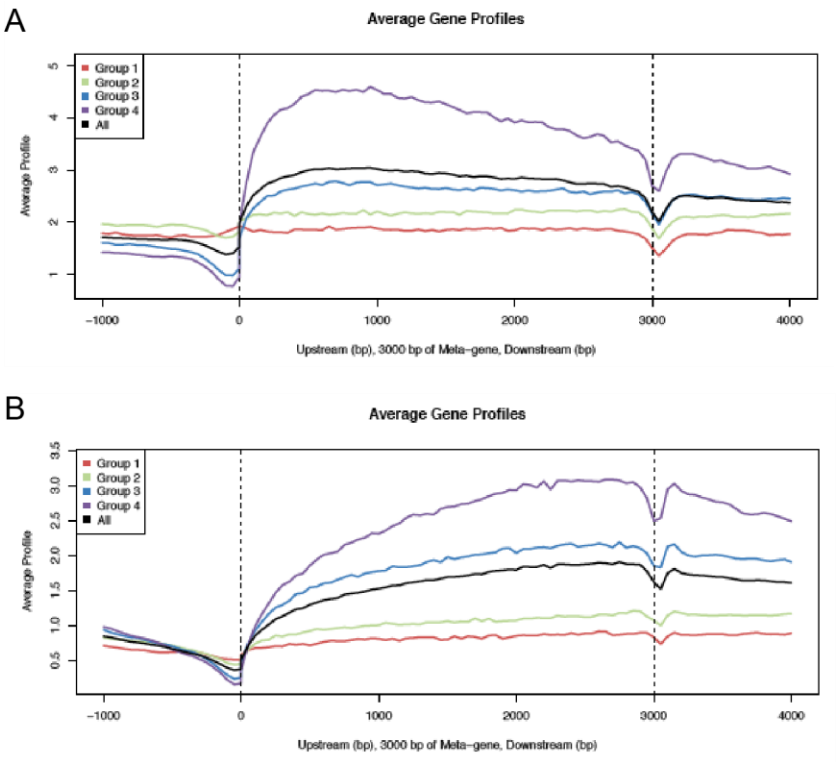

Figure 5.9.3 Different distribution of H4K20me1 and H3K36me3 in coding region of activated genes.

(A)&(B) The average ChIP enrichment signals from H4K20me1 (A) and H3K36me3 (B) in differentiating cells on the meta-gene of 3 kb. Average binding across subsets of genes ordered for their respective expression levels was plotted. Groups 1 to 4 are ordered for increasing expression level. The black color indicates all RefSeq genes.

5.10 The enrichment of H4K20me1 at the gene body is Pol II independent

To address whether the enrichment of H4K20me1 at the gene body is dependent on early elongating Pol II that could be distinguished from late elongation Pol II by CTD phosphorylation at Ser5 (Ser5P), I treated proliferating and differentiating C2C12 cells with three distinct transcription elongation inhibitors: α-Amanitin, Actinomycin D and DRB. While α-Amanitin binds to Pol II and blocks the incorporation of new ribonucleotides into the nascent RNA chains (de Mercoyrol et al., 1989), Actinomycin D intercalates into DNA thereby preventing the progression of RNA polymerases (Casse et al., 1999). DRB, a protein kinase inhibitor, blocks the CTD phosphorylation therefore impairs transcription initiation and elongation (Yamaguchi et al., 1999).

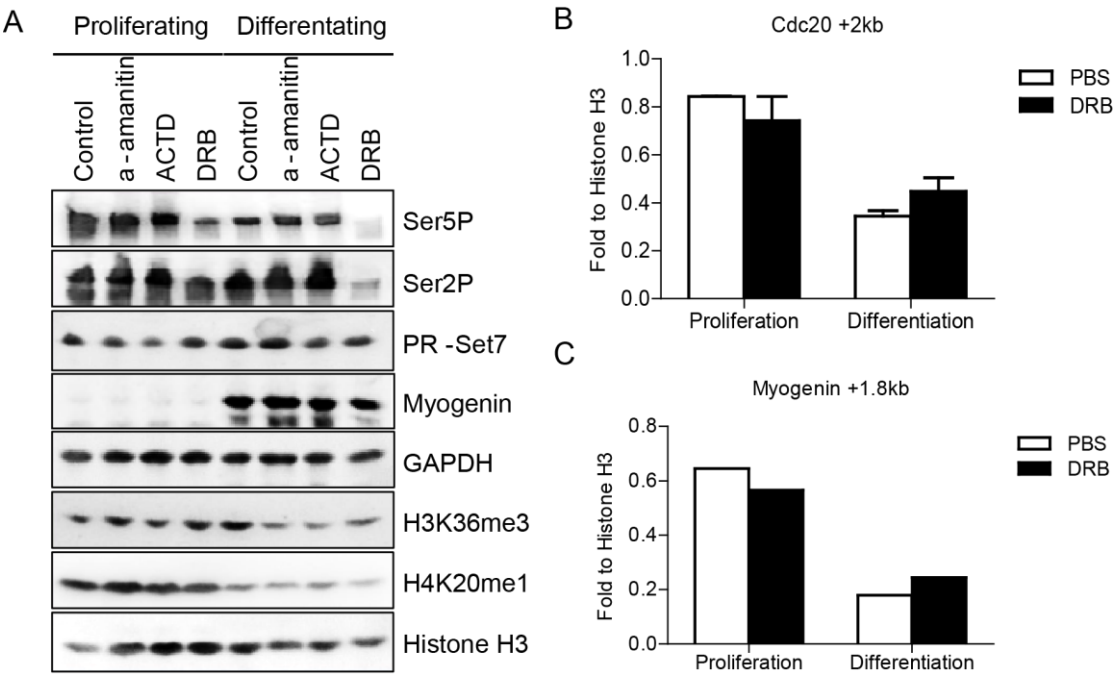

Figure 5.10 The enrichment of H4K20me1 at the gene body is independent on elongating Pol II

(A) Western blot using DRB treated proliferating and differentiating C2C12 cells showing that DRB inhibits Ser5 and Ser2 phosphorylation of Pol II without affecting the level of PR-Set7 and H4K20me1.

(B) &(C) ChIP-qPCR analysis showing unchanged level of H4K20me1 within the gene body in DRB treated and untreated C2C12 cells in both proliferating and differentiating stage.

Treatment of the cells for 3 hours with DRB led to a significant reduction of CTD phosphorylation and H3K36me3 in differentiated C2C12 cell, consistent with role of Set2 mediated H3K36me3 depending on elongating Pol II (Figure 5.11A). Interestingly neither H4K20me1 in histones nor its incorporation within the gene bodies of targeted gene such as Cdc20 and Myogenin changed upon DRB treatment

as compared to untreated cells (Figure 5.11B&C). These findings suggested that H4K20me1 incorporation within the coding region during transcription elongation is Pol II independent.

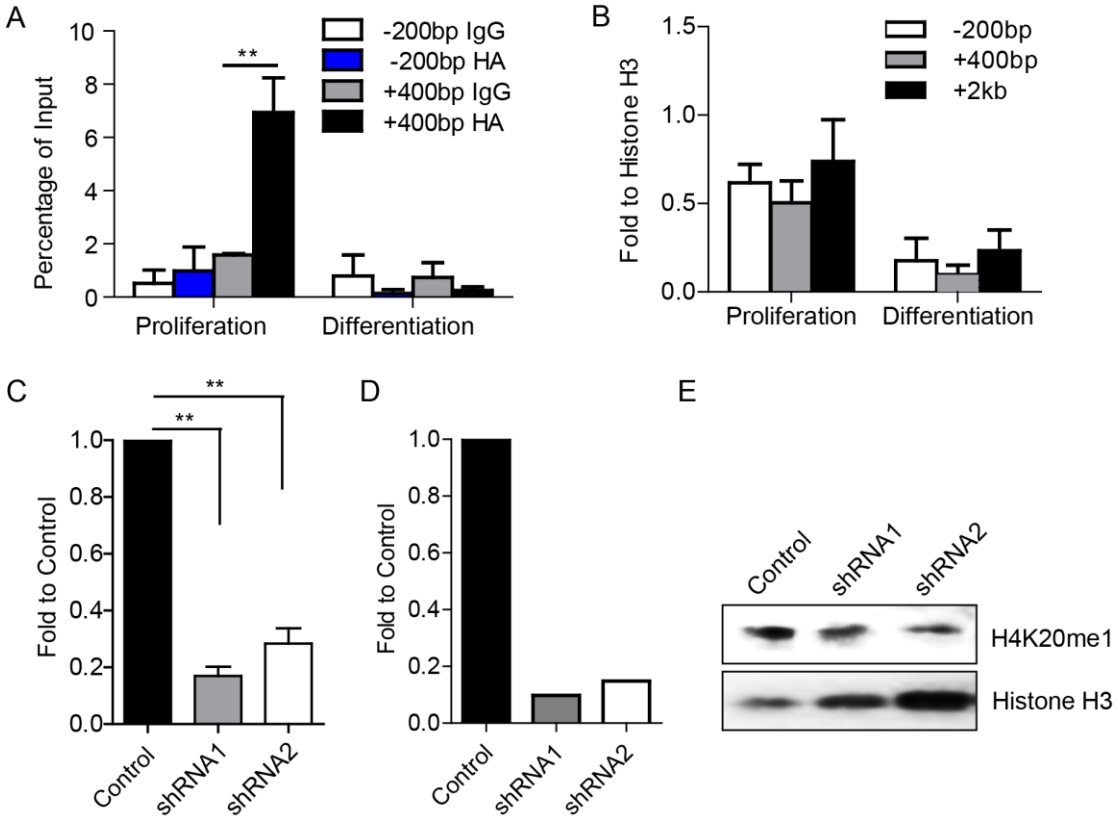

Figure 5.11 PR-Set7 and H4K20me1 are required for Cdc20 gene transcription

(A) ChIP-qPCR of H4K20me1 at three regulatory regions (-200bp, +400bp and +2kb) within Cdc20 locus in proliferating and differentiating C2C12 cells. The relative enrichment of H4K20me1 is normalized to histone H3. Error bars represent standard deviations of the mean.

(B) ChIP-qPCR of PR-Set7 binding to -200bp and +400bp of Cdc20 gene. ChIPs were performed using anti-HA antibodies in proliferating and differentiating stable C2C12 cell lines expressing HA-tagged PR-Set7. Error bars represent standard deviations of the mean (t test: **p < 0.01).

(C) RT-qPCR analysis showing reduction of PR-Set7 expression in stable C2C12 cell lines transfected with two shRNAs targeting PR-Set7 as compared to scramble shRNA. Error bars represent standard deviations of the mean (t-test: **p < 0.01).

(D) RT-qPCR analysis showing reduction of Cdc20 expression in stable C2C12 cell lines transfected with two shRNAs targeting PR-Set7 as compared to scramble RNA.

(E) Western blot assay showing decreased H4K20me1 level in stable C2C12 cell lines transfected with two shRNAs targeting PR-Set7 as compared to scramble RNA. Histone H3 is used as a protein loading control.

5.12 PR-Set7 mediated H4K20me1 is required for the transcription of Cdc20

PR-Set7/Set8/KMT5a has been shown to be the sole epigenetic modifying enzyme that catalyzes monomethylation of H4K20 (H4K20me1) (Schotta et al., 2008). To address whether PR-Set7 is associated with gene activation, chromatin IP using antibody against HA tag in C2C12 cells ectopically expressing PR-Set7-HA was carried out. PR-Set7 only bound to the gene body of Cdc20 gene in the proliferating but not differentiating cells (Figure 5.12A), which is consistent with the enrichment pattern of H4K20me1 (Figure 5.12B). This suggested that PR-Set7 positively correlates with gene transcription. Furthermore I performed PR-Set7 loss of function assays using two short hairpin RNAs (shRNAs) targeting murine Pr-set7 in C2C12 cells. PR-Set7 mRNA was significantly reduced as showed by RT-qPCR (Figure 5.12C). Consequently the level of H4K20me1 decreased as well (Figure 5.12D). Consistent with the role of PR-Set7 in transcription activation, the mRNA of targeted gene Cdc20 was strongly decreased (Figure 5.12E). Taken together these results indicated that PR-Set7 mediated H4K20me1 is required for transcription activation, a finding that is in contrast to a previous study claiming a role of PR-Set7 and H4K20me1 in transcription silencing (Congdon et al., 2010).

5.13 SILAC assay reveals interaction between PR-Set7 and multiple mRNA splicing factors

To start to elucidate the molecular mechanisms underlying PR-Set7/H4K20me1 mediated transcription activation, I identified PR-Set7 interaction partners within chromatin bound fractions using stable isotope labeling of amino acids in cell culture (SILAC)(Figure 5.13A). SILAC is the most commonly used method for metabolic labeling and depends on the incorporation of heavy isotope variants of arginine and lysine which, combined with tryptic protein digestion, ensures the labeling of all peptides except the very C-terminal ones. Compared to the “light” peptide, incorporation of “heavy” amino acids results in a defined mass shift that is detectable in MS survey scans. In brief, C2C12 cells that are ectopically expressing PR-Set7-HA were grown in heavy medium (Arg8, Lys10), while C2C12 cells with empty vector were labeled with nature arginine and lysine (light, Arg0, Lys0). Affinity purification of the HA-tagged PR-Set7 was then performed separately and immunoprecipitates were mixed before MS analysis from both cell lysates within proliferating and differentiating conditions (Figure 5.13A). In total, I identified 17 proteins that interact with PR-Set7 in proliferating and differentiating C2C12 cells. Interestingly among the PR-Set7 interaction partners several mRNA splicing factors such as Srrm2, Hnrnpa2b1, Prp8, Dnajc13 and Caper were identified. This suggested that PR-Set7

and H4K20me1 might be involved in co-transcription splicing thereby regulating transcriptional elongation during active gene expression. Further studies will focus on this hypothesis to elucidate the transcriptional role of PR-Set7/H4K20me1.

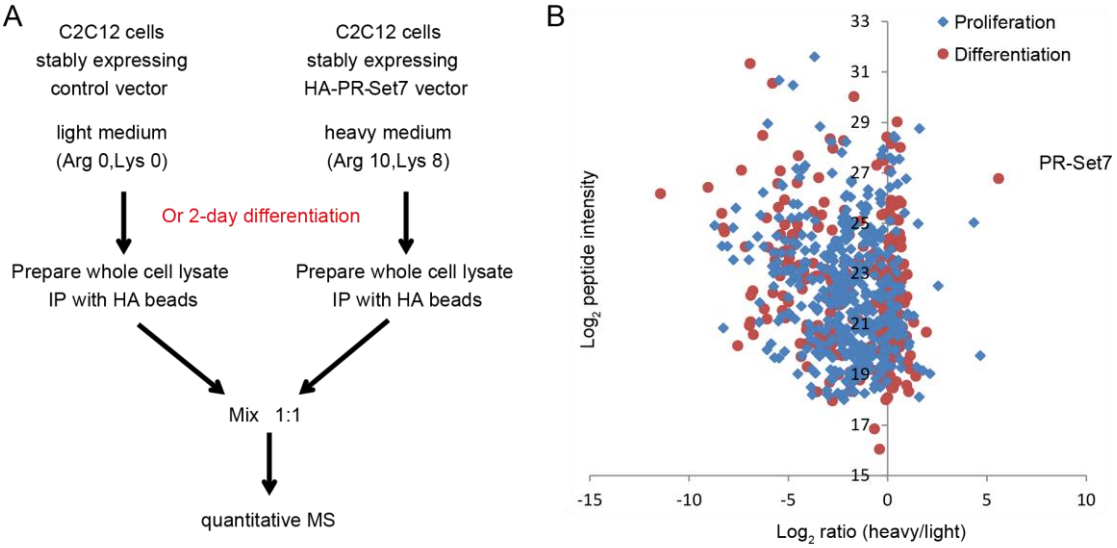

C

Gene name	log2 SILAC ratio Prolif.	log2 SILAC ratio Diff.
PR-Set7	4.35	5.60
Srrm2	2.14	1.94
Hnrnpa2b1	1.45	NaN
Prp8	1.10	1.13
Dnajc13	1.06	1.00
Caper	0.15	1.32

Figure 5.12 mRNA splicing factors are identified as PR-Set7 interaction partners by SILAC assay.

(A) Strategy of double-label SILAC experiment to identify the interaction partners of PR-Set7 in proliferating and differentiating C2C12 cells stably expressing HA-tagged PR-Set7.

(B) Scatter plot representing the proteins immunopurified together with PR-Set7 in proliferating and differentiating stable C2C12 cell lines. The summed peptide intensity distribution was plotted against the corresponding protein fold change (SILAC ratio) following immunoprecipitation.

(C) Table listing mRNA splicing factors that are identified as potential interaction partners of PR-Set7 by SILAC assay with the $\log_2$ SILAC ratio.

6 DISCUSSION

Adult muscle stem cells, also known as satellite cells, originate from muscle precursors during embryonic development and are required for adult muscle regeneration. Loss of satellite cells and deregulation of satellite cell homeostasis leads to deficient muscle repair under physiological conditions, during aging and pathological conditions such as muscular dystrophy. Here, I found that the protein arginine methyltransferase 5 (PRMT5) is highly enriched in satellite cells. Loss of PRMT5 in satellite cells of adult mice not only leads to a massive decline of the number of muscle stem cells during aging, but also completely abolishes muscle regeneration in both physiological and pathological conditions *in vivo*. Furthermore, I showed that PRMT5 is required for the proliferation of Pax7+/MyoD+ cells and formation of differentiated myogenic cells (Pax7-/MyoG+) but not for myofiber maturation (MyHC+). At the molecular level, PRMT5 directly modulates chromatin structure thereby epigenetic silencing the cell cycle inhibitor *p21* gene locus. Loss of p21 can partially restore the proliferation defects of PRMT5 deficient satellite cells. Interestingly, inactivation of PRMT5 in Pax7 positive precursors does neither inhibit cell expansion nor myotome formation during muscle development. Taken together these findings demonstrate the distinct genetic and epigenetic requirements of PRMT5 for Pax7+ muscle progenitor proliferation during muscle development and satellite cell proliferation during adult muscle regeneration (Figure 6).

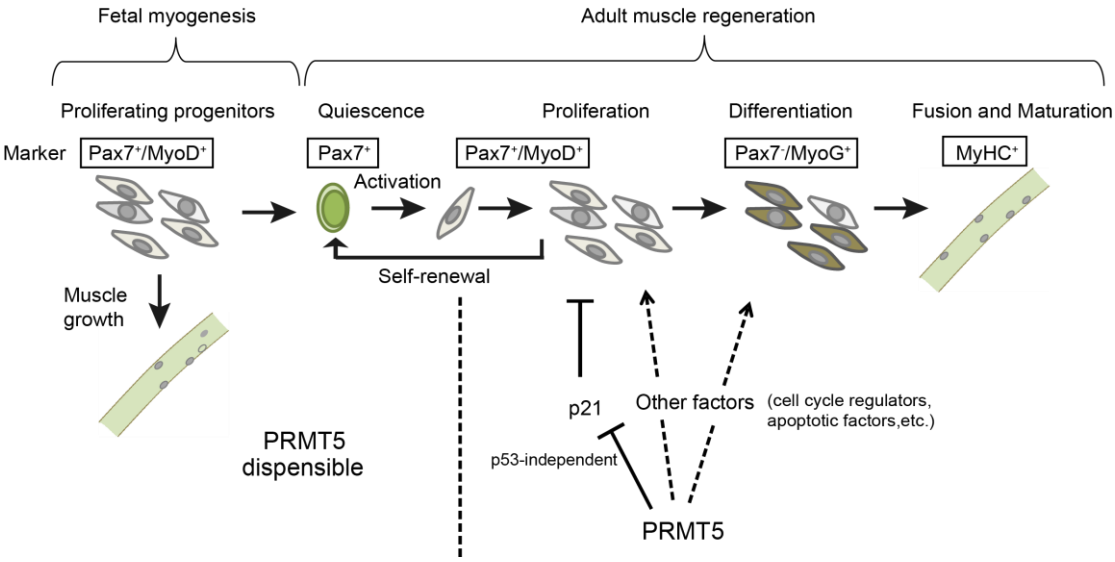

Figure 6 Model depicting distinct genetic requirement for PRMT5 in control of fetal myogenesis and regenerative myogenesis.

6.1 PRMT5 dependent mechanism of satellite cell proliferation

Previous studies have revealed an important function of PRMT5 for ES cell proliferation *in vitro* and neural progenitor cell proliferation during brain development, suggesting a general role of PRMT5 in cell proliferation control in different tissues and cell types (Bezzi et al., 2013; Gkountela et al., 2014; Tee et al., 2010). However, the function of PRMT5 in regulating proliferation is context dependent. A cellular feature that might confer different PRMT5 functions in a cell type specific manner is chromatin structure. For example, compared to the loose and open euchromatin structure found in undifferentiated ES cells (Meshorer and Misteli, 2006), quiescent satellite cells contain highly compacted and condensed heterochromatin (Gunther et al., 2013; Shi and Garry, 2006; Zhou et al., 2011). We could show that PRMT5 is highly enriched in the nucleus of satellite cells and suppresses *p21* gene transcription by heterochromatin organization thereby regulating satellite cell proliferation. Interestingly, in ES cells cytoplasmic PRMT5 plays an important role in regulating ES cell pluripotency by modulating the cytoplasmic LIF/Stat3 signaling pathway and indirectly suppressing genes that are associated with ES cell differentiation(Tee et al., 2010). Therefore, it seems that cytoplasmic or nuclear localization of PRMT5 could be involved in regulating proliferation in alternative ways in conjunction with distinct chromatin organizations in different cell types (Gu et al., 2012). Furthermore, nuclear PRMT5 appears to apply yet again distinct mechanisms to regulate neural progenitor and muscle stem cell proliferation. PRMT5 has been shown to regulate proliferation of NSCs by mediating alternative splicing events of Mdm4 that in turn leads to p53 stabilization, up-regulation of *p21* and cell cycle progression. Consistently, ablation of p53 partially rescues the proliferation defects of PRMT5 deficient NPCs *in vitro* and *in vivo* (Bezzi et al., 2013). However, in proliferating satellite cells, the up-regulation of *p21* gene expression upon PRMT5 ablation appears to be p53 independent since the binding of p53 to the *p21* locus is diminished with the absence of H3R8me2s and PRMT5 (Figure 5.6.4A). Furthermore, p53 expression in PRMT5 deficient SCs is not altered, both at the mRNA and protein level, even though alternative splicing of Mdm4 occur (Figure 5.6.4B,C and D). Additionally an increased p21 level is still observed in p53 and PRMT5 double deficient satellite cells as compared to the control cells (Figure 5.6.4E). In muscle stem cells, I could show that PRMT5 is required to reorganize chromatin structure of the *p21* gene locus and to silence *p21* gene expression. It is still an open question which transcription factors responsible for promoting transcription of the *p21* gene in PRMT5 deficient satellite cells. One of the candidates is the muscle specific transcription factor MyoD, which has been

shown to activate *p21* gene expression in cooperation with the transcriptional co-activator p300 in cultured myoblasts (de la Serna et al., 2006; Puri et al., 1997a; Puri et al., 1997b). Others might be Sp1/KLF, CREB and E2F1, which bind to the CpG island within the first intron of *p21* and activate *p21* transcription in cancer cells lines in the p53-independent way (Siatecka et al., 2010). Therefore, it will be interesting to test whether binding of these transcription factors to the *p21* locus are increased in satellite cells or muscle progenitors upon PRMT5 inactivation. Given that *p21* is not the only downstream target that mediates PRMT5 function in satellite cell proliferation, systematic RNA-seq and ChIP-seq assays are necessary for a comprehensive understanding of the PRMT5 dependent mechanism of satellite cell proliferation.

6.2 PRMT5 is required for satellite cell differentiation and muscle regeneration

While PRMT5 dependent control of proliferation in different stem cells is context dependent, an additional function of PRMT5 apparently exists in muscle stem cell differentiation. In vivo lineage tracing experiments using a Rosa26YFP reporter revealed that satellite cells without PRMT5 are unable to form MyoG+ cells on myofibers. This could not be attributed to a secondary effect of an earlier event disrupting satellite cell proliferation, since acute *in vitro* ablation of PRMT5 in proliferating SCs already expressing MyoD, also abolished terminal differentiation and inhibited formation of MyoG and MF20 positive cells. Interestingly this finding is consistent with previous *in vitro* studies showing that PRMT5 is required for differentiation of C2C12 myoblasts (Dacwag et al., 2009; Dacwag et al., 2007). Moreover the requirement of PRMT5 in satellite cell differentiation during regeneration is restricted to the myoblast stage, since the $HSA^{CreERT2}/Prmt5^{loxp/loxp}$ mice that allow ablation of PRMT5 in fully differentiated myocytes show normal regenerative capability compared to the wild type. Furthermore, differentiation of satellite cells lacking PRMT5 triggers cell apoptosis *in vitro*, which might be a reason for the loss of satellite cell numbers after ablation of PRMT5 over a prolonged time and in a regenerative environment as well. These observations, together with the finding that *p21* knockout could only partially rescue the proliferation defects but not the regeneration impairment in $Prmt5^{sKO}$ mice suggested that additional factors cooperate with or are targeted by PRMT5 at different stages of muscle regeneration (Figure 5.8). Conceivably, different cell types may express distinct recruitment factors or modulators of PRMT5, and PRMT5 may have distinct enzymatic substrates to

achieve cell type specific functions. To this end, cell type specific ChIP-seq experiments and the identification of cell type specific binding partners and substrates of PRMT5 will give more insight in elucidating the functions of PRMT5 in different contexts.

6.3 Precise cell proliferation control by PRMT5 in muscle progenitors and adult muscle stem cells

During development, myogenesis depends on highly proliferative muscle progenitor cells leading to pronounced increase of muscle mass. Similarly, regenerative myogenesis in adults relies on muscle stem cells to rebuild muscle mass after muscle injury. As such, regenerative myogenesis is reminiscent of developmental myogenesis under certain conditions (Parker et al., 2003). Along this line several factors and signaling pathways regulating muscle precursor cell expansion during development also play an important role in regulating satellite cell proliferation during regeneration. Prominent examples are the homeobox transcription factors Pax3 and the muscle regulatory factors (MRFs) such as MyoD, Myf5, MRF4 or MyoG, all of which follow similar sequential expression patterns and play similar roles during developmental and regenerative myogenesis (Braun and Gautel, 2011; Buckingham and Rigby, 2014; Le Grand and Rudnicki, 2007; Shi and Garry, 2006). However it has been suggested that distinct molecular processes distinguish cell proliferation between muscle precursors and adult muscle stem cells (Cornelison et al., 2004; Gunther et al., 2013; Lepper et al., 2009). Indeed, in this study I identified and characterized an essential role of the epigenetic modifier PRMT5 for muscle stem cell proliferation and muscle regeneration. Surprisingly, loss of Prmt5 does not affect Pax7+ muscle progenitor cell expansion and differentiation during muscle development.

One of the most obvious differences between developmental and regenerative myogenesis is the lack of quiescence of highly proliferative muscle progenitor cells during development, while satellite cells under non-regenerative physiological conditions are normally quiescent. During regeneration, and in contrast to muscle precursors, some activated satellite cells self-renew and return to quiescence to replenish the stem cell pool. This process has been attributed to asymmetric cell divisions of satellite cells, which might account for the functional differences of PRMT5 in muscle progenitors and satellite cells (Kuang et al., 2007). In the developing embryo rapidly dividing muscle precursors apparently do not receive signals from their microenvironment that would suffice for them to enter quiescence.

In contrast, it has been shown that signals emanating from the adult muscle stem cell niche play key roles in regulating stem cell asymmetry, fate and behavior (Chakkalakal et al., 2012). It is conceivable that PRMT5 mediated transcriptional and epigenetic control might be responsible for asymmetric division of satellite cells thereby differentially regulating adult stem cells and muscle progenitor cells (Bentzinger et al., 2013; Kuang et al., 2007; Yin et al., 2013a). Interestingly, a recent publication revealed that Prmt4, a protein arginine methyltransferase that is related to PRMT5 but catalyzes asymmetric but not symmetric arginine methylation in distinct histone residues, regulates asymmetric satellite cell division and muscle regeneration by methylating Pax7 directly and thereby influencing Pax7 mediated Myf5 gene expression (Kawabe et al., 2012). Whether Prmt4 would mediate epigenetic regulation of chromatin in satellite cell as an additional means to regulate asymmetric satellite cell division is still unknown. PRMT5 on the other hand appears not to control the transcription of myogenic factors such as Pax7 and Myf5 (Figure 5.6.1B), suggesting that PRMT5 might not directly control asymmetric division in satellite cells but rather controls proliferation in general by suppressing the cell cycle inhibitor p21. Notably, since adult muscle stem cells originate only from a minor fraction of Pax7+/MyoD+ muscle precursors during development (Kanisicak et al., 2009; Relaix et al., 2005; Schienda et al., 2006) (Seale et al., 2000), PRMT5 might not be responsible for the proliferation of the majority of Pax7+/MyoD+ progenitors but could instead mediate gene silencing in a subset of cells that will acquire quiescence and adult muscle stem cell features. Given that PRMT5 mediates *p21* gene silencing in adult satellite cells together with the observation that PRMT5 expression decreases within the myotome as muscle development proceeds (Figure S5), it is tempting to propose that PRMT5 may gradually diminish its expression in differentiating muscle tissue during early embryonic development and label a minor fraction of muscle precursor cells that will give rise to Pax7+/MyoD-/p21- adult muscle stem cells. In support of this hypothesis, we did not detect PRMT5 in the differentiated myofibers and only in satellite cells and myoblasts. Further lineage tracing experiments of Pax7+/PRMT5+ double positive descendants during development will be necessary to answer this question. This hypothesis also raises the idea that PRMT5 might control reentry of adult quiescent satellite cells into the cell cycle. Quiescent satellite cells express low levels of p21 and high levels of Pax7 that is counterintuitive because Pax7 expression is required for self-renewal of actively proliferating satellite cells (Gunther et al., 2013; Oustanina et al., 2004). It is conceivable that PRMT5 might regulate p21 expression levels as to retain satellite cells in a poised but quiescent state. Loss of PRMT5 results in up-regulation of p21 in satellite cells, and

this might increase the p21 dependent threshold that cannot be overcome for cell cycle reentry.

Recent studies have revealed distinct roles of Pax7 expressing progenitors during different time points along muscle development. While ablation of Pax7 expressing cells by $Pax7^{iCre+}$;$R26R^{DTA+}$ mice has little effect on embryonic myogenesis up to E14.5, there is a complete absence of fetal myogenic progenitors and myofibers upon depletion of Pax7 expressing cells from E14.5 to E18 (Hutcheson et al., 2009; Messina and Cossu, 2009). This finding together with the observations that Pax7 expressing cells are required for regenerative myogenesis (Gunther et al., 2013; Lepper et al., 2009) indicates that Pax7 expressing myogenic cells are mainly required for fetal myogenesis and adult muscle regeneration. If PRMT5 were critical for controlling embryonic but not fetal muscle progenitor cell expansion during development, inactivation of PRMT5 in Pax7 expressing cells will not influence developmental myogenesis. Therefore, ablation of PRMT5 within Pax3 or Myf5 lineages that are essential for early embryonic myogenesis will allow us to precisely delineate and narrow down the role of PRMT5 at different stages of muscle development. Along this line, comparative epigenetic, transcriptional and proteomic profiling of embryonic, fetal and adult Pax7 expressing cells will allow a more comprehensive understanding of the differences between developmental and regenerative myogenesis. Equally important will be to address how PRMT5 expression itself is regulated in these two settings as well.

6.4 Linking PRMT5 mediated satellite cell proliferation to Duchenne Muscular Dystrophy

Human Duchenne Muscular Dystrophy (DMD) is a severe muscle wasting disease in which diaphragm and skeletal muscles are characterized by constant muscle degeneration/regeneration cycles. A recent study demonstrated that while DMD pathology is driven by dystrophin deficiency in myofibers, DMD is ultimately a stem cell exhaustion disease (Sacco et al., 2010). Indeed, myoblasts from DMD patients exhibit severe proliferative defects *in vitro* (Blau et al., 1983; Blau et al., 1985). Consistently, Sacco et al. reported that telomere shortening occurring in mdx mice completely lacking telomerase activity (mdx/mTR2G mice) resulted in muscle stem cell proliferation defects and the phenotype in these mice recapitulates the gross muscle defects seen in human DMD (Mourkioti et al., 2013; Sacco et al., 2010). Interestingly, the pathology was only obvious in 72 weeks old mdx/mTR2G mice. The pivotal role of PRMT5 in satellite cell mediated muscle regeneration is underscored

by the finding that loss of PRMT5 not only results in a dramatic loss of satellite cells over time but also in severe muscle wasting in mdx mice. Remarkably, the pathology in PRMT5^{sKO}/mdx mice that is reminiscent of the dystrophic phenotype observed in DMD patients can be observed within only 90 days after induced deletion of PRMT5 and specifically in satellite cells. While we are still lacking detailed physiological analyses of muscle function in *Prmt5*^{sKO}/mdx mice, these findings provide an inducible and muscle stem cell specific genetic mouse model that enables to investigate early events during the onset and progression of DMD and might thus serve as a useful test system for therapeutic interventions.

It has not missed our attention that this model also fuels the debate on whether alternative stem cell types apart from Pax7+ SCs could contribute to muscle regeneration. As for mice lacking PRMT5 in Pax7 expressing satellite cells this does not seem to be the case. The finding that satellite cell specific deletion of PRMT5 results in progressive loss of satellite cells over time both under physiological and pathological conditions, together with the observation that damaged muscle of *Prmt5*^{sKO} mice could not be regenerated even 4 months after injury, indicates that 1) alternative stem cells to Pax7+ satellite cells cannot compensate for the regeneration impairment and satellite cell loss occurring in *Prmt5*^{sKO} or *Prmt5*^{sKO}/mdx mice, and 2) that Pax7+ cells are not sufficiently generated *de novo* if satellite cells are once lost given that Tamoxifen administration was applied only in the first 3 weeks. Intriguingly, it was recently shown that progressive loss of muscle stem cell numbers, activity and proliferation capacity during aging is associated with a high incidence of muscle stem cells that express elevated levels of p16 and p21, and this is due to elevated activity of the p38 mitogen-activated kinase pathway (Bernet et al., 2014; Cosgrove et al., 2014; Sousa-Victor et al., 2014). Strikingly, in the study by Sousa-Victor et al., PRMT5 expression has been shown to be reduced in 12-month-old SAMP8 mice that serve as a mouse model of progeria (Sousa-Victor et al., 2014). These findings together with the fact that PRMT5 inactivation results in elevated p21 levels, impaired proliferation and loss of satellite cells over time gives rise to the notion that epigenetic deregulation of muscle stem cells due to loss of PRMT5 activity might partially contribute to the loss of satellite cell mediated regeneration during aging.

6.5 PR-Set7, H4K20me1 and active transcription

Histone H4 Lys 20 mono-methylation (H4K20me1) has been implicated in regulating diverse processes such as cell cycle progression, DNA replication, DNA repair and gene regulation. H4K20me1 is catalyzed by the sole enzyme termed PR-Set7/Set8/KMT5 (Beck et al., 2012a; Schotta et al., 2008). Loss of PR-Set7

diminishes not only H4k20me1 but also H4K20me2 and H4K20me3. Consequently mice lacking PR-Set7 show major defects of early embryonic development (Oda et al., 2009). Despite numerous efforts, the role of H4K20me1 and PR-Set7 in gene transcription remains elusive. While initial studies suggested a role of PR-Set7 mediated H4K20me1 in transcriptional repression, recent epigenomic studies indicate a role of H4K20me1 in transcriptional activation (Abbas et al., 2010; Barski et al., 2007; Congdon et al., 2010; Wang et al., 2009). The released ChIP seq data from the human cell lines demonstrated that H4K20me1 is specifically enriched in intergenic regions and correlates with transcription activation. Along this line, ChIP-seq data of H4K20me1 in both proliferating and differentiating C2C12 cells show a positive correlation of this modification with gene transcription activity, high CpG content promoters, Pol II binding and other active transcription modifications such as H3K4me3, H3K36me3. Depletion of Pr-set7 by shRNAs reduces H4K20me1 and targeted gene repression. Interestingly this correlation with active transcription is more obvious in differentiating cells as compared to proliferating cells. Given that PR-Set7/H4K20me1 has been shown to actively regulate cell cycle and DNA replication, the less obvious correlation of ChIP-seq of H4K20me1 with transcription activation in proliferating cells might be due to the mixed mapping of H4K20me1 to sites of both DNA replication and gene transcription, which does not occur in differentiating cells with nearly no DNA replications. Furthermore transition from proliferating to differentiating C2C12 cells correlates with shifting of enrichment of H4K20me1 from the intergenic region to the intragenic region including TSS, introns and exons. Additional deep analyses of H4K20me1 ChIP-seq in differentiating C2C12 cells revealed that H4K20me1 predominantly peaks at the 5’ site of the gene body downstream from the TSS suggesting a role of H4K20me1 in early transcription elongation. This pattern of enrichment in the gene body is actually distinct from H3K36me3, whose enrichment peaks in the 3’ site near the transcription end site (TES) of the intron-containing genes. In yeast, it has been shown that the H3K36 methyltransferase Set2 binds directly to Pol II CTD phosphorylated on Ser2 (Ser2P), which also peaks at the 3’ site of the gene body, linking Set2 mediated H3K36me3 to transcriptional elongation coupled mRNA splicing of intron-containing genes (de Almeida et al., 2011). It seems that PR-Set7 mediated H4K20me1 might use similar mechanism as Set2 mediated H3K36me3 in control of transcriptional elongation by associating with Pol II Ser5P CTD. Indeed recent studies by Paula Vertino and colleagues demonstrated a dual role of PR-Set7 and histone H4K20me1 in the local regulation of RNA Pol II pausing by establishing both the H4K16ac and H4K20me3 marks (Kapoor-Vazirani and Vertino, 2014). Inhibition of the Ser5P CTD of Pol II by

DRB blocks transcription elongation but doesn't affect the H4K20me1 enrichment within the gene body. Therefore, it is still worth to address how the crosstalk between PR-Set7 induced H4K20me1 and MSL mediated H4K16ac is required for Pol II Ser5P and relieve of transcription pausing. The association of H4K20me1 in the gene body also implies a role of PR-Set7/H4K20me1 in transcriptional coupled splicing as well. In support of this several splicing factors including Srrm2, Hnrnpa2b1, Prp8, Dnajc13 and Caperas have been identified as PR-Set7 interaction partners using Co-IPand subsequent mass spectrometry. It will be very interesting to further analyze whether PR-Set7 and H4K20me1 are involved in co-transcriptional splicing thereby regulating transcriptional elongation during active gene expression in differentiating cells.

7 REFERENCES

Abbas, T., Shibata, E., Park, J., Jha, S., Karnani, N., and Dutta, A. (2010). CRL4(Cdt2) regulates cell proliferation and histone gene expression by targeting PR-Set7/Set8 for degradation. Molecular cell *40*, 9-21.

Abou-Khalil, R., Le Grand, F., Pallafacchina, G., Valable, S., Authier, F.J., Rudnicki, M.A., Gherardi, R.K., Germain, S., Chretien, F., Sotiropoulos, A.*, et al.* (2009). Autocrine and paracrine angiopoietin 1/Tie-2 signaling promotes muscle satellite cell self-renewal. Cell stem cell *5*, 298-309.

Alfaro, L.A., Dick, S.A., Siegel, A.L., Anonuevo, A.S., McNagny, K.M., Megeney, L.A., Cornelison, D.D., and Rossi, F.M. (2011). CD34 promotes satellite cell motility and entry into proliferation to facilitate efficient skeletal muscle regeneration. Stem Cells *29*, 2030-2041.

Ancelin, K., Lange, U.C., Hajkova, P., Schneider, R., Bannister, A.J., Kouzarides, T., and Surani, M.A. (2006). Blimp1 associates with Prmt5 and directs histone arginine methylation in mouse germ cells. Nat Cell Biol *8*, 623-630.

Anne, J., Ollo, R., Ephrussi, A., and Mechler, B.M. (2007). Arginine methyltransferase Capsuleen is essential for methylation of spliceosomal Sm proteins and germ cell formation in Drosophila. Development *134*, 137-146.

Asakura, A., Seale, P., Girgis-Gabardo, A., and Rudnicki, M.A. (2002). Myogenic specification of side population cells in skeletal muscle. J Cell Biol *159*, 123-134.

Asp, P., Blum, R., Vethantham, V., Parisi, F., Micsinai, M., Cheng, J., Bowman, C., Kluger, Y., and Dynlacht, B.D. (2011). Genome-wide remodeling of the epigenetic landscape during myogenic differentiation. Proceedings of the National Academy of Sciences of the United States of America *108*, E149-158.

Auclair, Y., and Richard, S. (2013). The role of arginine methylation in the DNA damage response. DNA repair *12*, 459-465.

Bandyopadhyay, S., Harris, D.P., Adams, G.N., Lause, G.E., McHugh, A., Tillmaand, E.G., Money, A., Willard, B., Fox, P.L., and Dicorleto, P.E. (2012). HOXA9 methylation by PRMT5 is essential for endothelial cell expression of leukocyte adhesion molecules. Mol Cell Biol *32*, 1202-1213.

Barski, A., Cuddapah, S., Cui, K., Roh, T.Y., Schones, D.E., Wang, Z., Wei, G., Chepelev, I., and Zhao, K. (2007). High-resolution profiling of histone methylations in the human genome. Cell *129*, 823-837.

Beck, D.B., Oda, H., Shen, S.S., and Reinberg, D. (2012a). PR-Set7 and H4K20me1: at the crossroads of genome integrity, cell cycle, chromosome condensation, and transcription. Genes & development *26*, 325-337.

Beck, D.B., Oda, H., Shen, S.S., and Reinberg, D. (2012b). PR-Set7 and H4K20me1: at the crossroads of genome integrity, cell cycle, chromosome condensation, and transcription. Genes Dev *26*, 325-337.

Bedford, M.T., and Clarke, S.G. (2009). Protein arginine methylation in mammals: who, what, and why. Molecular cell *33*, 1-13.

Bell, C.D., and Conen, P.E. (1968). Histopathological changes in Duchenne muscular dystrophy. Journal of the neurological sciences *7*, 529-544.

Bentzinger, C.F., Barzaghi, P., Lin, S., and Ruegg, M.A. (2005). Overexpression of mini-agrin in skeletal muscle increases muscle integrity and regenerative capacity in

laminin-alpha2-deficient mice. FASEB journal : official publication of the Federation of American Societies for Experimental Biology *19*, 934-942.

Bentzinger, C.F., Wang, Y.X., Dumont, N.A., and Rudnicki, M.A. (2013). Cellular dynamics in the muscle satellite cell niche. EMBO reports *14*, 1062-1072.

Bernet, J.D., Doles, J.D., Hall, J.K., Kelly Tanaka, K., Carter, T.A., and Olwin, B.B. (2014). p38 MAPK signaling underlies a cell-autonomous loss of stem cell self-renewal in skeletal muscle of aged mice. Nature medicine *20*, 265-271.

Bezzi, M., Teo, S.X., Muller, J., Mok, W.C., Sahu, S.K., Vardy, L.A., Bonday, Z.Q., and Guccione, E. (2013). Regulation of constitutive and alternative splicing by PRMT5 reveals a role for Mdm4 pre-mRNA in sensing defects in the spliceosomal machinery. Genes Dev *27*, 1903-1916.

Biressi, S., Tagliafico, E., Lamorte, G., Monteverde, S., Tenedini, E., Roncaglia, E., Ferrari, S., Cusella-De Angelis, M.G., Tajbakhsh, S., and Cossu, G. (2007). Intrinsic phenotypic diversity of embryonic and fetal myoblasts is revealed by genome-wide gene expression analysis on purified cells. Developmental biology *304*, 633-651.

Bischoff, R. (1986). Proliferation of muscle satellite cells on intact myofibers in culture. Developmental biology *115*, 129-139.

Blau, H.M., Webster, C., and Pavlath, G.K. (1983). Defective myoblasts identified in Duchenne muscular dystrophy. Proceedings of the National Academy of Sciences of the United States of America *80*, 4856-4860.

Blau, H.M., Webster, C., Pavlath, G.K., and Chiu, C.P. (1985). Evidence for defective myoblasts in Duchenne muscular dystrophy. Advances in experimental medicine and biology *182*, 85-110.

Bober, E., Brand-Saberi, B., Ebensperger, C., Wilting, J., Balling, R., Paterson, B.M., Arnold, H.H., and Christ, B. (1994). Initial steps of myogenesis in somites are independent of influence from axial structures. Development *120*, 3073-3082.

Bosnakovski, D., Xu, Z., Li, W., Thet, S., Cleaver, O., Perlingeiro, R.C., and Kyba, M. (2008). Prospective isolation of skeletal muscle stem cells with a Pax7 reporter. Stem Cells *26*, 3194-3204.

Braun, T., and Gautel, M. (2011). Transcriptional mechanisms regulating skeletal muscle differentiation, growth and homeostasis. Nat Rev Mol Cell Biol *12*, 349-361.

Braun, T., and Martire, A. (2007). Cardiac stem cells: paradigm shift or broken promise? A view from developmental biology. Trends in biotechnology *25*, 441-447.

Buckingham, M., and Rigby, P.W. (2014). Gene regulatory networks and transcriptional mechanisms that control myogenesis. Dev Cell *28*, 225-238.

Burkin, D.J., and Kaufman, S.J. (1999). The alpha7beta1 integrin in muscle development and disease. Cell Tissue Res *296*, 183-190.

Cao, Y., Kumar, R.M., Penn, B.H., Berkes, C.A., Kooperberg, C., Boyer, L.A., Young, R.A., and Tapscott, S.J. (2006). Global and gene-specific analyses show distinct roles for Myod and Myog at a common set of promoters. EMBO J *25*, 502-511.

Carlson, M.E., Hsu, M., and Conboy, I.M. (2008). Imbalance between pSmad3 and Notch induces CDK inhibitors in old muscle stem cells. Nature *454*, 528-532.

Casse, C., Giannoni, F., Nguyen, V.T., Dubois, M.F., and Bensaude, O. (1999). The transcriptional inhibitors, actinomycin D and alpha-amanitin, activate the HIV-1 promoter and favor phosphorylation of the RNA polymerase II C-terminal domain. The Journal of biological chemistry *274*, 16097-16106.

Chakkalakal, J.V., Jones, K.M., Basson, M.A., and Brack, A.S. (2012). The aged niche disrupts muscle stem cell quiescence. Nature *490*, 355-360.

Chang, B., Chen, Y., Zhao, Y., and Bruick, R.K. (2007). JMJD6 is a histone arginine demethylase. Science *318*, 444-447.

Chang, H.H., Hu, H.H., Lee, Y.J., Wei, H.M., Fan-June, M.C., Hsu, T.C., Tsay, G.J., and Li, C. (2013). Proteomic analyses and identification of arginine methylated proteins differentially recognized by autosera from anti-Sm positive SLE patients. J Biomed Sci *20*, 27.

Chang, T.H., Primig, M., Hadchouel, J., Tajbakhsh, S., Rocancourt, D., Fernandez, A., Kappler, R., Scherthan, H., and Buckingham, M. (2004). An enhancer directs differential expression of the linked Mrf4 and Myf5 myogenic regulatory genes in the mouse. Dev Biol *269*, 595-608.

Chen, C., Nott, T.J., Jin, J., and Pawson, T. (2011). Deciphering arginine methylation: Tudor tells the tale. Nature reviews Molecular cell biology *12*, 629-642.

Cheng, W.C., Chang, Y.N., and Wang, W.C. (2005). Structural basis for shikimate-binding specificity of Helicobacter pylori shikimate kinase. Journal of bacteriology *187*, 8156-8163.

Cheung, T.H., and Rando, T.A. (2013). Molecular regulation of stem cell quiescence. Nat Rev Mol Cell Biol *14*, 329-340.

Cho, E.C., Zheng, S., Munro, S., Liu, G., Carr, S.M., Moehlenbrink, J., Lu, Y.C., Stimson, L., Khan, O., Konietzny, R.*, et al.* (2012). Arginine methylation controls growth regulation by E2F-1. EMBO J *31*, 1785-1797.

Choudhury, A.R., Ju, Z., Djojosubroto, M.W., Schienke, A., Lechel, A., Schaetzlein, S., Jiang, H., Stepczynska, A., Wang, C., Buer, J.*, et al.* (2007). Cdkn1a deletion improves stem cell function and lifespan of mice with dysfunctional telomeres without accelerating cancer formation. Nat Genet *39*, 99-105.

Christov, C., Chretien, F., Abou-Khalil, R., Bassez, G., Vallet, G., Authier, F.J., Bassaglia, Y., Shinin, V., Tajbakhsh, S., Chazaud, B.*, et al.* (2007). Muscle satellite cells and endothelial cells: close neighbors and privileged partners. Molecular biology of the cell *18*, 1397-1409.

Chung, J., Karkhanis, V., Tae, S., Yan, F., Smith, P., Ayers, L.W., Agostinelli, C., Pileri, S., Denis, G.V., Baiocchi, R.A.*, et al.* (2013). Protein arginine methyltransferase 5 (PRMT5) inhibition induces lymphoma cell death through reactivation of the retinoblastoma tumor suppressor pathway and polycomb repressor complex 2 (PRC2) silencing. J Biol Chem *288*, 35534-35547.

Ciciliot, S., and Schiaffino, S. (2010). Regeneration of mammalian skeletal muscle. Basic mechanisms and clinical implications. Curr Pharm Des *16*, 906-914.

Cohn, R.D., Henry, M.D., Michele, D.E., Barresi, R., Saito, F., Moore, S.A., Flanagan, J.D., Skwarchuk, M.W., Robbins, M.E., Mendell, J.R.*, et al.* (2002). Disruption of DAG1 in differentiated skeletal muscle reveals a role for dystroglycan in muscle regeneration. Cell *110*, 639-648.

Conboy, I.M., Conboy, M.J., Smythe, G.M., and Rando, T.A. (2003). Notch-mediated restoration of regenerative potential to aged muscle. Science *302*, 1575-1577.

Conboy, M.J., Karasov, A.O., and Rando, T.A. (2007). High incidence of non-random template strand segregation and asymmetric fate determination in dividing stem cells and their progeny. PLoS Biol *5*, e102.

Congdon, L.M., Houston, S.I., Veerappan, C.S., Spektor, T.M., and Rice, J.C. (2010). PR-Set7-mediated monomethylation of histone H4 lysine 20 at specific genomic

regions induces transcriptional repression. Journal of cellular biochemistry *110*, 609-619.

Cornelison, D.D., Filla, M.S., Stanley, H.M., Rapraeger, A.C., and Olwin, B.B. (2001). Syndecan-3 and syndecan-4 specifically mark skeletal muscle satellite cells and are implicated in satellite cell maintenance and muscle regeneration. Dev Biol *239*, 79-94.

Cornelison, D.D., Olwin, B.B., Rudnicki, M.A., and Wold, B.J. (2000). MyoD(-/-) satellite cells in single-fiber culture are differentiation defective and MRF4 deficient. Dev Biol *224*, 122-137.

Cornelison, D.D., Wilcox-Adelman, S.A., Goetinck, P.F., Rauvala, H., Rapraeger, A.C., and Olwin, B.B. (2004). Essential and separable roles for Syndecan-3 and Syndecan-4 in skeletal muscle development and regeneration. Genes & development *18*, 2231-2236.

Cornelison, D.D., and Wold, B.J. (1997). Single-cell analysis of regulatory gene expression in quiescent and activated mouse skeletal muscle satellite cells. Dev Biol *191*, 270-283.

Cosgrove, B.D., Gilbert, P.M., Porpiglia, E., Mourkioti, F., Lee, S.P., Corbel, S.Y., Llewellyn, M.E., Delp, S.L., and Blau, H.M. (2014). Rejuvenation of the muscle stem cell population restores strength to injured aged muscles. Nature medicine *20*, 255-264.

Cosgrove, B.D., Sacco, A., Gilbert, P.M., and Blau, H.M. (2009). A home away from home: challenges and opportunities in engineering *in vitro* muscle satellite cell niches. Differentiation; research in biological diversity *78*, 185-194.

Cuthbert, G.L., Daujat, S., Snowden, A.W., Erdjument-Bromage, H., Hagiwara, T., Yamada, M., Schneider, R., Gregory, P.D., Tempst, P., Bannister, A.J.*, et al.* (2004). Histone deimination antagonizes arginine methylation. Cell *118*, 545-553.

Dacwag, C.S., Bedford, M.T., Sif, S., and Imbalzano, A.N. (2009). Distinct protein arginine methyltransferases promote ATP-dependent chromatin remodeling function at different stages of skeletal muscle differentiation. Mol Cell Biol *29*, 1909-1921.

Dacwag, C.S., Ohkawa, Y., Pal, S., Sif, S., and Imbalzano, A.N. (2007). The protein arginine methyltransferase Prmt5 is required for myogenesis because it facilitates ATP-dependent chromatin remodeling. Mol Cell Biol *27*, 384-394.

de Almeida, S.F., Grosso, A.R., Koch, F., Fenouil, R., Carvalho, S., Andrade, J., Levezinho, H., Gut, M., Eick, D., Gut, I.*, et al.* (2011). Splicing enhances recruitment of methyltransferase HYPB/Setd2 and methylation of histone H3 Lys36. Nature structural & molecular biology *18*, 977-983.

de Kermadec, J.M., Becane, H.M., Chenard, A., Tertrain, F., and Weiss, Y. (1994). Prevalence of left ventricular systolic dysfunction in Duchenne muscular dystrophy: an echocardiographic study. American heart journal *127*, 618-623.

de la Serna, I.L., Ohkawa, Y., Higashi, C., Dutta, C., Osias, J., Kommajosyula, N., Tachibana, T., and Imbalzano, A.N. (2006). The microphthalmia-associated transcription factor requires SWI/SNF enzymes to activate melanocyte-specific genes. The Journal of biological chemistry *281*, 20233-20241.

de Mercoyrol, L., Job, C., and Job, D. (1989). Studies on the inhibition by alpha-amanitin of single-step addition reactions and productive RNA synthesis catalysed by wheat-germ RNA polymerase II. The Biochemical journal *258*, 165-169.

Deaton, A.M., and Bird, A. (2011). CpG islands and the regulation of transcription. Genes & development *25*, 1010-1022.

Decary, S., Hamida, C.B., Mouly, V., Barbet, J.P., Hentati, F., and Butler-Browne, G.S. (2000). Shorter telomeres in dystrophic muscle consistent with extensive regeneration in young children. Neuromuscular disorders : NMD *10*, 113-120.

Dellavalle, A., Maroli, G., Covarello, D., Azzoni, E., Innocenzi, A., Perani, L., Antonini, S., Sambasivan, R., Brunelli, S., Tajbakhsh, S.*, et al.* (2011). Pericytes resident in postnatal skeletal muscle differentiate into muscle fibres and generate satellite cells. Nat Commun *2*, 499.

Deng, C., Zhang, P., Harper, J.W., Elledge, S.J., and Leder, P. (1995). Mice lacking p21CIP1/WAF1 undergo normal development, but are defective in G1 checkpoint control. Cell *82*, 675-684.

Dilworth, F.J., and Blais, A. (2011). Epigenetic regulation of satellite cell activation during muscle regeneration. Stem Cell Res Ther *2*, 18.

DiMario, J.X., Uzman, A., and Strohman, R.C. (1991). Fiber regeneration is not persistent in dystrophic (MDX) mouse skeletal muscle. Developmental biology *148*, 314-321.

Dobreva, G., and Braun, T. (2010). The yin and yang of polycomb repression in regenerating muscle. Cell Stem Cell *7*, 422-424.

Dong, F., Sun, X., Liu, W., Ai, D., Klysik, E., Lu, M.F., Hadley, J., Antoni, L., Chen, L., Baldini, A.*, et al.* (2006). Pitx2 promotes development of splanchnic mesoderm-derived branchiomeric muscle. Development *133*, 4891-4899.

DuBridge, R.B., Tang, P., Hsia, H.C., Leong, P.M., Miller, J.H., and Calos, M.P. (1987). Analysis of mutation in human cells by using an Epstein-Barr virus shuttle system. Molecular and cellular biology *7*, 379-387.

Eagle, M., Baudouin, S.V., Chandler, C., Giddings, D.R., Bullock, R., and Bushby, K. (2002). Survival in Duchenne muscular dystrophy: improvements in life expectancy since 1967 and the impact of home nocturnal ventilation. Neuromuscular disorders : NMD *12*, 926-929.

Eckert, D., Biermann, K., Nettersheim, D., Gillis, A.J., Steger, K., Jack, H.M., Muller, A.M., Looijenga, L.H., and Schorle, H. (2008). Expression of BLIMP1/PRMT5 and concurrent histone H2A/H4 arginine 3 dimethylation in fetal germ cells, CIS/IGCNU and germ cell tumors. BMC Dev Biol *8*, 106.

Fischer, A.H., Jacobson, K.A., Rose, J., and Zeller, R. (2008). Hematoxylin and eosin staining of tissue and cell sections. CSH Protoc *2008*, pdb prot4986.

Forcales, S.V., Albini, S., Giordani, L., Malecova, B., Cignolo, L., Chernov, A., Coutinho, P., Saccone, V., Consalvi, S., Williams, R.*, et al.* (2012). Signal-dependent incorporation of MyoD-BAF60c into Brg1-based SWI/SNF chromatin-remodelling complex. The EMBO journal *31*, 301-316.

Francetic, T., and Li, Q. (2011). Skeletal myogenesis and Myf5 activation. Transcription *2*, 109-114.

Franz, T., Kothary, R., Surani, M.A., Halata, Z., and Grim, M. (1993). The Splotch mutation interferes with muscle development in the limbs. Anat Embryol (Berl) *187*, 153-160.

Friesen, W.J., Paushkin, S., Wyce, A., Massenet, S., Pesiridis, G.S., Van Duyne, G., Rappsilber, J., Mann, M., and Dreyfuss, G. (2001). The methylosome, a 20S complex containing JBP1 and pICln, produces dimethylarginine-modified Sm proteins. Mol Cell Biol *21*, 8289-8300.

Fukada, S., Higuchi, S., Segawa, M., Koda, K., Yamamoto, Y., Tsujikawa, K., Kohama, Y., Uezumi, A., Imamura, M., Miyagoe-Suzuki, Y.*, et al.* (2004). Purification

and cell-surface marker characterization of quiescent satellite cells from murine skeletal muscle by a novel monoclonal antibody. Exp Cell Res *296*, 245-255.

Fulco, M., Schiltz, R.L., Iezzi, S., King, M.T., Zhao, P., Kashiwaya, Y., Hoffman, E., Veech, R.L., and Sartorelli, V. (2003). Sir2 regulates skeletal muscle differentiation as a potential sensor of the redox state. Mol Cell *12*, 51-62.

Gage, P.J., and Camper, S.A. (1997). Pituitary homeobox 2, a novel member of the bicoid-related family of homeobox genes, is a potential regulator of anterior structure formation. Hum Mol Genet *6*, 457-464.

Gary, J.D., and Clarke, S. (1998). RNA and protein interactions modulated by protein arginine methylation. Prog Nucleic Acid Res Mol Biol *61*, 65-131.

Gensch, N., Borchardt, T., Schneider, A., Riethmacher, D., and Braun, T. (2008). Different autonomous myogenic cell populations revealed by ablation of Myf5-expressing cells during mouse embryogenesis. Development *135*, 1597-1604.

George, R.M., Biressi, S., Beres, B.J., Rogers, E., Mulia, A.K., Allen, R.E., Rawls, A., Rando, T.A., and Wilson-Rawls, J. (2013). Numb-deficient satellite cells have regeneration and proliferation defects. Proc Natl Acad Sci U S A *110*, 18549-18554.

Gilbert, P.M., Havenstrite, K.L., Magnusson, K.E., Sacco, A., Leonardi, N.A., Kraft, P., Nguyen, N.K., Thrun, S., Lutolf, M.P., and Blau, H.M. (2010). Substrate elasticity regulates skeletal muscle stem cell self-renewal in culture. Science *329*, 1078-1081.

Giordani, L., and Puri, P.L. (2013). Epigenetic control of skeletal muscle regeneration: Integrating genetic determinants and environmental changes. FEBS J *280*, 4014-4025.

Girardot, M., Hirasawa, R., Kacem, S., Fritsch, L., Pontis, J., Kota, S.K., Filipponi, D., Fabbrizio, E., Sardet, C., Lohmann, F.*, et al.* (2014). PRMT5-mediated histone H4 arginine-3 symmetrical dimethylation marks chromatin at G + C-rich regions of the mouse genome. Nucleic Acids Res *42*, 235-248.

Gkountela, S., Li, Z., Chin, C.J., Lee, S.A., and Clark, A.T. (2014). PRMT5 is required for human embryonic stem cell proliferation but not pluripotency. Stem cell reviews *10*, 230-239.

Gonsalvez, G.B., Rajendra, T.K., Tian, L., and Matera, A.G. (2006). The Sm-protein methyltransferase, dart5, is essential for germ-cell specification and maintenance. Curr Biol *16*, 1077-1089.

Goulding, M., Lumsden, A., and Paquette, A.J. (1994). Regulation of Pax-3 expression in the dermomyotome and its role in muscle development. Development *120*, 957-971.

Greer, E.L., and Shi, Y. (2012). Histone methylation: a dynamic mark in health, disease and inheritance. Nature reviews Genetics *13*, 343-357.

Gros, J., Manceau, M., Thome, V., and Marcelle, C. (2005). A common somitic origin for embryonic muscle progenitors and satellite cells. Nature *435*, 954-958.

Gu, Z., Li, Y., Lee, P., Liu, T., Wan, C., and Wang, Z. (2012). Protein arginine methyltransferase 5 functions in opposite ways in the cytoplasm and nucleus of prostate cancer cells. PloS one *7*, e44033.

Guerci, A., Lahoute, C., Hebrard, S., Collard, L., Graindorge, D., Favier, M., Cagnard, N., Batonnet-Pichon, S., Precigout, G., Garcia, L.*, et al.* (2012). Srf-dependent paracrine signals produced by myofibers control satellite cell-mediated skeletal muscle hypertrophy. Cell metabolism *15*, 25-37.

Gunther, S., Kim, J., Kostin, S., Lepper, C., Fan, C.M., and Braun, T. (2013). Myf5-positive satellite cells contribute to Pax7-dependent long-term maintenance of adult muscle stem cells. Cell Stem Cell *13*, 590-601.

Gurung, B., Feng, Z., Iwamoto, D.V., Thiel, A., Jin, G., Fan, C.M., Ng, J.M., Curran, T., and Hua, X. (2013). Menin epigenetically represses Hedgehog signaling in MEN1 tumor syndrome. Cancer Res *73*, 2650-2658.

Haberland, M., Montgomery, R.L., and Olson, E.N. (2009). The many roles of histone deacetylases in development and physiology: implications for disease and therapy. Nat Rev Genet *10*, 32-42.

Haldar, M., Karan, G., Tvrdik, P., and Capecchi, M.R. (2008). Two cell lineages, myf5 and myf5-independent, participate in mouse skeletal myogenesis. Dev Cell *14*, 437-445.

Halevy, O., Novitch, B.G., Spicer, D.B., Skapek, S.X., Rhee, J., Hannon, G.J., Beach, D., and Lassar, A.B. (1995). Correlation of terminal cell cycle arrest of skeletal muscle with induction of p21 by MyoD. Science *267*, 1018-1021.

Hamed, M., Khilji, S., Chen, J., and Li, Q. (2013). Stepwise acetyltransferase association and histone acetylation at the Myod1 locus during myogenic differentiation. Sci Rep *3*, 2390.

Hawke, T.J., and Garry, D.J. (2001). Myogenic satellite cells: physiology to molecular biology. J Appl Physiol (1985) *91*, 534-551.

Heslop, L., Morgan, J.E., and Partridge, T.A. (2000). Evidence for a myogenic stem cell that is exhausted in dystrophic muscle. Journal of cell science *113 (Pt 12)*, 2299-2308.

Hosohata, K., Li, P., Hosohata, Y., Qin, J., Roeder, R.G., and Wang, Z. (2003). Purification and identification of a novel complex which is involved in androgen receptor-dependent transcription. Mol Cell Biol *23*, 7019-7029.

Hossain, M.A., Chung, C., Pradhan, S.K., and Johnson, T.L. (2013). The yeast cap binding complex modulates transcription factor recruitment and establishes proper histone H3K36 trimethylation during active transcription. Molecular and cellular biology *33*, 785-799.

Hsu, J.M., Chen, C.T., Chou, C.K., Kuo, H.P., Li, L.Y., Lin, C.Y., Lee, H.J., Wang, Y.N., Liu, M., Liao, H.W*., et al.* (2011). Crosstalk between Arg 1175 methylation and Tyr 1173 phosphorylation negatively modulates EGFR-mediated ERK activation. Nat Cell Biol *13*, 174-181.

Hutcheson, D.A., Zhao, J., Merrell, A., Haldar, M., and Kardon, G. (2009). Embryonic and fetal limb myogenic cells are derived from developmentally distinct progenitors and have different requirements for beta-catenin. Genes Dev *23*, 997-1013.

Jang, B., Ishigami, A., Maruyama, N., Carp, R.I., Kim, Y.S., and Choi, E.K. (2013). Peptidylarginine deiminase and protein citrullination in prion diseases: strong evidence of neurodegeneration. Prion *7*, 42-46.

Jansson, M., Durant, S.T., Cho, E.C., Sheahan, S., Edelmann, M., Kessler, B., and La Thangue, N.B. (2008). Arginine methylation regulates the p53 response. Nat Cell Biol *10*, 1431-1439.

Jelinic, P., Stehle, J.C., and Shaw, P. (2006). The testis-specific factor CTCFL cooperates with the protein methyltransferase PRMT7 in H19 imprinting control region methylation. PLoS Biol *4*, e355.

Jerome, L.A., and Papaioannou, V.E. (2001). DiGeorge syndrome phenotype in mice mutant for the T-box gene, Tbx1. Nat Genet *27*, 286-291.

Joe, A.W., Yi, L., Natarajan, A., Le Grand, F., So, L., Wang, J., Rudnicki, M.A., and Rossi, F.M. (2010a). Muscle injury activates resident fibro/adipogenic progenitors that facilitate myogenesis. Nat Cell Biol *12*, 153-163.

Joe, A.W., Yi, L., Natarajan, A., Le Grand, F., So, L., Wang, J., Rudnicki, M.A., and Rossi, F.M. (2010b). Muscle injury activates resident fibro/adipogenic progenitors that facilitate myogenesis. Nat Cell Biol *12*, 153-163.

Juan, A.H., Derfoul, A., Feng, X., Ryall, J.G., Dell'Orso, S., Pasut, A., Zare, H., Simone, J.M., Rudnicki, M.A., and Sartorelli, V. (2011). Polycomb EZH2 controls self-renewal and safeguards the transcriptional identity of skeletal muscle stem cells. Genes Dev *25*, 789-794.

Kang, J.S., and Krauss, R.S. (2010). Muscle stem cells in developmental and regenerative myogenesis. Curr Opin Clin Nutr Metab Care *13*, 243-248.

Kanisicak, O., Mendez, J.J., Yamamoto, S., Yamamoto, M., and Goldhamer, D.J. (2009). Progenitors of skeletal muscle satellite cells express the muscle determination gene, MyoD. Dev Biol *332*, 131-141.

Kapoor-Vazirani, P., and Vertino, P.M. (2014). A dual role for the histone methyltransferase PR-SET7/SETD8 and histone H4 lysine 20 monomethylation in the local regulation of RNA polymerase II pausing. The Journal of biological chemistry *289*, 7425-7437.

Karkhanis, V., Hu, Y.J., Baiocchi, R.A., Imbalzano, A.N., and Sif, S. (2011). Versatility of PRMT5-induced methylation in growth control and development. Trends in biochemical sciences *36*, 633-641.

Kassar-Duchossoy, L., Giacone, E., Gayraud-Morel, B., Jory, A., Gomes, D., and Tajbakhsh, S. (2005). Pax3/Pax7 mark a novel population of primitive myogenic cells during development. Genes Dev *19*, 1426-1431.

Kawabe, Y., Wang, Y.X., McKinnell, I.W., Bedford, M.T., and Rudnicki, M.A. (2012). Carm1 regulates Pax7 transcriptional activity through MLL1/2 recruitment during asymmetric satellite stem cell divisions. Cell Stem Cell *11*, 333-345.

Keller, C., Hansen, M.S., Coffin, C.M., and Capecchi, M.R. (2004). Pax3:Fkhr interferes with embryonic Pax3 and Pax7 function: implications for alveolar rhabdomyosarcoma cell of origin. Genes Dev *18*, 2608-2613.

Kelly, R.G., Jerome-Majewska, L.A., and Papaioannou, V.E. (2004). The del22q11.2 candidate gene Tbx1 regulates branchiomeric myogenesis. Hum Mol Genet *13*, 2829-2840.

Kolodziej, S., Kuvardina, O.N., Oellerich, T., Herglotz, J., Backert, I., Kohrs, N., Buscato, E., Wittmann, S.K., Salinas-Riester, G., Bonig, H.*, et al.* (2014). PADI4 acts as a coactivator of Tal1 by counteracting repressive histone arginine methylation. Nature communications *5*, 3995.

Kuang, S., Kuroda, K., Le Grand, F., and Rudnicki, M.A. (2007). Asymmetric self-renewal and commitment of satellite stem cells in muscle. Cell *129*, 999-1010.

Kwak, Y.T., Guo, J., Prajapati, S., Park, K.J., Surabhi, R.M., Miller, B., Gehrig, P., and Gaynor, R.B. (2003). Methylation of SPT5 regulates its interaction with RNA polymerase II and transcriptional elongation properties. Mol Cell *11*, 1055-1066.

LaBarge, M.A., and Blau, H.M. (2002). Biological progression from adult bone marrow to mononucleate muscle stem cell to multinucleate muscle fiber in response to injury. Cell *111*, 589-601.

Lacroix, M., El Messaoudi, S., Rodier, G., Le Cam, A., Sardet, C., and Fabbrizio, E. (2008). The histone-binding protein COPR5 is required for nuclear functions of the protein arginine methyltransferase PRMT5. EMBO reports *9*, 452-458.

Lagha, M., Sato, T., Bajard, L., Daubas, P., Esner, M., Montarras, D., Relaix, F., and Buckingham, M. (2008). Regulation of skeletal muscle stem cell behavior by Pax3 and Pax7. Cold Spring Harb Symp Quant Biol *73*, 307-315.

Lai, K.M., Gonzalez, M., Poueymirou, W.T., Kline, W.O., Na, E., Zlotchenko, E., Stitt, T.N., Economides, A.N., Yancopoulos, G.D., and Glass, D.J. (2004). Conditional activation of akt in adult skeletal muscle induces rapid hypertrophy. Mol Cell Biol *24*, 9295-9304.

Langmead, B. (2010). Aligning short sequencing reads with Bowtie. Curr Protoc Bioinformatics *Chapter 11*, Unit 11 17.

Le Grand, F., and Rudnicki, M.A. (2007). Skeletal muscle satellite cells and adult myogenesis. Current opinion in cell biology *19*, 628-633.

Le Guezennec, X., Vermeulen, M., Brinkman, A.B., Hoeijmakers, W.A., Cohen, A., Lasonder, E., and Stunnenberg, H.G. (2006). MBD2/NuRD and MBD3/NuRD, two distinct complexes with different biochemical and functional properties. Mol Cell Biol *26*, 843-851.

LeBlanc, S.E., Konda, S., Wu, Q., Hu, Y.J., Oslowski, C.M., Sif, S., and Imbalzano, A.N. (2012). Protein arginine methyltransferase 5 (Prmt5) promotes gene expression of peroxisome proliferator-activated receptor gamma2 (PPARgamma2) and its target genes during adipogenesis. Mol Endocrinol *26*, 583-597.

Lee, J.Y., Qu-Petersen, Z., Cao, B., Kimura, S., Jankowski, R., Cummins, J., Usas, A., Gates, C., Robbins, P., Wernig, A*., et al.* (2000). Clonal isolation of muscle-derived cells capable of enhancing muscle regeneration and bone healing. J Cell Biol *150*, 1085-1100.

Lepper, C., Conway, S.J., and Fan, C.M. (2009). Adult satellite cells and embryonic muscle progenitors have distinct genetic requirements. Nature *460*, 627-631.

Lepper, C., Partridge, T.A., and Fan, C.M. (2011). An absolute requirement for Pax7-positive satellite cells in acute injury-induced skeletal muscle regeneration. Development *138*, 3639-3646.

Lim, J.H., Choi, Y.J., Cho, C.H., and Park, J.W. (2012). Protein arginine methyltransferase 5 is an essential component of the hypoxia-inducible factor 1 signaling pathway. Biochem Biophys Res Commun *418*, 254-259.

Liu, F., Zhao, X., Perna, F., Wang, L., Koppikar, P., Abdel-Wahab, O., Harr, M.W., Levine, R.L., Xu, H., Tefferi, A*., et al.* (2011). JAK2V617F-mediated phosphorylation of PRMT5 downregulates its methyltransferase activity and promotes myeloproliferation. Cancer Cell *19*, 283-294.

Liu, K., Guo, Y., Liu, H., Bian, C., Lam, R., Liu, Y., Mackenzie, F., Rojas, L.A., Reinberg, D., Bedford, M.T*., et al.* (2012). Crystal structure of TDRD3 and methyl-arginine binding characterization of TDRD3, SMN and SPF30. PloS one *7*, e30375.

Liu, L., Cheung, T.H., Charville, G.W., Hurgo, B.M., Leavitt, T., Shih, J., Brunet, A., and Rando, T.A. (2013). Chromatin modifications as determinants of muscle stem cell quiescence and chronological aging. Cell Rep *4*, 189-204.

Lu, J., McKinsey, T.A., Zhang, C.L., and Olson, E.N. (2000). Regulation of skeletal myogenesis by association of the MEF2 transcription factor with class II histone deacetylases. Mol Cell *6*, 233-244.

Lu, J.R., Bassel-Duby, R., Hawkins, A., Chang, P., Valdez, R., Wu, H., Gan, L., Shelton, J.M., Richardson, J.A., and Olson, E.N. (2002). Control of facial muscle development by MyoR and capsulin. Science *298*, 2378-2381.

Macleod, K.F., Sherry, N., Hannon, G., Beach, D., Tokino, T., Kinzler, K., Vogelstein, B., and Jacks, T. (1995). p53-dependent and independent expression of p21 during cell growth, differentiation, and DNA damage. Genes Dev *9*, 935-944.

Mal, A., Sturniolo, M., Schiltz, R.L., Ghosh, M.K., and Harter, M.L. (2001). A role for histone deacetylase HDAC1 in modulating the transcriptional activity of MyoD: inhibition of the myogenic program. EMBO J *20*, 1739-1753.

Margueron, R., and Reinberg, D. (2011). The Polycomb complex PRC2 and its mark in life. Nature *469*, 343-349.

McKinnell, I.W., Ishibashi, J., Le Grand, F., Punch, V.G., Addicks, G.C., Greenblatt, J.F., Dilworth, F.J., and Rudnicki, M.A. (2008). Pax7 activates myogenic genes by recruitment of a histone methyltransferase complex. Nature cell biology *10*, 77-84.

McKinsey, T.A., Zhang, C.L., Lu, J., and Olson, E.N. (2000a). Signal-dependent nuclear export of a histone deacetylase regulates muscle differentiation. Nature *408*, 106-111.

McKinsey, T.A., Zhang, C.L., and Olson, E.N. (2000b). Activation of the myocyte enhancer factor-2 transcription factor by calcium/calmodulin-dependent protein kinase-stimulated binding of 14-3-3 to histone deacetylase 5. Proc Natl Acad Sci U S A *97*, 14400-14405.

Megeney, L.A., and Rudnicki, M.A. (1995). Determination versus differentiation and the MyoD family of transcription factors. Biochem Cell Biol *73*, 723-732.

Meinen, S., Barzaghi, P., Lin, S., Lochmuller, H., and Ruegg, M.A. (2007). Linker molecules between laminins and dystroglycan ameliorate laminin-alpha2-deficient muscular dystrophy at all disease stages. The Journal of cell biology *176*, 979-993.

Meister, G., and Fischer, U. (2002). Assisted RNP assembly: SMN and PRMT5 complexes cooperate in the formation of spliceosomal UsnRNPs. EMBO J *21*, 5853-5863.

Meshorer, E., and Misteli, T. (2006). Chromatin in pluripotent embryonic stem cells and differentiation. Nature reviews Molecular cell biology *7*, 540-546.

Messina, G., Biressi, S., Monteverde, S., Magli, A., Cassano, M., Perani, L., Roncaglia, E., Tagliafico, E., Starnes, L., Campbell, C.E.*, et al.* (2010). Nfix regulates fetal-specific transcription in developing skeletal muscle. Cell *140*, 554-566.

Messina, G., and Cossu, G. (2009). The origin of embryonic and fetal myoblasts: a role of Pax3 and Pax7. Genes Dev *23*, 902-905.

Miranda, T.B., Miranda, M., Frankel, A., and Clarke, S. (2004). PRMT7 is a member of the protein arginine methyltransferase family with a distinct substrate specificity. The Journal of biological chemistry *279*, 22902-22907.

Mitchell, K.J., Pannerec, A., Cadot, B., Parlakian, A., Besson, V., Gomes, E.R., Marazzi, G., and Sassoon, D.A. (2010). Identification and characterization of a non-satellite cell muscle resident progenitor during postnatal development. Nat Cell Biol *12*, 257-266.

Montarras, D., Morgan, J., Collins, C., Relaix, F., Zaffran, S., Cumano, A., Partridge, T., and Buckingham, M. (2005). Direct isolation of satellite cells for skeletal muscle regeneration. Science *309*, 2064-2067.

Mourkioti, F., Kustan, J., Kraft, P., Day, J.W., Zhao, M.M., Kost-Alimova, M., Protopopov, A., DePinho, R.A., Bernstein, D., Meeker, A.K.*, et al.* (2013). Role of telomere dysfunction in cardiac failure in Duchenne muscular dystrophy. Nature cell biology *15*, 895-904.

Murphy, M., and Kardon, G. (2011). Origin of vertebrate limb muscle: the role of progenitor and myoblast populations. Current topics in developmental biology *96*, 1-32.

Murphy, M.M., Lawson, J.A., Mathew, S.J., Hutcheson, D.A., and Kardon, G. (2011). Satellite cells, connective tissue fibroblasts and their interactions are crucial for muscle regeneration. Development *138*, 3625-3637.

Nagamatsu, G., Kosaka, T., Kawasumi, M., Kinoshita, T., Takubo, K., Akiyama, H., Sudo, T., Kobayashi, T., Oya, M., and Suda, T. (2011). A germ cell-specific gene, Prmt5, works in somatic cell reprogramming. J Biol Chem *286*, 10641-10648.

Nagata, Y., Partridge, T.A., Matsuda, R., and Zammit, P.S. (2006). Entry of muscle satellite cells into the cell cycle requires sphingolipid signaling. J Cell Biol *174*, 245-253.

Nameroff, M., and Rhodes, L.D. (1989). Differential response among cells in the chick embryo myogenic lineage to photosensitization by Merocyanine 540. Journal of cellular physiology *141*, 475-482.

Ng, J.K., Kawakami, Y., Buscher, D., Raya, A., Itoh, T., Koth, C.M., Rodriguez Esteban, C., Rodriguez-Leon, J., Garrity, D.M., Fishman, M.C.*, et al.* (2002). The limb identity gene Tbx5 promotes limb initiation by interacting with Wnt2b and Fgf10. Development *129*, 5161-5170.

Oda, H., Okamoto, I., Murphy, N., Chu, J., Price, S.M., Shen, M.M., Torres-Padilla, M.E., Heard, E., and Reinberg, D. (2009). Monomethylation of histone H4-lysine 20 is involved in chromosome structure and stability and is essential for mouse development. Molecular and cellular biology *29*, 2278-2295.

Olguin, H.C., and Pisconti, A. (2012). Marking the tempo for myogenesis: Pax7 and the regulation of muscle stem cell fate decisions. J Cell Mol Med *16*, 1013-1025.

Otani, J., Nankumo, T., Arita, K., Inamoto, S., Ariyoshi, M., and Shirakawa, M. (2009). Structural basis for recognition of H3K4 methylation status by the DNA methyltransferase 3A ATRX-DNMT3-DNMT3L domain. EMBO Rep *10*, 1235-1241.

Oustanina, S., Hause, G., and Braun, T. (2004). Pax7 directs postnatal renewal and propagation of myogenic satellite cells but not their specification. The EMBO journal *23*, 3430-3439.

Pal, S., Baiocchi, R.A., Byrd, J.C., Grever, M.R., Jacob, S.T., and Sif, S. (2007). Low levels of miR-92b/96 induce PRMT5 translation and H3R8/H4R3 methylation in mantle cell lymphoma. EMBO J *26*, 3558-3569.

Pal, S., Vishwanath, S.N., Erdjument-Bromage, H., Tempst, P., and Sif, S. (2004). Human SWI/SNF-associated PRMT5 methylates histone H3 arginine 8 and negatively regulates expression of ST7 and NM23 tumor suppressor genes. Mol Cell Biol *24*, 9630-9645.

Palacios, D., Mozzetta, C., Consalvi, S., Caretti, G., Saccone, V., Proserpio, V., Marquez, V.E., Valente, S., Mai, A., Forcales, S.V.*, et al.* (2010). TNF/p38alpha/polycomb signaling to Pax7 locus in satellite cells links inflammation to the epigenetic control of muscle regeneration. Cell Stem Cell *7*, 455-469.

Pannerec, A., Marazzi, G., and Sassoon, D. (2012). Stem cells in the hood: the skeletal muscle niche. Trends Mol Med *18*, 599-606.

Parise, G., McKinnell, I.W., and Rudnicki, M.A. (2008). Muscle satellite cell and atypical myogenic progenitor response following exercise. Muscle Nerve *37*, 611-619.

Parker, M.H., Seale, P., and Rudnicki, M.A. (2003). Looking back to the embryo: defining transcriptional networks in adult myogenesis. Nature reviews Genetics *4*, 497-507.

Parker, S.B., Eichele, G., Zhang, P., Rawls, A., Sands, A.T., Bradley, A., Olson, E.N., Harper, J.W., and Elledge, S.J. (1995). p53-independent expression of p21Cip1 in muscle and other terminally differentiating cells. Science *267*, 1024-1027.

Pastoret, C., and Sebille, A. (1993). Further aspects of muscular dystrophy in mdx mice. Neuromuscul Disord *3*, 471-475.

Penn, B.H., Bergstrom, D.A., Dilworth, F.J., Bengal, E., and Tapscott, S.J. (2004). A MyoD-generated feed-forward circuit temporally patterns gene expression during skeletal muscle differentiation. Genes Dev *18*, 2348-2353.

Petrof, B.J., Shrager, J.B., Stedman, H.H., Kelly, A.M., and Sweeney, H.L. (1993). Dystrophin protects the sarcolemma from stresses developed during muscle contraction. Proceedings of the National Academy of Sciences of the United States of America *90*, 3710-3714.

Polesskaya, A., Duquet, A., Naguibneva, I., Weise, C., Vervisch, A., Bengal, E., Hucho, F., Robin, P., and Harel-Bellan, A. (2000). CREB-binding protein/p300 activates MyoD by acetylation. J Biol Chem *275*, 34359-34364.

Polesskaya, A., Seale, P., and Rudnicki, M.A. (2003). Wnt signaling induces the myogenic specification of resident CD45+ adult stem cells during muscle regeneration. Cell *113*, 841-852.

Powers, M.A., Fay, M.M., Factor, R.E., Welm, A.L., and Ullman, K.S. (2011). Protein arginine methyltransferase 5 accelerates tumor growth by arginine methylation of the tumor suppressor programmed cell death 4. Cancer Res *71*, 5579-5587.

Puri, P.L., Avantaggiati, M.L., Balsano, C., Sang, N., Graessmann, A., Giordano, A., and Levrero, M. (1997a). p300 is required for MyoD-dependent cell cycle arrest and muscle-specific gene transcription. The EMBO journal *16*, 369-383.

Puri, P.L., Iezzi, S., Stiegler, P., Chen, T.T., Schiltz, R.L., Muscat, G.E., Giordano, A., Kedes, L., Wang, J.Y., and Sartorelli, V. (2001). Class I histone deacetylases sequentially interact with MyoD and pRb during skeletal myogenesis. Mol Cell *8*, 885-897.

Puri, P.L., Sartorelli, V., Yang, X.J., Hamamori, Y., Ogryzko, V.V., Howard, B.H., Kedes, L., Wang, J.Y., Graessmann, A., Nakatani, Y.*, et al.* (1997b). Differential roles of p300 and PCAF acetyltransferases in muscle differentiation. Molecular cell *1*, 35-45.

Qu-Petersen, Z., Deasy, B., Jankowski, R., Ikezawa, M., Cummins, J., Pruchnic, R., Mytinger, J., Cao, B., Gates, C., Wernig, A.*, et al.* (2002). Identification of a novel population of muscle stem cells in mice: potential for muscle regeneration. J Cell Biol *157*, 851-864.

Ramon-Maiques, S., Kuo, A.J., Carney, D., Matthews, A.G., Oettinger, M.A., Gozani, O., and Yang, W. (2007). The plant homeodomain finger of RAG2 recognizes histone H3 methylated at both lysine-4 and arginine-2. Proceedings of the National Academy of Sciences of the United States of America *104*, 18993-18998.

Rank, G., Cerruti, L., Simpson, R.J., Moritz, R.L., Jane, S.M., and Zhao, Q. (2010). Identification of a PRMT5-dependent repressor complex linked to silencing of human fetal globin gene expression. Blood *116*, 1585-1592.

Ratajczak, M.Z., Majka, M., Kucia, M., Drukala, J., Pietrzkowski, Z., Peiper, S., and Janowska-Wieczorek, A. (2003). Expression of functional CXCR4 by muscle satellite cells and secretion of SDF-1 by muscle-derived fibroblasts is associated with the presence of both muscle progenitors in bone marrow and hematopoietic stem/progenitor cells in muscles. Stem Cells *21*, 363-371.

Relaix, F., Montarras, D., Zaffran, S., Gayraud-Morel, B., Rocancourt, D., Tajbakhsh, S., Mansouri, A., Cumano, A., and Buckingham, M. (2006). Pax3 and Pax7 have distinct and overlapping functions in adult muscle progenitor cells. J Cell Biol *172*, 91-102.

Relaix, F., Rocancourt, D., Mansouri, A., and Buckingham, M. (2005). A Pax3/Pax7-dependent population of skeletal muscle progenitor cells. Nature *435*, 948-953.

Rudnicki, M.A., Le Grand, F., McKinnell, I., and Kuang, S. (2008). The molecular regulation of muscle stem cell function. Cold Spring Harb Symp Quant Biol *73*, 323-331.

Sacco, A., Mourkioti, F., Tran, R., Choi, J., Llewellyn, M., Kraft, P., Shkreli, M., Delp, S., Pomerantz, J.H., Artandi, S.E.*, et al.* (2010). Short telomeres and stem cell exhaustion model Duchenne muscular dystrophy in mdx/mTR mice. Cell *143*, 1059-1071.

Sambasivan, R., Gayraud-Morel, B., Dumas, G., Cimper, C., Paisant, S., Kelly, R.G., and Tajbakhsh, S. (2009). Distinct regulatory cascades govern extraocular and pharyngeal arch muscle progenitor cell fates. Dev Cell *16*, 810-821.

Sambasivan, R., Yao, R., Kissenpfennig, A., Van Wittenberghe, L., Paldi, A., Gayraud-Morel, B., Guenou, H., Malissen, B., Tajbakhsh, S., and Galy, A. (2011). Pax7-expressing satellite cells are indispensable for adult skeletal muscle regeneration. Development *138*, 3647-3656.

Schienda, J., Engleka, K.A., Jun, S., Hansen, M.S., Epstein, J.A., Tabin, C.J., Kunkel, L.M., and Kardon, G. (2006). Somitic origin of limb muscle satellite and side population cells. Proceedings of the National Academy of Sciences of the United States of America *103*, 945-950.

Schotta, G., Sengupta, R., Kubicek, S., Malin, S., Kauer, M., Callen, E., Celeste, A., Pagani, M., Opravil, S., De La Rosa-Velazquez, I.A.*, et al.* (2008). A chromatin-wide transition to H4K20 monomethylation impairs genome integrity and programmed DNA rearrangements in the mouse. Genes & development *22*, 2048-2061.

Seale, P., Sabourin, L.A., Girgis-Gabardo, A., Mansouri, A., Gruss, P., and Rudnicki, M.A. (2000). Pax7 is required for the specification of myogenic satellite cells. Cell *102*, 777-786.

Serra, C., Palacios, D., Mozzetta, C., Forcales, S.V., Morantte, I., Ripani, M., Jones, D.R., Du, K., Jhala, U.S., Simone, C.*, et al.* (2007). Functional interdependence at the chromatin level between the MKK6/p38 and IGF1/PI3K/AKT pathways during muscle differentiation. Molecular cell *28*, 200-213.

Shi, X., and Garry, D.J. (2006). Muscle stem cells in development, regeneration, and disease. Genes Dev *20*, 1692-1708.

Shinin, V., Gayraud-Morel, B., Gomes, D., and Tajbakhsh, S. (2006). Asymmetric division and cosegregation of template DNA strands in adult muscle satellite cells. Nat Cell Biol *8*, 677-687.

Siatecka, M., Lohmann, F., Bao, S., and Bieker, J.J. (2010). EKLF directly activates the p21WAF1/CIP1 gene by proximal promoter and novel intronic regulatory regions during erythroid differentiation. Mol Cell Biol *30*, 2811-2822.

Simone, C., Forcales, S.V., Hill, D.A., Imbalzano, A.N., Latella, L., and Puri, P.L. (2004). p38 pathway targets SWI-SNF chromatin-remodeling complex to muscle-specific loci. Nature genetics *36*, 738-743.

Soleimani, V.D., Punch, V.G., Kawabe, Y., Jones, A.E., Palidwor, G.A., Porter, C.J., Cross, J.W., Carvajal, J.J., Kockx, C.E., van, I.W.F.*, et al.* (2012). Transcriptional dominance of Pax7 in adult myogenesis is due to high-affinity recognition of homeodomain motifs. Dev Cell *22*, 1208-1220.

Sousa-Victor, P., Gutarra, S., Garcia-Prat, L., Rodriguez-Ubreva, J., Ortet, L., Ruiz-Bonilla, V., Jardi, M., Ballestar, E., Gonzalez, S., Serrano, A.L.*, et al.* (2014). Geriatric muscle stem cells switch reversible quiescence into senescence. Nature *506*, 316-321.

Spencer, S.L., Cappell, S.D., Tsai, F.C., Overton, K.W., Wang, C.L., and Meyer, T. (2013). The proliferation-quiescence decision is controlled by a bifurcation in CDK2 activity at mitotic exit. Cell *155*, 369-383.

Straub, V., Rafael, J.A., Chamberlain, J.S., and Campbell, K.P. (1997). Animal models for muscular dystrophy show different patterns of sarcolemmal disruption. The Journal of cell biology *139*, 375-385.

Tae, S., Karkhanis, V., Velasco, K., Yaneva, M., Erdjument-Bromage, H., Tempst, P., and Sif, S. (2011). Bromodomain protein 7 interacts with PRMT5 and PRC2, and is involved in transcriptional repression of their target genes. Nucleic Acids Res *39*, 5424-5438.

Tajbakhsh, S., Rocancourt, D., and Buckingham, M. (1996). Muscle progenitor cells failing to respond to positional cues adopt non-myogenic fates in myf-5 null mice. Nature *384*, 266-270.

Tajbakhsh, S., Rocancourt, D., Cossu, G., and Buckingham, M. (1997). Redefining the genetic hierarchies controlling skeletal myogenesis: Pax-3 and Myf-5 act upstream of MyoD. Cell *89*, 127-138.

Takahashi, K., and Yamanaka, S. (2006). Induction of pluripotent stem cells from mouse embryonic and adult fibroblast cultures by defined factors. Cell *126*, 663-676.

Tan, C.P., and Nakielny, S. (2006). Control of the DNA methylation system component MBD2 by protein arginine methylation. Mol Cell Biol *26*, 7224-7235.

Tee, W.W., Pardo, M., Theunissen, T.W., Yu, L., Choudhary, J.S., Hajkova, P., and Surani, M.A. (2010). Prmt5 is essential for early mouse development and acts in the cytoplasm to maintain ES cell pluripotency. Genes Dev *24*, 2772-2777.

Tripsianes, K., Madl, T., Machyna, M., Fessas, D., Englbrecht, C., Fischer, U., Neugebauer, K.M., and Sattler, M. (2011). Structural basis for dimethylarginine recognition by the Tudor domains of human SMN and SPF30 proteins. Nature structural & molecular biology *18*, 1414-1420.

Tsutsui, T., Fukasawa, R., Shinmyouzu, K., Nakagawa, R., Tobe, K., Tanaka, A., and Ohkuma, Y. (2013). Mediator complex recruits epigenetic regulators via its two cyclin-dependent kinase subunits to repress transcription of immune response genes. J Biol Chem *288*, 20955-20965.

Urciuolo, A., Quarta, M., Morbidoni, V., Gattazzo, F., Molon, S., Grumati, P., Montemurro, F., Tedesco, F.S., Blaauw, B., Cossu, G.*, et al.* (2013). Collagen VI regulates satellite cell self-renewal and muscle regeneration. Nature communications *4*, 1964.

Ustanina, S., Carvajal, J., Rigby, P., and Braun, T. (2007). The myogenic factor Myf5 supports efficient skeletal muscle regeneration by enabling transient myoblast amplification. Stem cells *25*, 2006-2016.

Vagin, V.V., Wohlschlegel, J., Qu, J., Jonsson, Z., Huang, X., Chuma, S., Girard, A., Sachidanandam, R., Hannon, G.J., and Aravin, A.A. (2009). Proteomic analysis of murine Piwi proteins reveals a role for arginine methylation in specifying interaction with Tudor family members. Genes Dev *23*, 1749-1762.

Wang, A., Ren, L., Abenes, G., and Hai, R. (2009). Genome sequence divergences and functional variations in human cytomegalovirus strains. FEMS immunology and medical microbiology *55*, 23-33.

Wang, L., Pal, S., and Sif, S. (2008). Protein arginine methyltransferase 5 suppresses the transcription of the RB family of tumor suppressors in leukemia and lymphoma cells. Mol Cell Biol *28*, 6262-6277.

Wang, Y., Wysocka, J., Sayegh, J., Lee, Y.H., Perlin, J.R., Leonelli, L., Sonbuchner, L.S., McDonald, C.H., Cook, R.G., Dou, Y.*, et al.* (2004). Human PAD4 regulates histone arginine methylation levels via demethylimination. Science *306*, 279-283.

Webby, C.J., Wolf, A., Gromak, N., Dreger, M., Kramer, H., Kessler, B., Nielsen, M.L., Schmitz, C., Butler, D.S., Yates, J.R., 3rd*, et al.* (2009). Jmjd6 catalyses lysyl-hydroxylation of U2AF65, a protein associated with RNA splicing. Science *325*, 90-93.

Wei, H., Mundade, R., Lange, K.C., and Lu, T. (2014). Protein arginine methylation of non-histone proteins and its role in diseases. Cell cycle *13*, 32-41.

Wei, H., Wang, B., Miyagi, M., She, Y., Gopalan, B., Huang, D.B., Ghosh, G., Stark, G.R., and Lu, T. (2013). PRMT5 dimethylates R30 of the p65 subunit to activate NF-kappaB. Proc Natl Acad Sci U S A *110*, 13516-13521.

Wei, T.Y., Juan, C.C., Hisa, J.Y., Su, L.J., Lee, Y.C., Chou, H.Y., Chen, J.M., Wu, Y.C., Chiu, S.C., Hsu, C.P.*, et al.* (2012). Protein arginine methyltransferase 5 is a potential oncoprotein that upregulates G1 cyclins/cyclin-dependent kinases and the phosphoinositide 3-kinase/AKT signaling cascade. Cancer Sci *103*, 1640-1650.

White, R.B., Bierinx, A.S., Gnocchi, V.F., and Zammit, P.S. (2010). Dynamics of muscle fibre growth during postnatal mouse development. BMC Dev Biol *10*, 21.

Wilson, A., and Trumpp, A. (2006). Bone-marrow haematopoietic-stem-cell niches. Nature reviews Immunology *6*, 93-106.

Woodhouse, S., Pugazhendhi, D., Brien, P., and Pell, J.M. (2013). Ezh2 maintains a key phase of muscle satellite cell expansion but does not regulate terminal differentiation. Journal of cell science *126*, 565-579.

Xu, X., Hoang, S., Mayo, M.W., and Bekiranov, S. (2010). Application of machine learning methods to histone methylation ChIP-Seq data reveals H4R3me2 globally represses gene expression. BMC Bioinformatics *11*, 396.

Yablonka-Reuveni, Z., Day, K., Vine, A., and Shefer, G. (2008). Defining the transcriptional signature of skeletal muscle stem cells. J Anim Sci *86*, E207-216.

Yaffe, D., and Saxel, O. (1977). Serial passaging and differentiation of myogenic cells isolated from dystrophic mouse muscle. Nature *270*, 725-727.

Yamaguchi, Y., Takagi, T., Wada, T., Yano, K., Furuya, A., Sugimoto, S., Hasegawa, J., and Handa, H. (1999). NELF, a multisubunit complex containing RD, cooperates with DSIF to repress RNA polymerase II elongation. Cell *97*, 41-51.

Yan, F., Alinari, L., Lustberg, M.E., Martin, L.K., Cordero-Nieves, H.M., Banasavadi-Siddegowda, Y., Virk, S., Barnholtz-Sloan, J., Bell, E.H., Wojton, J.*, et al.* (2014).

Genetic validation of the protein arginine methyltransferase PRMT5 as a candidate therapeutic target in glioblastoma. Cancer Res *74*, 1752-1765.

Yang, Y., and Bedford, M.T. (2013). Protein arginine methyltransferases and cancer. Nature reviews Cancer *13*, 37-50.

Yin, H., Pasut, A., Soleimani, V.D., Bentzinger, C.F., Antoun, G., Thorn, S., Seale, P., Fernando, P., van Ijcken, W., Grosveld, F.*, et al.* (2013a). MicroRNA-133 controls brown adipose determination in skeletal muscle satellite cells by targeting Prdm16. Cell Metab *17*, 210-224.

Yin, H., Price, F., and Rudnicki, M.A. (2013b). Satellite cells and the muscle stem cell niche. Physiol Rev *93*, 23-67.

Zacharias, A.L., Lewandoski, M., Rudnicki, M.A., and Gage, P.J. (2011). Pitx2 is an upstream activator of extraocular myogenesis and survival. Dev Biol *349*, 395-405.

Zammit, P.S., Golding, J.P., Nagata, Y., Hudon, V., Partridge, T.A., and Beauchamp, J.R. (2004). Muscle satellite cells adopt divergent fates: a mechanism for self-renewal? J Cell Biol *166*, 347-357.

Zammit, P.S., Relaix, F., Nagata, Y., Ruiz, A.P., Collins, C.A., Partridge, T.A., and Beauchamp, J.R. (2006). Pax7 and myogenic progression in skeletal muscle satellite cells. J Cell Sci *119*, 1824-1832.

Zhang, Y., Jurkowska, R., Soeroes, S., Rajavelu, A., Dhayalan, A., Bock, I., Rathert, P., Brandt, O., Reinhardt, R., Fischle, W.*, et al.* (2010). Chromatin methylation activity of Dnmt3a and Dnmt3a/3L is guided by interaction of the ADD domain with the histone H3 tail. Nucleic Acids Res *38*, 4246-4253.

Zhang, Y., Liu, T., Meyer, C.A., Eeckhoute, J., Johnson, D.S., Bernstein, B.E., Nusbaum, C., Myers, R.M., Brown, M., Li, W.*, et al.* (2008). Model-based analysis of ChIP-Seq (MACS). Genome Biol *9*, R137.

Zhao, Q., Rank, G., Tan, Y.T., Li, H., Moritz, R.L., Simpson, R.J., Cerruti, L., Curtis, D.J., Patel, D.J., Allis, C.D.*, et al.* (2009). PRMT5-mediated methylation of histone H4R3 recruits DNMT3A, coupling histone and DNA methylation in gene silencing. Nat Struct Mol Biol *16*, 304-311.

Zhou, Y., Kim, J., Yuan, X., and Braun, T. (2011). Epigenetic modifications of stem cells: a paradigm for the control of cardiac progenitor cells. Circulation research *109*, 1067-1081.

Zhou, Z., Sun, X., Zou, Z., Sun, L., Zhang, T., Guo, S., Wen, Y., Liu, L., Wang, Y., Qin, J.*, et al.* (2010). PRMT5 regulates Golgi apparatus structure through methylation of the golgin GM130. Cell Res *20*, 1023-1033.

8 APPENDIX

8.1 Abbreviations

%	Percent
°C	Degree Celsius
A	Adenine
ATP	Adenosine triphosphate
BMP	Bone morphogenetic protein
bp	Base pairs
BSA	Bovine serum albumin
C	Cytosine
CDK	Cyclin-dependent kinase
cDNA	Complementary DNA
ChIP	Chromatin immunoprecipitation
cm	Centimeter
CMV	Cytomegalovirus
Co-IP	Co-immunopricipitation
CpG	Cytosine-guanine dinucleotide
CREB	cAMP response element-binding protein
CTX	Cobra cardiotoxin
CXCR-4	C-X-C chemokine receptor type 4
DAPI	4',6-diamidino-2-phenylindole
DMD	Duchenne muscular dystrophy
DMEM	Dulbecco's Modified Eagle Medium
DMSO	Dimethyl sulfoxide
DNA	Deoxyribonucleic acid
Dnajc13	DnaJ (Hsp40) homolog, subfamily C, member 13
DNMT	DNA methyltransferase
DRB	5,6-dichloro-1-β-D-ribofuranosyl-1H-benzimidazole
DTA	Diphtheria toxin A
DTT	Dithiothreitol
E. coli	*Escherichia coli*
ECL	Enhanced chemi-luminescence
ECM	Extracellular matrix

EDL	Extensor digitorum longus
EDTA	Ethylenediaminetetraacetic acid
EdU	5-ethynyl-2'-deoxyuridine
ES	Embryonic stem cell
FAPs	Fibro-adipogenic progenitors
FCS	Fetal calf serum
FGF	Fibroblast growth factor
g	Gram
G	Guanine
g	Gravitational acceleration
GAPDH	Glyceraldehyde 3-phosphate dehydrogenase
GFP	Green fluorescent protein
h	Hour
H&E	Hematoxylin and eosin
H3K27me3	Histone H3 trimethyl Lysine 27
H3K36me3	Histone H3 trimethyl Lysine 36
H3K9me3	Histone H3 trimethyl Lysine 9
H3R8me2s	Histone H3 symetrical dimethyl Arginine 8
H4K20me1	Histone H4 monomethyl Lysine 20
H4K20me2	Histone H4 dimethyl Lysine 20
H4K20me3	Histone H4 trimethyl Lysine 20
H4K4me3	Histone H4 trimethyl Lysine 4
H4R3me2s	Histone H4 symetrical dimethyl Arginine 3
HA	Hemagglutinin
HBS	HEPES Buffered Saline
HDAC	Histone deacetylases
HE	Hematoxylin and eosin
HEPES	4-(2-hydroxyethyl)-1-piperazineethanesulfonic acid
Hnrnpa2b1	Heterogeneous Nuclear Ribonucleoprotein A2/B1
HRP	Horseradish peroxidase
HSA	Human skeletal actin
IF	Immunofluorescence
IGF	Insulin-like growth factor
IgG	Immunoglobulin G
IP	Immunoprecipitation

JNK	c-Jun N-terminal kinases
kb	kilo-base pairs
kDa	kilodalton
kg	kilogram
KO	Knock Out
M	molar
MEF2	Myocyte enhancer factor 2
min	Minute
ml	milliliter
mm	millimeter
mM	millimolar
MNase	Micrococcal Nuclease
MPI	Max-Planck Institute
Mrf4	myogenic regulatory factor 4
mRNA	messenger RNA
MS	Mass spectrometry
Myf5	Myogenic factor 5
MyoD	Myogenic differentiation
NFκB	Nuclear factor kappa-light-chain-enhancer of activated B cells
NP-40	Nonidet P-40
NSC	neural stem cell
P300	E1A binding protein p300
Pax3	Pair box transcription factor 3
Pax7	Pair box transcription factor 7
PBS	Phosphate Buffered Saline
PCAF	P300/CBP-associated factor
PcG	Polycomb-group
PCR	Polymerase chain reaction
PenStrep	Penicillin Streptomycin
PFA	Paraformaldehyde
Pitx2	Pituitary homeobox 2
PMSF	Phenyl methyl sulfonyl fluoride
Pol II	RNA Polymerase II
PRC2	Polycomb repressive complex 2
PRMT5	Protein arginine methyl transferase 5

Prp8	pre-mRNA processing factor 8
PR-Set7	PR/SET Domain-Containing Protein 7
qPCR	quantitative PCR
rDNA	Ribosomal DNA
RNA	Ribonucleic acid
rpm	Rotations per minute
rRNA	Ribosomal RNA
RT	Room temperature
RT-qPCR	Quantitative reverse transcription polymerase chain reaction
s	Second
SC	Satellite cell
SDS	Sodium dodecyl sulfate
SDS-PAGE	Sodium dodecyl sulfate polyacrylamide gel electrophoresis
shRNA	Small hairpin RNA
SILAC	Stable isotope labeling with amino acids in cell culture
Srrm2	Serine/Arginine Repetitive Matrix 2
SSC	Saline-sodium citrate buffer
STAT	Signal transducer and activator of transcription
SWI/SNF	SWItch/Sucrose Non Fermentable
T	Thymine
TA	Tibialis anterior
TBS	Tris-Buffered Saline
Tbx1	T-box transcription factor 1
TES	Transcription end site
TFBS	Transcription factor binding sites
TrxG	Trithorax group
TSS	Transcription start site
Tween 20	Polyoxyethylene-sorbitan-monolaurate
V	Volt
WT	Wild type
YFP	Yellow fluorescent protein
µg	micro gram
µl	micro liter
µM	micro molar
µm	micro meter

8.2 Lists of figures

8.3 Acknowledgements

First of all, I would like to express my sincere gratitude to my Ph.D. supervisor Prof. Dr. Dr. Thomas Braun for providing me the opportunity to pursue my doctor degree in his laboratory. His excellent knowledge, generous guidance and constant support impressed me deeply and enabled me to develop a good understanding and performing of my project.

I am most grateful to my direct supervisor Dr. Yonggang Zhou for consigning this interesting and challenging topic to me and guiding me these years. He is always a friend and a guide, providing me unconditional support, guidance, encouragement, and advice whenever I needed any help during my study. His dedication to science and pursuit of perfection will always inspire me to grow further not only in my scientific career but also my whole life in the future.

I express my appreciation to Prof. Dr. Lienhard Schmitz for his willingness to be my second corrector and for his valuable advice as my thesis committees. I am grateful for a very supporting and inspiring atmosphere I enjoyed at the MPI of Heart and lung research, thanking to all AG Braun members. Many thanks go to my group members who are also my close friends, Dr. Xuejun Yuan, Angelina Georgieva, Dr. Verawan Boonsanay, Dr. Hui Qi for the friendly working atmosphere and a lot of helpful discussion especially Xuejun for ChIP methodological training. Thanks also go to Dr. Johnny Kim, Dr. Shuichi Watanabe and Dr. Stefan Günter for theoretical and practical help especially regarding satellite cells isolation and culture and RNA sequencing. I would also like to express my appreciation to Dr. Marcus Krüger and his group for the SILAC assay, to Dr. Astrid Wietelmann for the MRI, and to Dr. Marek Bartkuhn for the ChIP-seq data analysis.

Finally, my special gratitude and love go to my family. I could not have done my PhD study without their love and support. I thank my parents who have always been my biggest supporter with their abiding love through thick and thin, and my husband Yi Cai for all the bitter and sweet we have been through together as well as for his remarkable patience and unwavering love supporting me over the course of my research. I dedicate this dissertation to them.